

Riccati quadratic differential systems

Joan C. Artés, Jaume Llibre

Departament de Matemàtiques, Universitat Autònoma de Barcelona

D. Schlomiuk

Département de Mathématiques et de Statistiques

Université de Montréal

Nicolae Vulpe

Vladimir Andrunakievichi Institute of Mathematics
and Computer Science, Moldova

Abstract

In this article we study the family of quadratic Riccati differential systems. This family was studied before and phase portraits were given but the complete topological classification was still missing. Our first goal in this work is to provide the complete topological classification of this family of systems and we obtained a total of 119 phase portraits either non-degenerate or degenerate. Furthermore we not only provide the complete topological classification but we also give the full bifurcation diagram of this family in the 12 parameter space of coefficients of the systems. This bifurcation diagram is given in terms of invariant polynomials and it is thus completely independent of the normal forms in which the systems may be presented. This bifurcation diagram provides an algorithm to decide for any given quadratic system in any form it may be presented, whether it is a Riccati system or not, and in case it is to specify its phase portrait. All this was made possible because the authors exploited to the full the algebraic geometric properties of this class of systems, namely that this is the family of quadratic systems that either have two parallel invariant straight lines or are limit points within quadratic systems of this more generic subfamily. We also provide a critical review of previous work on the quadratic Riccati family.

1 Introduction and the statement of the main theorem

We consider here polynomial differential systems

$$\frac{dx}{dt} = P(x, y), \quad \frac{dy}{dt} = Q(x, y), \quad (1)$$

where $P, Q \in \mathbb{R}[x, y]$ i.e. P, Q are polynomials in x, y with real coefficients. We call *degree* of a system (1) the number $\tilde{m} = \max(\deg(P), \deg(Q))$. Among the planar polynomial differential systems the simplest are the quadratic ones, i.e. $\tilde{m} = 2$ and they are of the form:

$$\frac{dx}{dt} = a + cx + dy + gx^2 + 2hxy + ky^2, \quad \frac{dy}{dt} = b + ex + fy + lx^2 + 2mxy + ny^2. \quad (2)$$

We call *cubic* a system (1) with $\tilde{m} = 3$.

Studies on some quadratic systems are old as it is the case with the Riccati systems. They go back over 300 years (see [12] for their history).

Definition 1.1. *The quadratic Riccati systems are of the form:*

$$\frac{dx}{dt} = a + cx + gx^2, \quad \frac{dy}{dt} = b + ex + fy + lx^2 + 2mxy + ny^2. \quad (3)$$

Notation 1.1. *We denote the family of quadratic Riccati differential systems by the symbol QS_{Ric} .*

As indicated in [12] the first time that Riccati equations occurred in the literature was in 1694 in a paper of Johann I. Bernoulli. They are however called after Jacopo F. Riccati who first mentioned them in 1718 in a letter to Giovanni Poleni, where the Riccati equations were not necessarily quadratic. Apart from Johann I. Bernoulli, several members of the Bernoulli family had contributions on this subject. Initially the problem was to solve the equations, at least in some particular cases, using separation of variables. Seeing that for the higher degree equations the generic case was hard to treat, Riccati proposed to consider the particular quadratic case. This case proved to be useful in areas of applied mathematics, for example in control theory. For more applications consult [13].

In [13] the authors say in their abstract that they “give the complete description of the phase portraits in the Poincaré disk (i.e. in the compactification of \mathbb{R}^2 adding the circle \mathbb{S}^1 of the infinity) modulo topological equivalence” of the Riccati systems with $n(b^2 + e^2 + l^2) \neq 0$. The motivation for this exclusion was firstly that for $n = 0$ the systems are Liénard and secondly that in case $b = e = l = 0$ the systems are Bernoulli equations. We point out however that any Bernoulli system can be transformed by only using a translation $y \rightarrow y + \alpha$, $\alpha \neq 0$ into a Riccati system with new coefficients $a, c, g, b', e', f', l', m', n'$ such that $b'^2 + c'^2 + l'^2 \neq 0$ and hence it is useless to add this restriction.

The problem of classifying topologically any quadratic family of equations is global in the parameter space as we want phase portraits on the Poincaré disk for *all* values of the parameters of the equations. In particular the Riccati family depends on nine parameters (modulo rescaling only eight) and clearly we expect to have many phase portraits. It is therefore convenient to split the family into smaller ones where we have fewer phase portraits and hence we have a better control not to miss any.

In [13] the authors' starting point was to do exactly this, i.e. to split the Riccati family into several smaller families which have far fewer phase portraits. They provided five normal forms that cover the whole Riccati family, each one with fewer parameters. Their main theorem says that they obtained 74 phase portraits. To prove their theorem the authors used the classical method, i.e. firstly one calculates the finite singularities and their local phase portraits (topological types), then one passes to the calculation of the infinite singularities and their types and afterwards one tries to complete the study by determining the separatrices, the connections and the limit cycles if they exist. At the end however they still missed some portraits. In order to avoid missing phase portraits or repeating them and also to obtain a truly global picture allowing the gluing together of normal forms it is convenient to use algebraic invariants as the ones introduced in Section 2. These are based on the algebraic invariant theory developed by Sibirski and his school [24].

At the beginning of this century global geometric tools began to be used see for example [14, 16]. Furthermore using these tools together with polynomial invariants a number of families of quadratic or cubic differential systems were topologically classified.

An interesting case is the study of all Lotka-Volterra differential systems, well known for their many applications. We recall that a Lotka-Volterra differential system is defined to be a quadratic system (1) with $P(x, y) = x(ax + by + c)$ and $Q(x, y) = y(dx + ey + f)$, with $a, \dots, f \in \mathbb{R}$.

As in the Riccati family the phase portraits of the Lotka-Volterra family were studied first by using only the classical methods and three papers were written in this way, none of them

complete and each of them with repeated phase portraits and some with errors.

These Lotka-Volterra systems have an algebraic geometric property, namely they possess two distinct real invariant lines ($x = 0, y = 0$) intersecting in the finite plane (at $(0, 0)$). This geometric property actually defines them as any quadratic system possessing two real invariant lines intersecting at a finite point can be brought via an affine transformation to one of this form. To obtain the global topological classification the authors of [22] used this algebraic geometric property valid for *all* Lotka-Volterra systems and the notion of *configuration of invariant lines* introduced by them in [16].

Definition 1.2. *We call configuration of invariant lines (or simply configuration) of a system (1) the set of all its invariant lines (real or complex), each endowed with its own multiplicity and together with all the real singular points of the system located on these lines, each one endowed with its own multiplicity.*

The notion of multiplicity of an invariant line was introduced in [16].

Definition 1.3. *We say that an invariant straight line $L(x, y) = ux + vy + w = 0$, $(u, v) \neq (0, 0)$, $(u, v, w) \in \mathbb{C}^3$ for a real polynomial differential system (S) has multiplicity m if there exists a sequence of real polynomial systems (S_k) $k \geq 1$ converging to (S) , such that each (S_k) has m distinct (complex) invariant straight lines $L_k^j = u_k^j x + v_k^j y + w_k^j = 0$, $j = 0, \dots, m$, converging to $L = 0$ as $k \rightarrow \infty$, i.e. $[u_k^j : v_k^j : w_k^j] \rightarrow [u : v : w]$ as $k \rightarrow \infty$ in $\mathbf{P}_2(\mathbb{C})$ and this does not occur for $m + 1$.*

An analogous definition of multiplicity of the line at infinity was also introduced in [16].

Definition 1.4. *We say that the line at infinity is an invariant line of multiplicity m for a system (S) of the form (1) if and only if there exists a sequence of systems (S_i) of the form (1) tending to (S) when $i \rightarrow \infty$ and (S_i) have $m - 1$ distinct invariant affine lines $L_i^j = u_i^j x + v_i^j y + w_i^j = 0$ $(u_i^j, v_i^j) \neq (0, 0)$, $(u_i^j, v_i^j, w_i^j) \in \mathbb{C}^3$, $(j = 1, \dots, m - 1)$ such that for every j , $(u_i^j, v_i^j, w_i^j) \rightarrow (0, 0, 1)$ and they do not have m invariant such lines L_j^i $j = 1, \dots, m$ satisfying the above mentioned conditions.*

Note that in the previous definition the multiplicity is m because apart from the $m - 1$ lines we must also take into account the line at infinity that is invariant.

In the above definitions the convergence of the systems means convergence of the coefficients of the systems in the $(N - 1)$ -dimensional sphere \mathbb{S}^{N-1} after time rescaling by the square root of the sum of the squares of the $N = (m + 1)(m + 2)$ coefficients of the systems involved where $m = \deg(S)$.

Definition 1.5. *We call total multiplicity of invariant lines of a polynomial system (1) the sum of multiplicities of all its invariant lines including the multiplicity of the line at infinity.*

A quadratic system (1) is *non-degenerate* if the polynomials P, Q have no common real factors other than constants.

Proposition 1.1 (Corollary 5 [1]). *A non-degenerate quadratic system could have invariant lines, including the line at infinity, of total multiplicity at most six.*

Notation 1.2. *We denote by $\mathbf{QSL}_{\geq n}$, the family of non-degenerate quadratic systems possessing invariant lines of total multiplicity at least n , ($1 \leq n \leq 6$).*

Like in the case of the Lotka-Volterra differential systems the quadratic Riccati systems have invariant lines so we can use this geometric property in order to first find their possible configurations of invariant lines and classify the whole family in subfamilies of systems according to their configurations.

We note that although in the topological equivalence relation the presence of an invariant line in a system does not count as it can be deformed by a homeomorphism, the affine transformations preserve the invariant lines and the finer affine equivalence relation was thus instrumental in better controlling the process of getting information and proving the result. Any polynomial system (1) has singularities, but the condition to possess invariant lines is a substantial restriction that turns out to be valuable for handling the large number of phase portraits. Furthermore although a configuration of invariant lines is not a phase portrait it is at least part of one and occasionally this information even leads to a single phase portrait. The presence of an invariant line or the topological type of a singularity are both affine invariants.

The above observations show that whenever the systems have some algebraic geometric property, it is useful to pay attention and use it for the topological classifications. In particular, the family $\mathbf{QSL}_{\geq 2}$ is an interesting object to study and this provides us with additional motivation for this work as $\mathbf{QS}_{Ric} \subset \mathbf{QSL}_{\geq 3} \subset \mathbf{QSL}_{\geq 2}$.

Our topological classification of \mathbf{QS}_{Ric} was the only piece so far lacking in the global topological classification of $\mathbf{QSL}_{\geq 3}$. Indeed, the case when we have two affine invariant lines intersecting in the finite space is solved (if the lines are real this is the Lotka-Volterra case and if they are complex this problem was solved in [23]). The Riccati systems cover the case of two parallel lines, real or complex that intersect at infinity and their limiting cases.

All that remains to do in order to obtain the topological classification of $\mathbf{QSL}_{\geq 2}$ is to construct all phase portraits of quadratic systems having exactly two invariant lines, both simple, i.e. a real simple affine line and the line at infinity simple, or no affine invariant line and the line at infinity double.

Knowing the configuration of invariant lines of a system gives a part of the information on the phase portrait that can then be completed by adding what else is missing, for example the proof of absence of limit cycles as it is the case for the quadratic Riccati family, or the proof of presence of limit cycles a fact occurring in other families such as for example the family of quadratic systems possessing two complex invariant lines intersecting at a finite point (see [23]).

Our goal in this paper is to obtain the topological classification of the quadratic Riccati family (that is the classification of the phase portraits of this family in the Poincaré disk according to the topological equivalence relation) and for this we rely on the geometric classification of this family, by this meaning the classification in terms of configurations of invariant lines of this family. For this last classification we rely on [10] where at the beginning we have the following lemma:

Lemma 1.1. *If a quadratic system (1) possesses two distinct parallel invariant affine lines (real or complex) this system could be brought via a real affine transformation to a quadratic Riccati system (3).*

We denote by \mathbf{QSL}^{2P} the class of non-degenerate quadratic systems which via an affine transformation could be brought to the canonical form (3). The notation \mathbf{QSL}^{2P} brings into focus the principal property of Riccati systems, i.e. that generically they have two parallel invariant lines.

In [10] all the configurations of invariant lines (real or complex) were obtained for the family \mathbf{QSL}^{2P} . Also, the bifurcation diagram of these configurations in the 12-dimensional space of coefficients of systems in this family was obtained in terms of invariant polynomials. To reach our goal of obtaining the topological classification all that remains to be done is to obtain the phase portraits for each one of the configurations.

We have $\mathbf{QS}_{Ric} \subset \mathbf{QSL}^{2P}$ and any system in \mathbf{QSL}^{2P} is affinely equivalent to one in \mathbf{QS}_{Ric} . Clearly the two families \mathbf{QS}_{Ric} and \mathbf{QSL}^{2P} thus have the same set of phase portraits. Our goal now is to find all phase portraits of \mathbf{QSL}^{2P} .

When in the systems of the Lemma 1.1 we have $c^2 - 4ag \neq 0$ then $a + cx + gx^2$ splits into two distinct factors giving two invariant straight lines intersecting at infinity, parallel to the y -axis. But the family $\mathbf{QSL}^{2\mathbf{P}}$ contains also the limit cases, i.e. when $c^2 - 4ag = 0$. If $g = 0$ and $c \neq 0$ (or $g = c = 0$), systems (3) possess only one (respectively do not possess any) invariant straight line in the direction $x = 0$. If $a = c = 0$ the y -axis $x = 0$ is a double affine line.

Theorem 1.1 ([10]). *Assume that a quadratic non-degenerate system (S) belongs to $\mathbf{QSL}^{2\mathbf{P}}$, then (S) possesses one of the 111 distinct configurations of invariant straight lines presented in Figures 1–4.*

In this theorem we mentioned that the 111 configuration are distinct. We need to specify when two configurations are to be considered as distinct or equivalently. We first introduce some notions.

Suppose we have an invariant straight line $l = ax + by + c = 0$, with $a, b, c \in \mathbb{R}$. Let $L = aX + bY + cZ = 0$ be its projective completion in the complex projective plane $\mathbb{P}_2(\mathbb{C})$.

Definition 1.6. *We call total curve $F(X, Y, Z) = 0$ of a configuration C of invariant straight lines with projective invariant straight lines $L_i = 0$, where $F = \prod L_i^{m_i} \prod Z^m$, m_i is the multiplicity of $L_i = 0$ and m is the multiplicity of $Z = 0$.*

Definition 1.7. *We say that two configurations C_1 and C_2 of invariant straight lines are equivalent if the following conditions are satisfied:*

- 1) *we have a bijection f from the set of invariant straight lines of C_1 to the set of invariant straight lines of C_2 ;*
- 2) *for each straight line L of C_1 we have a bijection r of the set of real singularities (finite and infinite) of L to the set of real singularities of $f(L)$, sending a finite (respectively infinite) singularity to a finite (respectively infinite) singularity and preserving their multiplicities;*
- 3) *each such map r conserves the multiplicity of the real singular points considered as simple or multiple singular points of the total curve $F = 0$.*

Our goals in this paper are:

- to find all phase portraits of the family $\mathbf{QSL}^{2\mathbf{P}}$;
- this classification should be done in the twelve parameters space \mathbb{R}^{12} independently of the normal forms the systems may be presented;
- to determine the bifurcation diagram of the phase portraits in the same space \mathbb{R}^{12} of the coefficients of systems.

Our main result in this paper is the following theorem:

Main Theorem. *The following statements hold:*

- (i) *The family $\mathbf{QSL}^{2\mathbf{P}}$ (as well as the family \mathbf{QS}_{Ric}) possesses a total of 119 topologically distinct phase portraits given in Figures 5 and 6.*
- (ii) *The topological classification is done using algebraic invariants and hence it is independent of the normal forms in which the systems may be presented.*
- (iii) *The bifurcation diagram of the phase portraits of systems in the family $\mathbf{QSL}^{2\mathbf{P}}$ is done in the twelve-dimensional parameter space \mathbb{R}^{12} and it is presented in Diagrams j for $j \in \{5, 6, 7, 8\}$. These diagrams give an algorithm to determine for any given system if it belongs or not to the family $\mathbf{QSL}^{2\mathbf{P}}$ and in case it belongs to this family, it gives the specific phase portrait.*

Remark 1.1. *Phase portraits for the quadratic Riccati family were given before in [13]. However this is the first time that a complete topological classification of this family was achieved. This family has numerous phase portraits and to be able to obtain a complete list of them we not only relied on the classical methods but also used modern ones, practically all methods for topologically classifying large families of quadratic systems available to us today. We give in the Appendix a critical review of [13] that also sums up all the methods we used in this work.*

The main tool we used for obtaining the global topological classification of this family was the geometry of the systems expressed in their 111 distinct configurations of invariant straight lines. The presence of the invariant straight lines was instrumental for obtaining most of the phase portraits. These configurations were obtained in [10] and are presented here in Figures i with $i \in \{1, 2, 3, 4\}$. We point out that this classification of configurations of the family \mathbf{QSL}^{2P} was done in [10] in terms of algebraic invariants and hence it is independent of the normal forms in which the systems may be presented. In [10] we also have the bifurcation diagrams of these configurations.

The main idea of the proof of our main theorem is first to pick a specific configuration and then follow the bifurcation diagram calculating the invariants that lead to the chosen configuration, and then calculating its resulting normal form. Once we have this normal form we calculate the phase portraits for that specific configuration by the usual classical method. Doing this for each one of the 111 configurations of invariant invariant straight lines we obtain all the phase portraits of the family \mathbf{QSL}^{2P} . We note that the splitting of this family into smaller families leading to normal forms for these subfamilies is done here according to the geometry of the systems and not in an arbitrary way, a fact that eliminates repeating calculations.

We also provide the bifurcation diagram of the phase portraits in the twelve-dimensional space \mathbb{R}^{12} . This diagram, done in terms of algebraic invariants is also an algorithm for deciding for any system given in any normal form if it is or not a Riccati system, and if it is then to provide with its phase portrait.

As we see both geometric and algebraic tools were used. But for some configurations more tools were needed. In the cases where there exist several potential phase portraits we needed to rely on papers (on structurally stable [2], codimension 1 systems [4] and a paper on codimension 2 systems [8]) that have studied the realizability of those potential phase portraits. We also had to check if these phase portraits were compatible or not with the geometric property expressed in the existence of invariant straight lines as in Riccati systems. This geometric property of the Riccati systems was instrumental in eliminating some of the potential phase portraits.

This paper thus relies on most of the diverse available techniques (geometric, algebraic, analytical and topological) in the *global* topological classifications of families of planar polynomial vector fields.

Our article is organized as follows: In Section 2 we exhibit the main polynomial invariants that intervene in this classification. In Section 3 we present some preliminary results involving the use of polynomial invariants, in particular we present the bifurcation diagram in the 12-dimensional space of the parameters, in terms of invariant polynomials of the configurations of the family \mathbf{QSL}^{2P} obtained in [10]. The actual calculation of the phase portraits of the Riccati systems is done in Section 4 which is split into 5 subsections.

2 The main invariant polynomials associated to the class \mathbf{QS}_{Ric}

Consider quadratic systems of the form (2). It is known that on the set \mathbf{QS} acts the group $Aff(2, \mathbb{R})$ of affine transformations on the plane (cf. [17]). For every subgroup $G \subseteq Aff(2, \mathbb{R})$

we have an induced action of G on \mathbf{QS} . We can identify the set \mathbf{QS} of systems (2) with a subset of \mathbb{R}^{12} via the map $\mathbf{QS} \rightarrow \mathbb{R}^{12}$ which associates to each system (2) the 12-tuple $\tilde{a} = (a, c, d, g, h, k, b, e, f, l, m, n)$ of its coefficients. We associate to this group action polynomials in x, y and parameters which behave well with respect to this action, the GL -comitants (GL -invariants), the T -comitants (affine invariants) and the CT -comitants. For their definitions as well as their detailed constructions we refer the reader to the paper [17] (see also [5]).

Next we define the following 40 invariant polynomials needed for the class \mathbf{QS}_{Ric} :

$$\left\{ \mu_0, \dots, \mu_4, \mathbf{D}, \mathbf{R}, \mathbf{U}, \eta, B_1, B_2, B_3, \widetilde{M}, C_2, \theta, \theta_3, \theta_5, \widetilde{K}, \widetilde{N}, \right. \\ \left. \widetilde{D}, H_1, H_3, \dots, H_{12}, H_{15}, H_{16}, D_1, N_1, N_2, N_5, N_6, \mathcal{G}_2, \mathcal{G}_3 \right\}. \quad (4)$$

According to [5] (see also [9]) we apply the differential operator $\mathcal{L} = x \cdot \mathbf{L}_2 - y \cdot \mathbf{L}_1$ acting on $\mathbb{R}[\tilde{a}, x, y]$ with

$$\mathbf{L}_1 = 2a \frac{\partial}{\partial c} + c \frac{\partial}{\partial g} + \frac{1}{2} d \frac{\partial}{\partial h} + 2b \frac{\partial}{\partial e} + e \frac{\partial}{\partial l} + \frac{1}{2} f \frac{\partial}{\partial m}, \\ \mathbf{L}_2 = 2a \frac{\partial}{\partial d} + d \frac{\partial}{\partial k} + \frac{1}{2} c \frac{\partial}{\partial h} + 2b \frac{\partial}{\partial f} + f \frac{\partial}{\partial n} + \frac{1}{2} e \frac{\partial}{\partial m},$$

to construct several invariant polynomials from the set (4). More precisely using this operator and the affine invariant $\mu_0 = \text{Res}_x(p_2(\tilde{a}, x, y), q_2(\tilde{a}, x, y))/y^4$ we construct the following polynomials

$$\mu_i(\tilde{a}, x, y) = \frac{1}{i!} \mathcal{L}^{(i)}(\mu_0), \quad i = 1, \dots, 4, \quad \text{where } \mathcal{L}^{(i)}(\mu_0) = \mathcal{L}(\mathcal{L}^{(i-1)}(\mu_0)).$$

Using these invariant polynomials we define some new ones, which according to [5] are responsible for the number and multiplicities of the finite singular points of (2):

$$\mathbf{D} = \left[3((\mu_3, \mu_3)^{(2)}, \mu_2)^{(2)} - (6\mu_0\mu_4 - 3\mu_1\mu_3 + \mu_2^2, \mu_4)^{(4)} \right] / 48, \\ \mathbf{P} = 12\mu_0\mu_4 - 3\mu_1\mu_3 + \mu_2^2, \\ \mathbf{R} = 3\mu_1^2 - 8\mu_0\mu_2, \\ \mathbf{S} = \mathbf{R}^2 - 16\mu_0^2\mathbf{P}, \\ \mathbf{T} = 18\mu_0^2(3\mu_3^2 - 8\mu_2\mu_4) + 2\mu_0(2\mu_2^3 - 9\mu_1\mu_2\mu_3 + 27\mu_1^2\mu_4) - \mathbf{P}\mathbf{R}, \\ \mathbf{U} = \mu_3^2 - 4\mu_2\mu_4.$$

In what follows we also need the so-called *transvectant of order k* (see [11], [15]) of two polynomials $f, g \in \mathbb{R}[\tilde{a}, x, y]$

$$(f, g)^{(k)} = \sum_{h=0}^k (-1)^h \binom{k}{h} \frac{\partial^k f}{\partial x^{k-h} \partial y^h} \frac{\partial^k g}{\partial x^h \partial y^{k-h}}.$$

In order to construct the remaining invariant polynomials contained in the set (4) we first need to define some elemental bricks which help us to construct these elements of the set.

We remark that the following polynomials in $\mathbb{R}[\tilde{a}, x, y]$ are the simplest invariant polynomials of degree one with respect to the coefficients of the differential systems (2) which are GL -comitants:

$$C_i(x, y) = yp_i(x, y) - xq_i(x, y), \quad i = 0, 1, 2; \\ D_i(x, y) = \frac{\partial}{\partial x} p_i(x, y) + \frac{\partial}{\partial y} q_i(x, y), \quad i = 1, 2.$$

Apart from these simple invariant polynomials we shall also make use of the following nine GL -invariant polynomials:

$$T_1 = (C_0, C_1)^{(1)}, \quad T_2 = (C_0, C_2)^{(1)}, \quad T_3 = (C_0, D_2)^{(1)}, \\ T_4 = (C_1, C_1)^{(2)}, \quad T_5 = (C_1, C_2)^{(1)}, \quad T_6 = (C_1, C_2)^{(2)}, \\ T_7 = (C_1, D_2)^{(1)}, \quad T_8 = (C_2, C_2)^{(2)}, \quad T_9 = (C_2, D_2)^{(1)}.$$

These are of degree two with respect to the coefficients of systems (2).

We next define a list of T -comitants:

$$\begin{aligned}
\hat{A}(\tilde{a}) &= (C_1, T_8 - 2T_9 + D_2^2)^{(2)}/144, \\
\hat{B}(\tilde{a}, x, y) &= \left\{ 16D_1(D_2, T_8)^{(1)}(3C_1D_1 - 2C_0D_2 + 4T_2) + 32C_0(D_2, T_9)^{(1)}(3D_1D_2 \right. \\
&\quad - 5T_6 + 9T_7) + 2(D_2, T_9)^{(1)}(27C_1T_4 - 18C_1D_1^2 - 32D_1T_2 + 32(C_0, T_5)^{(1)}) \\
&\quad + 6(D_2, T_7)^{(1)}[8C_0(T_8 - 12T_9) - 12C_1(D_1D_2 + T_7) + D_1(26C_2D_1 + 32T_5) \\
&\quad + C_2(9T_4 + 96T_3)] + 6(D_2, T_6)^{(1)}[32C_0T_9 - C_1(12T_7 + 52D_1D_2) \\
&\quad - 32C_2D_1^2] + 48D_2(D_2, T_1)^{(1)}(2D_2^2 - T_8) + 6D_1D_2T_4(T_8 - 7D_2^2 - 42T_9) \\
&\quad - 32D_1T_8(D_2, T_2)^{(1)} + 9D_2^2T_4(T_6 - 2T_7) - 16D_1(C_2, T_8)^{(1)}(D_1^2 + 4T_3) \\
&\quad + 12D_1(C_1, T_8)^{(2)}(C_1D_2 - 2C_2D_1) + 12D_1(C_1, T_8)^{(1)}(T_7 + 2D_1D_2) \\
&\quad + 96D_2^2[D_1(C_1, T_6t)^{(1)} + D_2(C_0, T_6)^{(1)}] - 4D_1^3D_2(D_2^2 + 3T_8 + 6T_9) \\
&\quad \left. - 16D_1D_2T_3(2D_2^2 + 3T_8) + 6D_1^2D_2^2(7T_6 + 2T_7) - 252D_1D_2T_4T_9 \right\} / (2^8 3^3), \\
\hat{D}(\tilde{a}, x, y) &= [2C_0(T_8 - 8T_9 - 2D_2^2) + C_1(6T_7 - T_6) - (C_1, T_5)^{(1)} - 9D_1^2C_2 \\
&\quad + 6D_1(C_1D_2 - T_5)]/36, \\
\hat{E}(\tilde{a}, x, y) &= [D_1(2T_9 - T_8) - 3(C_1, T_9)^{(1)} - D_2(3T_7 + D_1D_2)]/72, \\
\hat{F}(\tilde{a}, x, y) &= [6D_1^2(D_2^2 - 4T_9) + 4D_1D_2(T_6 + 6T_7) + 48C_0(D_2, T_9)^{(1)} - 9D_2^2T_4 \\
&\quad + 288D_1\hat{E} - 24(C_2, \hat{D})^{(2)} + 120(D_2, \hat{D})^{(1)} - 36C_1(D_2, T_7)^{(1)} \\
&\quad + 8D_1(D_2, T_5)^{(1)}]/144, \\
\hat{K}(\tilde{a}, x, y) &= (T_8 + 4T_9 + 4D_2^2)/72, \\
\hat{H}(\tilde{a}, x, y) &= (-T_8 + 8T_9 + 2D_2^2)/72,
\end{aligned}$$

as well as the needed bricks:

$$\begin{aligned}
A_2(\tilde{a}) &= (C_2, \hat{D})^{(3)}/12, & A_8(\tilde{a}) &= ((\hat{D}, \hat{H})^{(2)}, D_2)^{(1)}/8, \\
A_{11}(\tilde{a}) &= (\hat{F}, \hat{K})^{(2)}/4, & A_{20}(\tilde{a}) &= ((C_2, \hat{D})^{(2)}, \hat{F})^{(2)}/16, \\
A_{21}(\tilde{a}) &= ((\hat{D}, \hat{D})^{(2)}, \hat{K})^{(2)}/16, & A_{39}(\tilde{a}) &= (((\hat{D}, \hat{D})^{(2)}, \hat{F})^{(1)}, \hat{H})^{(2)}/64, \\
A_{42}(\tilde{a}) &= (((\hat{D}, \hat{F})^{(2)}, \hat{F})^{(1)}, D_2)^{(1)}/16.
\end{aligned}$$

Now we can define the remaining invariant polynomials of the set (4):

$$\begin{aligned}
\tilde{K}(\tilde{a}, x, y) &= 4\hat{K} \equiv \text{Jacob}(p_2(\tilde{a}, x, y), q_2(\tilde{a}, x, y)), \\
\tilde{M}(\tilde{a}, x, y) &= (C_2, C_2)^{(2)} \equiv 2\text{Hess}(C_2(\tilde{a}, x, y)), \\
\tilde{N}(\tilde{a}, x, y) &= \tilde{K} - 4\hat{H}, \\
\eta(\tilde{a}) &= (\tilde{M}, \tilde{M})^{(2)}/384 \equiv \text{Discrim}(C_2(\tilde{a}, x, y)), \\
\theta(\tilde{a}) &= -(\tilde{N}, \tilde{N})^{(2)}/2 \equiv \text{Discrim}(\tilde{N}(\tilde{a}, x, y)); \\
\theta_3(\tilde{a}) &= A_8 + A_{11}, \\
B_1(\tilde{a}) &= \text{Res}_x(C_2, \tilde{D})/y^9 = -2^{-9}3^{-8}(B_2, B_3)^{(4)}, \\
B_2(\tilde{a}, x, y) &= (B_3, B_3)^{(2)} - 6B_3(C_2, \tilde{D})^{(3)}, \\
B_3(\tilde{a}, x, y) &= (C_2, \tilde{D})^{(1)} \equiv \text{Jacob}(C_2, \tilde{D}),
\end{aligned}$$

$$\begin{aligned}
H_1(\tilde{a}) &= -((C_2, C_2)^{(2)}, C_2)^{(1)}, D)^{(3)}, \\
H_3(\tilde{a}, x, y) &= (C_2, D)^{(2)}, \\
H_4(\tilde{a}) &= ((C_2, D)^{(2)}, (C_2, D_2)^{(1)})^{(2)}, \\
H_5(\tilde{a}) &= ((C_2, C_2)^{(2)}, (D, D)^{(2)})^{(2)} + 8((C_2, D)^{(2)}, (D, D_2)^{(1)})^{(2)}, \\
H_6(\tilde{a}, x, y) &= 16N^2(C_2, D)^{(2)} + H_2^2(C_2, C_2)^{(2)}, \\
H_7(\tilde{a}) &= (\tilde{N}, C_1)^{(2)}, \\
H_8(\tilde{a}) &= 9((C_2, D)^{(2)}, (D, D_2)^{(1)})^{(2)} + 2[(C_2, D)^{(3)}]^2, \\
H_9(\tilde{a}) &= -(((\tilde{D}, \tilde{D})^{(2)}, \tilde{D})^{(1)}, \tilde{D})^{(3)}, \\
H_{10}(\tilde{a}) &= ((\tilde{N}, \tilde{D})^{(2)}, D_2)^{(1)}, \\
H_{11}(\tilde{a}, x, y) &= 8\hat{H}[(C_2, \tilde{D})^{(2)} + 8(\tilde{D}, D_2)^{(1)}] + 3[(C_1, 2\hat{H} - \tilde{N})^{(1)} - 2D_1\tilde{N}]^2, \\
H_{12}(\tilde{a}, x, y) &= (\tilde{D}, \tilde{D})^{(2)} \equiv \text{Hessian}(\tilde{D}), \\
H_{15}(\tilde{a}) &= ((\tilde{D}, \tilde{D})^{(2)}, -4\hat{H})^{(2)}, \\
H_{16}(\tilde{a}) &= 14A_2^4 - A_2^2(10A_{20} + 33A_{21}) - 2A_2(15A_{39} + A_{42}), \\
\mathcal{G}_2(\tilde{a}) &= 8H_8 - 9H_5, \\
\mathcal{G}_3(\tilde{a}) &= (\mu_0 - \eta)H_1 - 6\eta(H_4 + 12H_{10}).
\end{aligned}$$

We remark that the above invariant polynomials were constructed and used in [7, 20, 21].

3 Preliminary results involving the use of polynomial invariants

The following two lemmas reveal the geometrical meaning of the invariant polynomials B_1 , B_2 , B_3 , θ and \tilde{N} .

Lemma 3.1 ([16]). *For the existence of an invariant straight line in one (respectively 2; 3 distinct) directions in the affine plane it is necessary that $B_1 = 0$ (respectively $B_2 = 0$; $B_3 = 0$).*

Lemma 3.2 ([16]). *A necessary condition for the existence of one couple (respectively, two couples) of parallel invariant straight lines of a system (2) corresponding to $\mathbf{a} \in \mathbb{R}^{12}$ is the condition $\theta(\mathbf{a}) = 0$ (respectively, $\tilde{N}(\mathbf{a}, x, y) = 0$).*

We remark that the invariant polynomials $\mu_i(\tilde{a}, x, y)$ ($i = 0, 1, \dots, 4$) defined earlier are responsible for the total multiplicity of the finite singularities of quadratic systems (2). Moreover they detect whether a quadratic system is degenerate or not. More exactly, according to [9] (see also [5] we have the following lemma.

Lemma 3.3. *Consider a quadratic system (S) with coefficients $\mathbf{a} \in \mathbb{R}^{12}$. Then:*

- (i) *The total multiplicity of the finite singularities of this system is $4 - k$ if and only if for every i such that $0 \leq i \leq k - 1$ we have $\mu_i(\mathbf{a}, x, y) = 0$ in $\mathbb{R}[x, y]$ and $\mu_k(\mathbf{a}, x, y) \neq 0$.*
- (ii) *The system (S) is degenerate (i.e. $\gcd(p, q) \neq \text{constant}$) if and only if $\mu_i(\mathbf{a}, x, y) = 0$ in $\mathbb{R}[x, y]$ for every $i = 0, 1, 2, 3, 4$.*

On the other hand the invariant polynomials η , \tilde{M} and C_2 govern the number of real and complex infinite singularities. More precisely, according to [24] (see also [17]) we have the next result.

Lemma 3.4. *The number of infinite singularities (real and complex) of a quadratic system in QS is determined by the following conditions:*

- (i) 3 real if $\eta > 0$;
- (ii) 1 real and 2 imaginary if $\eta < 0$;
- (iii) 2 real if $\eta = 0$ and $\widetilde{M} \neq 0$;
- (iv) 1 real if $\eta = \widetilde{M} = 0$ and $C_2 \neq 0$;
- (v) ∞ if $\eta = \widetilde{M} = C_2 = 0$.

Moreover, the quadratic systems (2), for each one of these cases, can be brought via a linear transformation to the corresponding case of the following canonical systems $(\mathbf{S}_I) - (\mathbf{S}_V)$:

$$\begin{cases} \dot{x} &= a + cx + dy + gx^2 + (h-1)xy, \\ \dot{y} &= b + ex + fy + (g-1)xy + hy^2; \end{cases} \quad (\mathbf{S}_I)$$

$$\begin{cases} \dot{x} &= a + cx + dy + gx^2 + (h+1)xy, \\ \dot{y} &= b + ex + fy - x^2 + gxy + hy^2; \end{cases} \quad (\mathbf{S}_{II})$$

$$\begin{cases} \dot{x} &= a + cx + dy + gx^2 + hxy, \\ \dot{y} &= b + ex + fy + (g-1)xy + hy^2; \end{cases} \quad (\mathbf{S}_{III})$$

$$\begin{cases} \dot{x} &= a + cx + dy + gx^2 + hxy, \\ \dot{y} &= b + ex + fy - x^2 + gxy + hy^2; \end{cases} \quad (\mathbf{S}_{IV})$$

$$\begin{cases} \dot{x} &= a + cx + dy + x^2, \\ \dot{y} &= b + ex + fy + xy. \end{cases} \quad (\mathbf{S}_V)$$

Now we define the affine comitants which are responsible for the existence of invariant lines for a non-degenerate quadratic system (2).

Let us apply a translation $x = x' + x_0$, $y = y' + y_0$ to the polynomials $p(\tilde{a}, x, y)$ and $q(\tilde{a}, x, y)$. We obtain $\hat{p}(\hat{a}(\tilde{a}, x_0, y_0), x', y') = p(\tilde{a}, x' + x_0, y' + y_0)$, $\hat{q}(\hat{a}(\tilde{a}, x_0, y_0), x', y') = q(\tilde{a}, x' + x_0, y' + y_0)$. Let us construct the following polynomials

$$\Gamma_i(\tilde{a}, x_0, y_0) \equiv \text{Res}_{x'} \left(C_i(\hat{a}(\tilde{a}, x_0, y_0), x', y'), C_0(\hat{a}(\tilde{a}, x_0, y_0), x', y') \right) / (y')^{i+1},$$

$$\Gamma_i(\tilde{a}, x_0, y_0) \in \mathbb{R}[\tilde{a}, x_0, y_0], \quad (i = 1, 2).$$

Notation 3.1.

$$\tilde{\mathcal{E}}_i(\tilde{a}, x, y) = \Gamma_i(\tilde{a}, x_0, y_0)|_{\{x_0=x, y_0=y\}} \in \mathbb{R}[\tilde{a}, x, y] \quad (i = 1, 2). \quad (5)$$

Observation 3.1. We note that the polynomials $\tilde{\mathcal{E}}_1(\tilde{a}, x, y)$ and $\tilde{\mathcal{E}}_2(\tilde{a}, x, y)$ thus constructed are affine comitants of systems (2) and are homogeneous polynomials in the coefficients a, \dots, n and non-homogeneous in x, y and

$$\deg_{\tilde{a}} \tilde{\mathcal{E}}_1 = 3, \quad \deg_{(x,y)} \tilde{\mathcal{E}}_1 = 5, \quad \deg_{\tilde{a}} \tilde{\mathcal{E}}_2 = 4, \quad \deg_{(x,y)} \tilde{\mathcal{E}}_2 = 6.$$

Notation 3.2. Let $\mathcal{E}_i(\tilde{a}, X, Y, Z)$ ($i = 1, 2$) be the homogenization of $\tilde{\mathcal{E}}_i(\tilde{a}, x, y)$, i.e.

$$\mathcal{E}_1(\tilde{a}, X, Y, Z) = Z^5 \tilde{\mathcal{E}}_1(\tilde{a}, X/Z, Y/Z), \quad \mathcal{E}_2(\tilde{a}, X, Y, Z) = Z^6 \tilde{\mathcal{E}}_2(\tilde{a}, X/Z, Y/Z)$$

and $\mathcal{H}(\tilde{a}, X, Y, Z) = \text{gcd} \left(\mathcal{E}_1(\tilde{a}, X, Y, Z), \mathcal{E}_2(\tilde{a}, X, Y, Z) \right)$ in $\mathbb{R}[\tilde{a}, X, Y, Z]$.

The geometrical meaning of these affine comitants is given by the two following lemmas (see [16]):

Lemma 3.5. *The straight line $\mathcal{L}(x, y) \equiv ux + vy + w = 0$, $u, v, w \in \mathbb{C}$, $(u, v) \neq (0, 0)$ is an invariant line for a quadratic system (2) if and only if the polynomial $\mathcal{L}(x, y)$ is a common factor of the polynomials $\tilde{\mathcal{E}}_1(\mathbf{a}, x, y)$ and $\tilde{\mathcal{E}}_2(\mathbf{a}, x, y)$ over \mathbb{C} , i.e.*

$$\tilde{\mathcal{E}}_i(\mathbf{a}, x, y) = (ux + vy + w)\tilde{W}_i(x, y) \quad (i = 1, 2),$$

where $\tilde{W}_i(x, y) \in \mathbb{C}[x, y]$.

Lemma 3.6. *1) If $\mathcal{L}(x, y) \equiv ux + vy + w = 0$, $u, v, w \in \mathbb{C}$, $(u, v) \neq (0, 0)$ is an invariant straight line of multiplicity k for a quadratic system (2) corresponding to a point $\mathbf{a} \in \mathbb{R}^{12}$ then $\mathcal{L}(x, y)^k \mid \gcd(\tilde{\mathcal{E}}_1, \tilde{\mathcal{E}}_2)$ in $\mathbb{C}[x, y]$, i.e. there exist $W_i(\mathbf{a}, x, y) \in \mathbb{C}[x, y]$ ($i = 1, 2$) such that*

$$\tilde{\mathcal{E}}_i(\mathbf{a}, x, y) = (ux + vy + w)^k W_i(\mathbf{a}, x, y), \quad i = 1, 2. \quad (6)$$

2) If the line $l_\infty : Z = 0$ is of multiplicity $k > 1$ then $Z^{k-1} \mid \gcd(\mathcal{E}_1, \mathcal{E}_2)$, in other words we have $Z^{k-1} \mid \mathcal{H}(\mathbf{a}, X, Y, Z)$.

In [10] the classification of the family \mathbf{QSL}^{2P} of quadratic differential systems possessing two parallel invariant affine lines according to their configurations of invariant lines is given. Since the family \mathbf{QS}_{Ric} of quadratic Riccati systems is a subfamily of \mathbf{QSL}^{2P} it is clear that this classification is a very useful one in order to classify topologically the family \mathbf{QS}_{Ric} .

We mention that in [10, see Theorem 5.1] the authors determined the necessary and sufficient conditions for an arbitrary non-degenerate quadratic system to belong to the family \mathbf{QSL}^{2P} . We have the following lemma.

Lemma 3.7. *An arbitrary quadratic system (2) belongs to the class \mathbf{QSL}^{2P} if and only if $\theta = B_1 = H_7 = 0$ and one of the following conditions is satisfied:*

- (i) *If $\eta > 0$ then either $\tilde{N} \neq 0$, or $\tilde{N} = 0$, $\theta_3 = 0$.*
- (ii) *If $\eta < 0$ then $\tilde{N} \neq 0$.*
- (iii) *If $\eta = 0$, $\tilde{M} \neq 0$ then either $\tilde{N} \neq 0$, or $\tilde{N} = 0$, $\tilde{K} \neq 0$, $\theta_3 = 0$, or $\tilde{N} = \tilde{K} = 0$, $B_2 \neq 0$, $\theta_5 = 0$, or $\tilde{N} = \tilde{K} = B_2 = 0$.*
- (iv) *If $\eta = \tilde{M} = 0$, $C_2 \neq 0$ then either $\tilde{N} \neq 0$, or $\tilde{N} = B_2 = 0$.*
- (v) *If $\eta = \tilde{M} = C_2 = 0$.*

Remark 3.1. *We point out that in the statement (iv) of the above lemma (which is the same as in [10, see Theorem 5.1]) it is claimed that in the case $\tilde{N} = 0$ the condition $B_2 = 0$ is necessary for a quadratic system to be in the class \mathbf{QSL}^{2P} . However this condition was omitted in Diagram 4 of [10]. Here we presented Diagrams 1 to 4 given in [10] but with the correction to Diagram 4 by addition of the corresponding branch.*

According to [10, see Theorem 6.1] the next theorem describes all the configurations which could have systems in \mathbf{QSL}^{2P} as well as the corresponding invariant criteria for their realization.

Theorem 3.1. *If a quadratic non-degenerate system (S) belongs to the class of systems \mathbf{QSL}^{2P} , then this system possesses one of the configurations of invariant lines indicated below if and only if the corresponding conditions are satisfied respectively:*

- (i) *For $\eta > 0$ the system (S) possesses one of the configurations given in Figure 1 if and only if one of the sets of conditions given in the Diagram 1 is satisfied, correspondingly.*
- (ii) *For $\eta < 0$ the system (S) possesses one of the configurations given in Figure 2 if and only if the one of the sets of conditions given in the Diagram 2 is satisfied, correspondingly.*

- (iii) For $\eta = 0$ and $\widetilde{M} \neq 0$ the system (S) possesses one of the configurations given in Figure 3 if and only if one of the sets of conditions given in the Diagram 3 is satisfied, correspondingly.
- (iv) For $\eta = \widetilde{M} = 0$ the system (S) possesses one of the configurations given in Figure 4 if and only if one of the sets of conditions given in the Diagram 4 is satisfied, correspondingly.

4 Phase portraits of the Riccati systems

Theorem 4.1. *If a quadratic system (S) belongs to the class of Riccati systems \mathbf{QS}_{Ric} , then system (S) possesses one of the following phase portraits if and only if the corresponding conditions are satisfied respectively:*

- (i) For $\eta > 0$ a non-degenerate (respectively, degenerate) system (S) possesses one of the phase portraits Ric. 1–Ric. 27 (respectively, Ric. D_1 –Ric. D_3) given in Figure 5 (respectively, Figure 6) if and only if one of the sets of conditions given in Diagram 5 is satisfied, correspondingly.
- (ii) For $\eta < 0$ a non-degenerate (respectively, degenerate) system (S) possesses one of the phase portraits Ric. 28–Ric. 35 (respectively, Ric. D_4 , Ric. 28d and Ric. 35d) if and only if one of the sets of conditions given in Diagram 6 is satisfied, correspondingly. The phase portraits Ric. 28–Ric. 35 (respectively, Ric. D_4) are given in Figure 5 (respectively, Figure 6), whereas Ric. 28d and Ric. 35d are topologically equivalent to Ric. 28 and Ric. 35, correspondingly.
- (iii) For $\eta = 0$ and $\widetilde{M} \neq 0$ a non-degenerate (respectively, degenerate) system (S) possesses one of the phase portraits Ric. 36–Ric. 76 (respectively, Ric. D_5 –Ric. D_{18} and Ric. 53d) if and only if one of the sets of conditions given in Diagram 7 is satisfied, correspondingly. The phase portraits Ric. 36–Ric. 76 (respectively, Ric. D_5 –Ric. D_{18}) are given in Figure 5 (respectively, Figure 6), whereas Ric. 53d is topologically equivalent to Ric. 53.
- (iv) For $\eta = \widetilde{M} = 0$ a non-degenerate (respectively, degenerate) system (S) possesses one of the phase portraits Ric. 28 and Ric. 77–Ric. 93 (respectively, Ric. D_{19} –Ric. D_{26} and Ric. 28d) if and only if one of the sets of conditions given in Diagram 8 is satisfied, correspondingly. The phase portraits Ric. 28 and Ric. 77–Ric. 93 (respectively, Ric. D_{19} –Ric. D_{26}) are given in Figure 5 (respectively, Figure 6), whereas Ric. 28d is topologically equivalent to Ric. 28.

Proof of Theorem 4.1: First of all we prove the following lemma.

Lemma 4.1. *Consider an arbitrary quadratic system (2) and assume that its phase portrait possesses a separatrix connection between two singularities p_1 and p_2 at least one of them being finite. Suppose that this connection is not part of an invariant straight line. Then inside the region R bordered by this separatrix and the segment $\overline{p_1 p_2}$ there necessarily exists either one singularity or at least one of the points p_1 or p_2 is a non-elemental singularity which is α – (or ω –) limit for orbits that reach the singular point inside the region R .*

Proof: According to [3, Lemma 3.4] (see also [26]) if a straight line in a quadratic system passes through two finite singularities p_1 and p_2 then either this straight line is invariant or the trajectories of the flow cross the segment $\overline{p_1 p_2}$ in opposite direction as they cross the half lines $\overline{\infty p_1}$ and $\overline{p_2 \infty}$.

On the other hand by Lemma [3, Lemma 3.5] (see also [26]) the straight line connecting one finite singular point and a couple of infinite singular points in a quadratic system is either

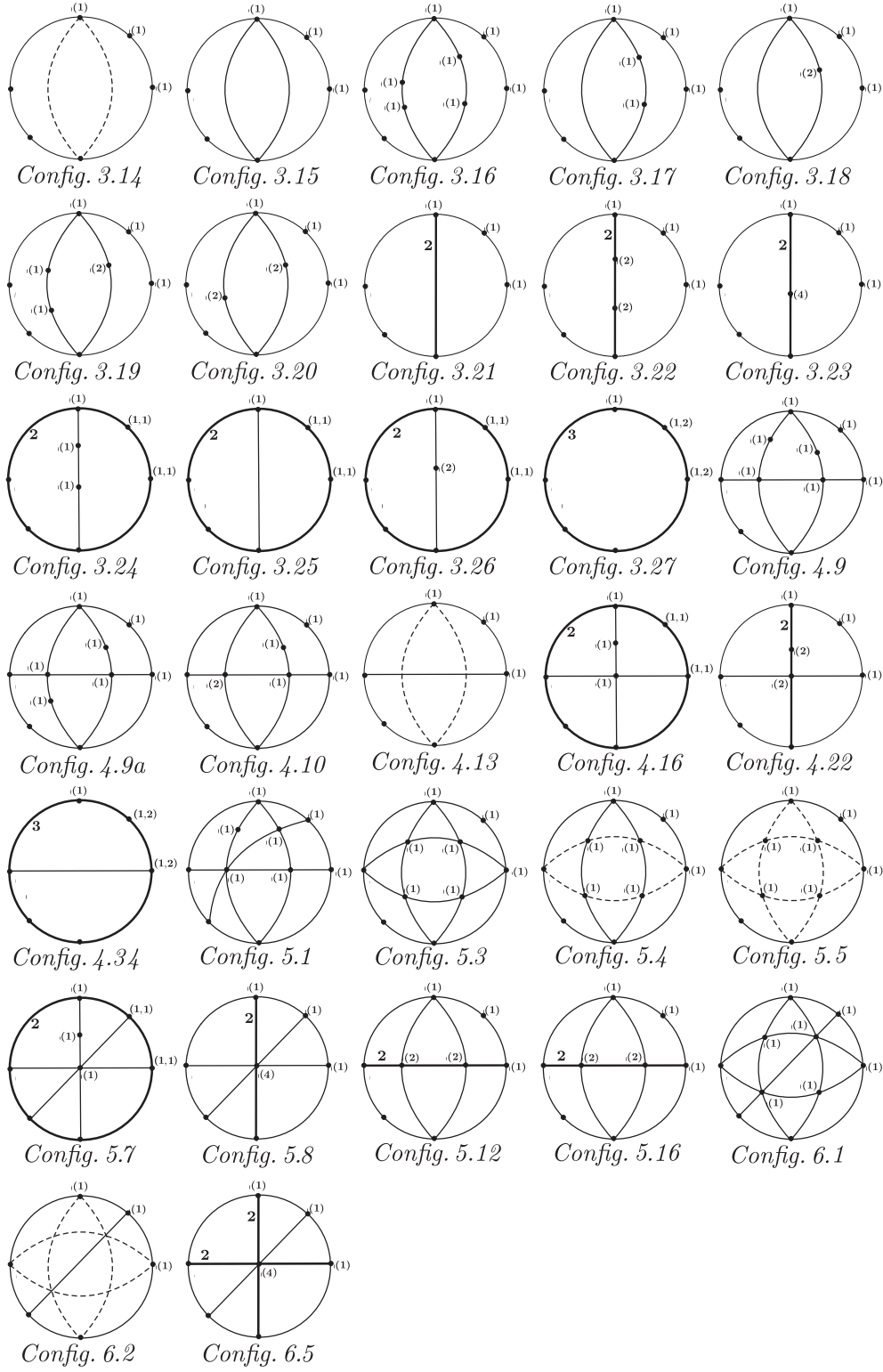


Figure 1: The configurations of quadratic systems in $\mathbf{QSL}^{2\mathbf{P}}$ (case $\eta > 0$)

formed by trajectories or it is a line with exactly one contact point. This contact point is the finite singularity. For the latter case the flow goes in different directions on each half line.

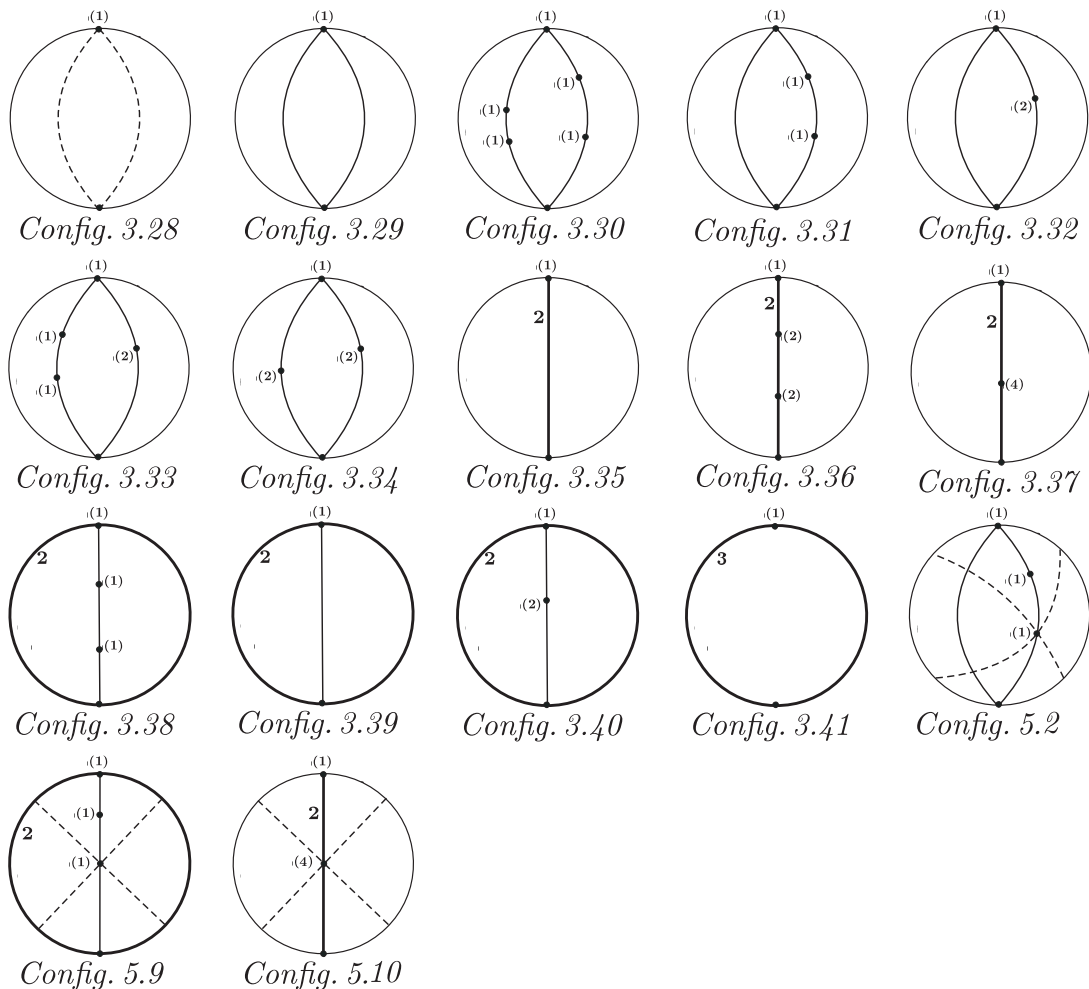


Figure 2: The configurations of quadratic systems in \mathbf{QSL}^{2P} (case $\eta < 0$)

An orbit passing through a point inside R can neither have its α - nor ω -limit inside the closure \bar{R} of R . Thus the orbits must come from outside \bar{R} and proceed by going out of it, forcing then the existence of at least one contact point on the segment $\overline{p_1 p_2}$ which contradicts Lemma 3.4 (or Lemma 3.5) from [3]. \blacksquare

Corollary 4.1. *If the phase portrait of a quadratic system possesses a separatrix connection between two singularities p_1 and p_2 at least one of them being finite and the region R is defined like in previous lemma and does not contain the required elements imposed by Lemma 4.1 then the region R is empty and the separatrix connection is part of an invariant straight line.*

Remark 4.1. *We point out that Section 4.5 is dedicated to degenerate Riccati systems. According to Lemma 5.2 (iii) from [5] a quadratic system is degenerate if and only if the conditions $\mu_i = 0$ for all $i \in \{0, 1, 2, 3, 4\}$ are fulfilled. So in what follows up to Section 4.5 we consider that systems in \mathbf{QS}_{Ric} are non-degenerate, i.e. at least one of the polynomials μ_i , $i \in \{0, 1, 2, 3, 4\}$ does not vanish.*

Following Theorem 3.1 we consider the cases given by the following three invariant polynomials: η , \widetilde{M} and C_2 .

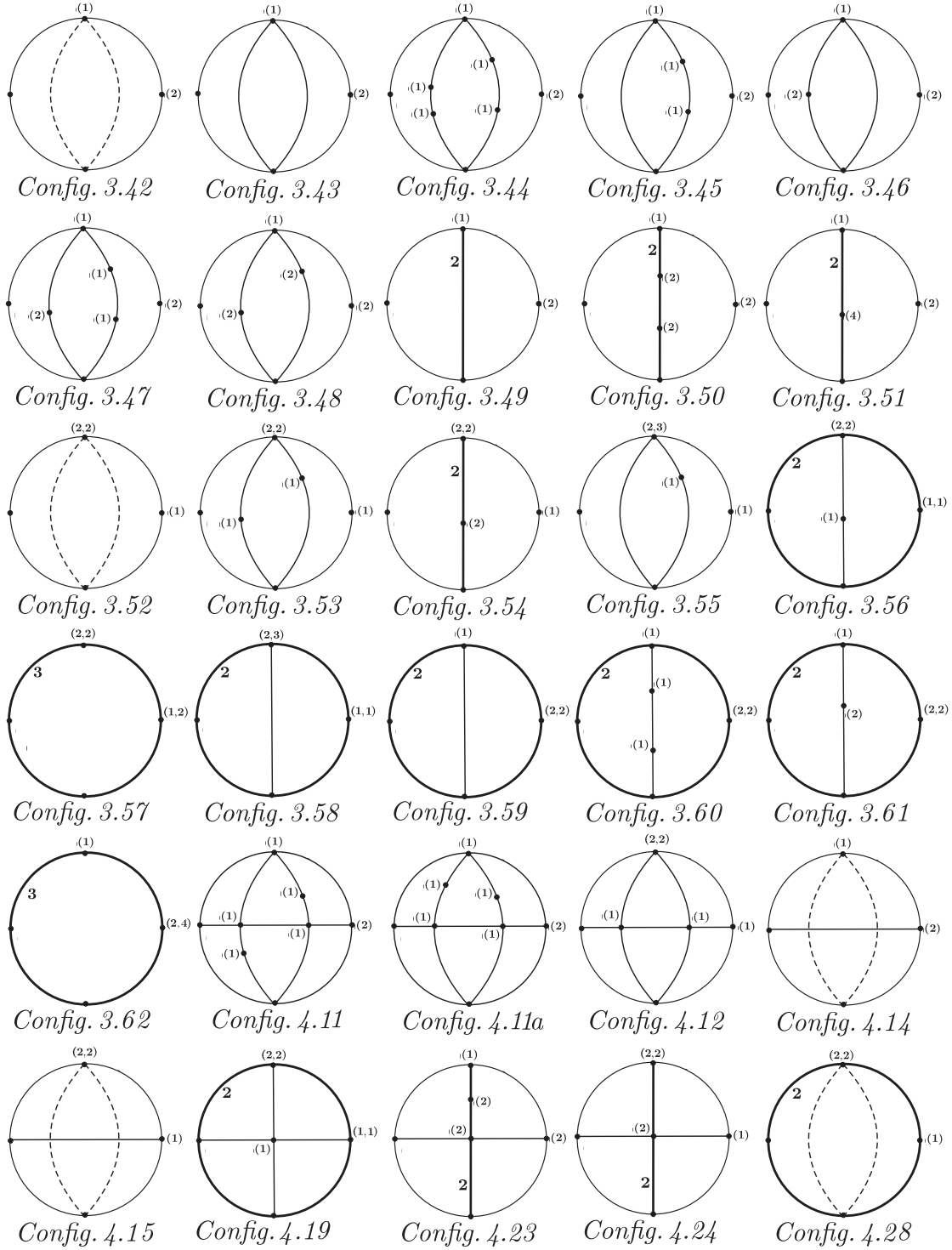


Figure 3: The configurations of quadratic systems in \mathbf{QSL}^{2P} (case $\eta = 0 \neq \widetilde{M}$)

4.1 The case $\eta > 0$

According to the Diagram 1 we examine two subcases: $\widetilde{N} \neq 0$ and $\widetilde{N} = 0$.

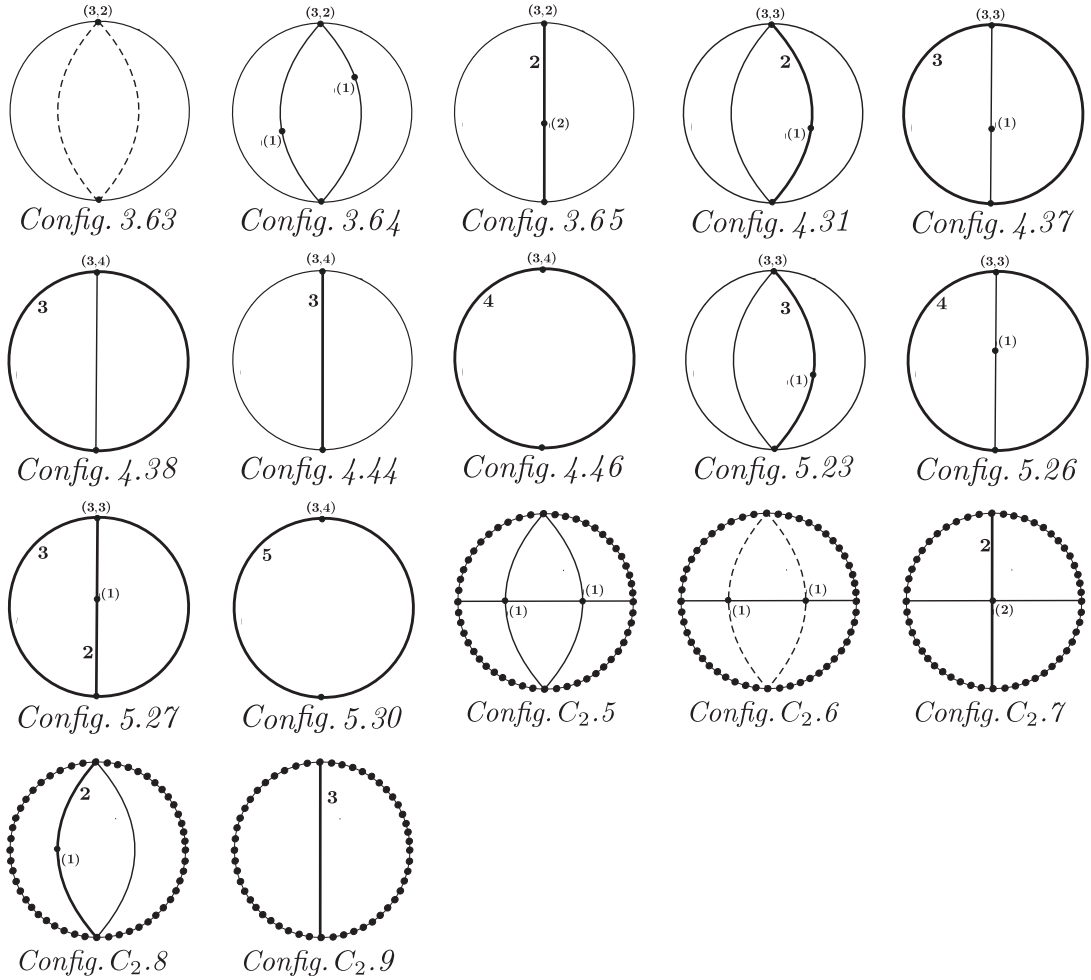


Figure 4: The configurations of quadratic systems in \mathbf{QSL}^{2P} (case $\eta = \widetilde{M} = 0$)

We observe that for these systems $\mu_0 = g^2 \geq 0$ and since $\eta > 0$ considering [7] (see Diagram 1 on the page 36) we have the next remark.

Remark 4.2. *In the case $\mu_0 \neq 0$ (then $\mu_0 > 0$) systems (8) possess at infinity one saddle and two nodes, all elemental.*

Since by Lemma 3.1 the condition $B_2 = 0$ is necessary for the existence of invariant lines at least in two directions, we consider two possibilities: $B_2 = 0$ and $B_2 \neq 0$. Even if in the Diagram 1 the case $B_2 = 0$ follows after $B_2 \neq 0$ we begin here with $B_2 = 0$. Our motivation is because in the case $B_2 = 0$ the systems belong to a higher codimension subfamilies and these subfamilies form an skeleton from which the systems with $B_2 \neq 0$ will bifurcate.

4.1.1.1 The possibility $B_2 = 0$. According to Diagram 1 we examine two cases: $B_3 \neq 0$ and $B_3 = 0$.

4.1.1.1.1 The case $B_3 \neq 0$. Then by Lemma 3.1 we could not have invariant lines in three directions and we examine the corresponding cases provided by Diagram 1. Following this diagram we consider each one of the configurations of invariant lines in order to determine how many topological phase portraits could be obtained from each one of the configurations.

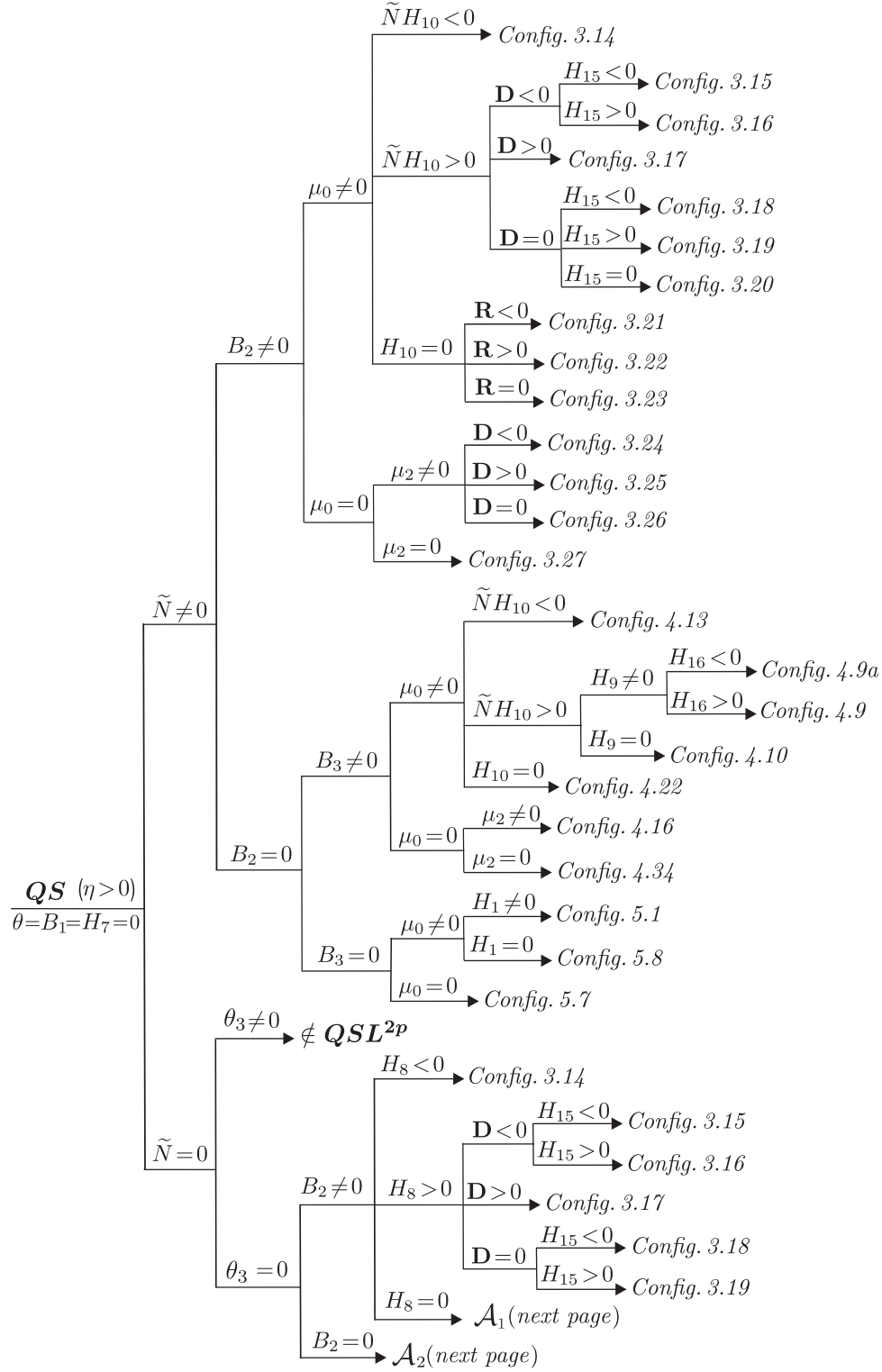


Diagram 1: The invariant criteria for configurations of systems in QSL^{2p} (case $\eta > 0$)

1: $\mu_0 \neq 0, \tilde{N}H_{10} < 0 \Rightarrow \text{Config. 4.13}$. Since we are in the class of quadratic systems possessing invariant lines of total multiplicity 4 we shall use the classification given in [21]. According to this classification the configuration *Config. 4.13* leads to the two phase portraits: *Portrait 4.13(a)*

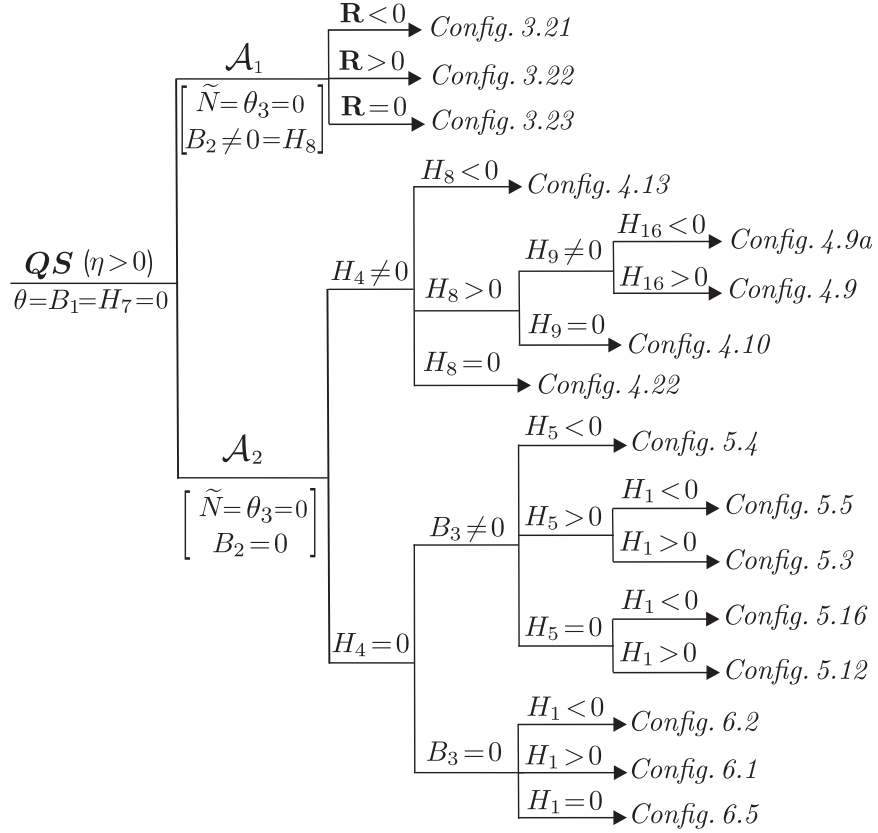


Diagram 1 (*continued*): The invariant criteria for configurations of systems in \mathbf{QSL}^{2p} (case $\eta > 0$)

and *Portrait 4.13(b)*. However we have detected an inexactitude concerning these two phase portraits. More exactly we have the next remark.

Remark 4.3. *In Table 2 [21, page 55] it is claimed that in the case $\tilde{N} \neq 0$ we have *Portrait 4.13(a)* if $\mathcal{G}_2 < 0$ and *Portrait 4.13(b)* if $\mathcal{G}_2 > 0$. On the other hand in the proof of the Main Theorem (see page 68) we find an opposite affirmation, i.e. we have *Portrait 4.13(a)* if $\mathcal{G}_2 > 0$ and *Portrait 4.13(b)* if $\mathcal{G}_2 < 0$. This is correct and in Table 2 the conditions $\mathcal{G}_2 < 0$ and $\mathcal{G}_2 > 0$ from the 3rd column and 1st and 2nd lines, respectively, must be interchanged.*

We denote the phase portraits *Portrait 4.13(b)* and *Portrait 4.13(a)* by *Ric. 1* and *Ric. 2*.

For each branch of the Diagrams 1 to 4 for the configurations of the family \mathbf{QSL}^{2p} leading to a specific configuration we find the phase portraits of the systems having that configuration of invariant lines and complete these diagrams by adding the branch of these various phase portraits. Many of these phase portraits have been encountered before in the papers on $\mathbf{QSL}_{\geq 3}$. Since this paper is the first one that has the complete topological classification of Riccati systems, we denote a phase portrait of the Riccati family by *Ric. i* starting with the two phase portraits *Ric. 1* and *Ric. 2* just introduced here above and of course taking care not to repeat anyone of these phase portrait in this list.

Thus considering Remark 4.3 we get *Ric. 1* if $\mathcal{G}_2 < 0$ and *Ric. 2* if $\mathcal{G}_2 > 0$.

2: $\mu_0 \neq 0, \tilde{N}H_{10} > 0, H_9 \neq 0$ and either (i) $H_{16} < 0 \Rightarrow \text{Config. } 4.9a$ or (ii) $H_{16} > 0 \Rightarrow \text{Config. } 4.9$. We examine these two cases together because in the paper [21] (as well as in [18]) there is omitted the configuration *Config. 4.9a*. This mistake was corrected in [10] (see Remark 6.2 and Lemma 6.1) where a new invariant polynomial H_{16} was defined. This invariant

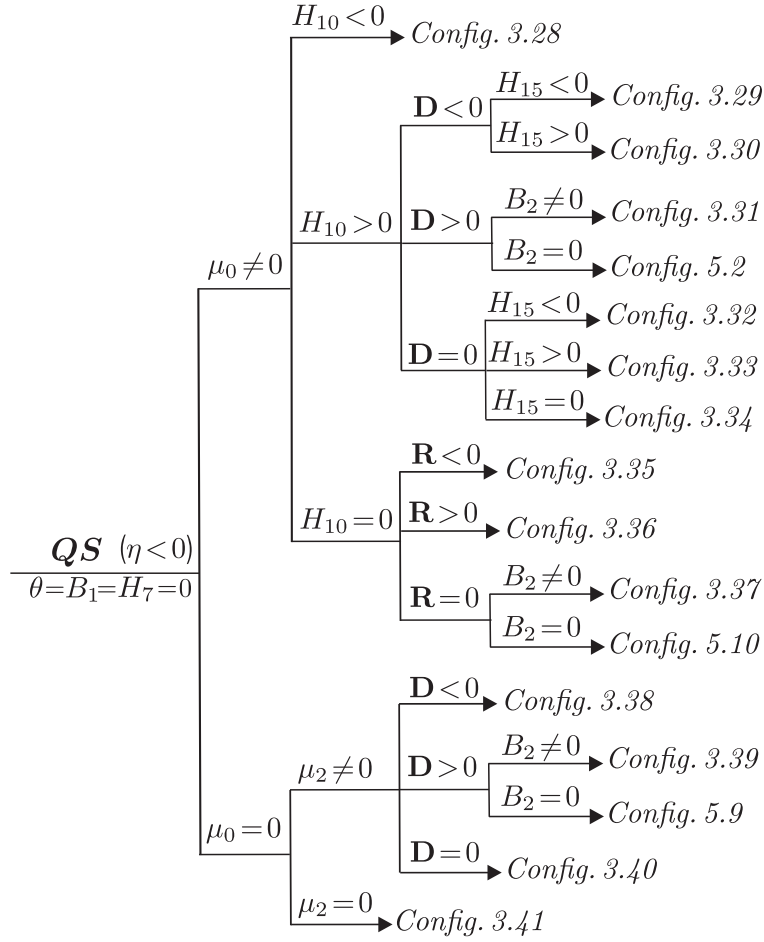


Diagram 2: The invariant criteria for configurations of systems in QSL^{2P} (case $\eta < 0$)

distinguishes these two configurations as it is indicated above. To be more precise we present here jointly one result from [10] (see Lemma 6.1) and one result from [21] (see Table 2).

Lemma 4.2. *Assume that for an arbitrary quadratic system (2) the conditions $\eta > 0$, $\theta = H_7 = B_2 = 0$, $\mu_0 B_3 H_4 H_9 \neq 0$ and $\tilde{N}H_{10} > 0$ are satisfied. Then the configuration of the invariant lines of this system corresponds to Config. 4.9a if $H_{16} < 0$ and to Config. 4.9 if $H_{16} > 0$. Moreover the phase portrait of this system corresponds to one of the portraits given below if and only if the corresponding set of the conditions hold:*

$$Portrait 4.9(a) \Leftrightarrow \mathcal{G}_2 > 0, H_4 > 0, \mathcal{G}_3 < 0;$$

$$Portrait 4.9(b) \Leftrightarrow \text{either } \mathcal{G}_2 > 0, H_4 < 0 \text{ or } \mathcal{G}_2 < 0;$$

$$Portrait 4.9(c) \Leftrightarrow \mathcal{G}_2 > 0, H_4 > 0, \mathcal{G}_3 > 0.$$

Next we would like to distinguish which of these three phase portraits is generated by the configuration *Config. 4.9a* and which by *Config. 4.9*.

Assume that for an arbitrary quadratic system (2) the conditions provided by Lemma 4.2 are satisfied. Then as it was shown in [10] (see the proof of Lemma 6.1), this system could be brought via an affine transformation and time rescaling to the 2-parameter family of systems

$$\dot{x} = x^2 - 1, \quad \dot{y} = y(y + ax + b). \quad (9)$$

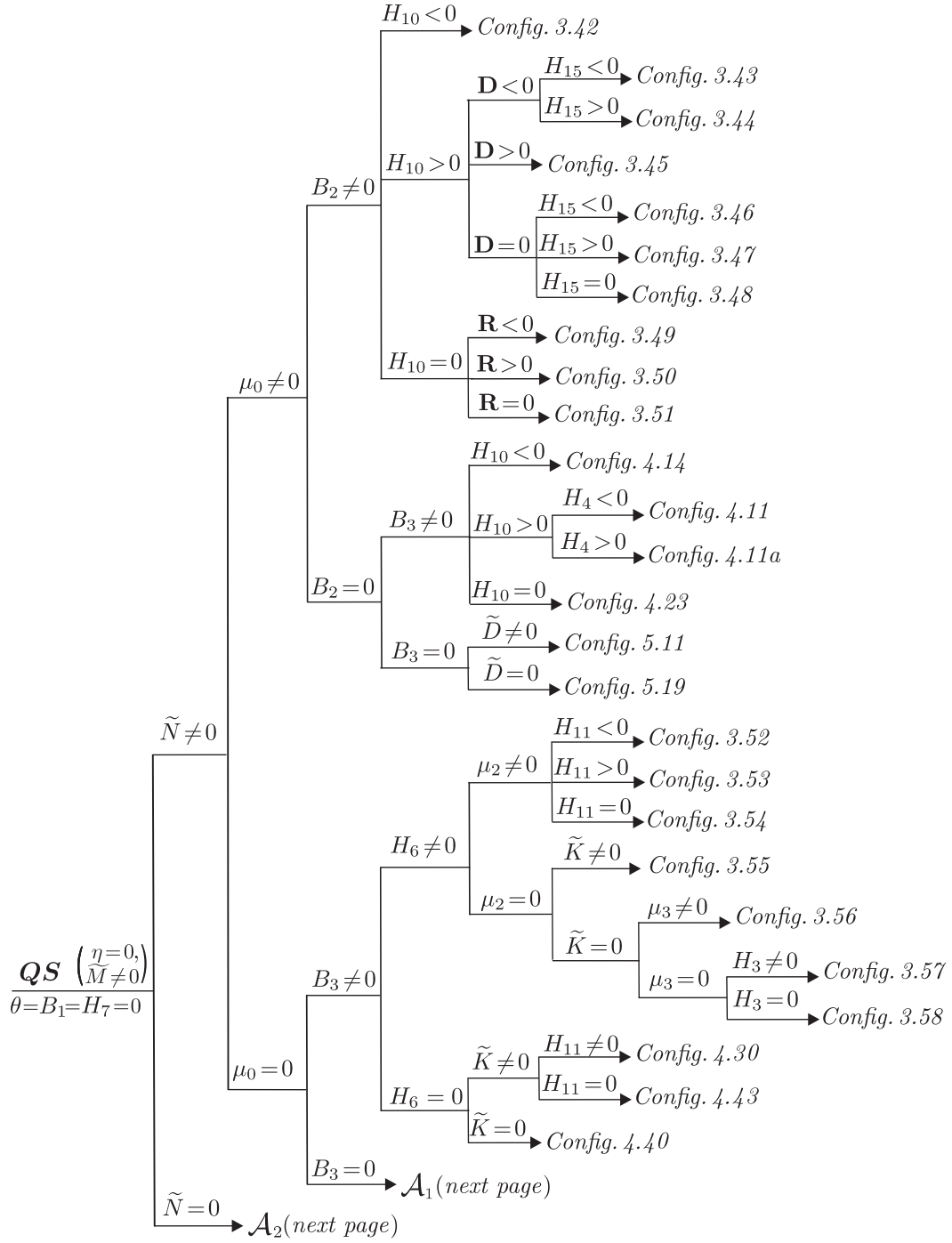


Diagram 3: The invariant criteria for configurations of systems in \mathbf{QSL}^{2p} (case $\eta = 0 \neq \widetilde{M}$)

For these systems we calculate

$$H_4 = -48a[(a-2)^2 - b^2], \quad H_{16} = 180(b^2 - a^2)[(a-2)^2 - b^2]^2,$$

$$\mathcal{G}_2 = 13824(a-1)(b^2 - a^2), \quad \mathcal{G}_3 = 288a(a-1)[(a-2)^2 - b^2].$$

Considering these expressions it is not too difficult to prove the following implications:

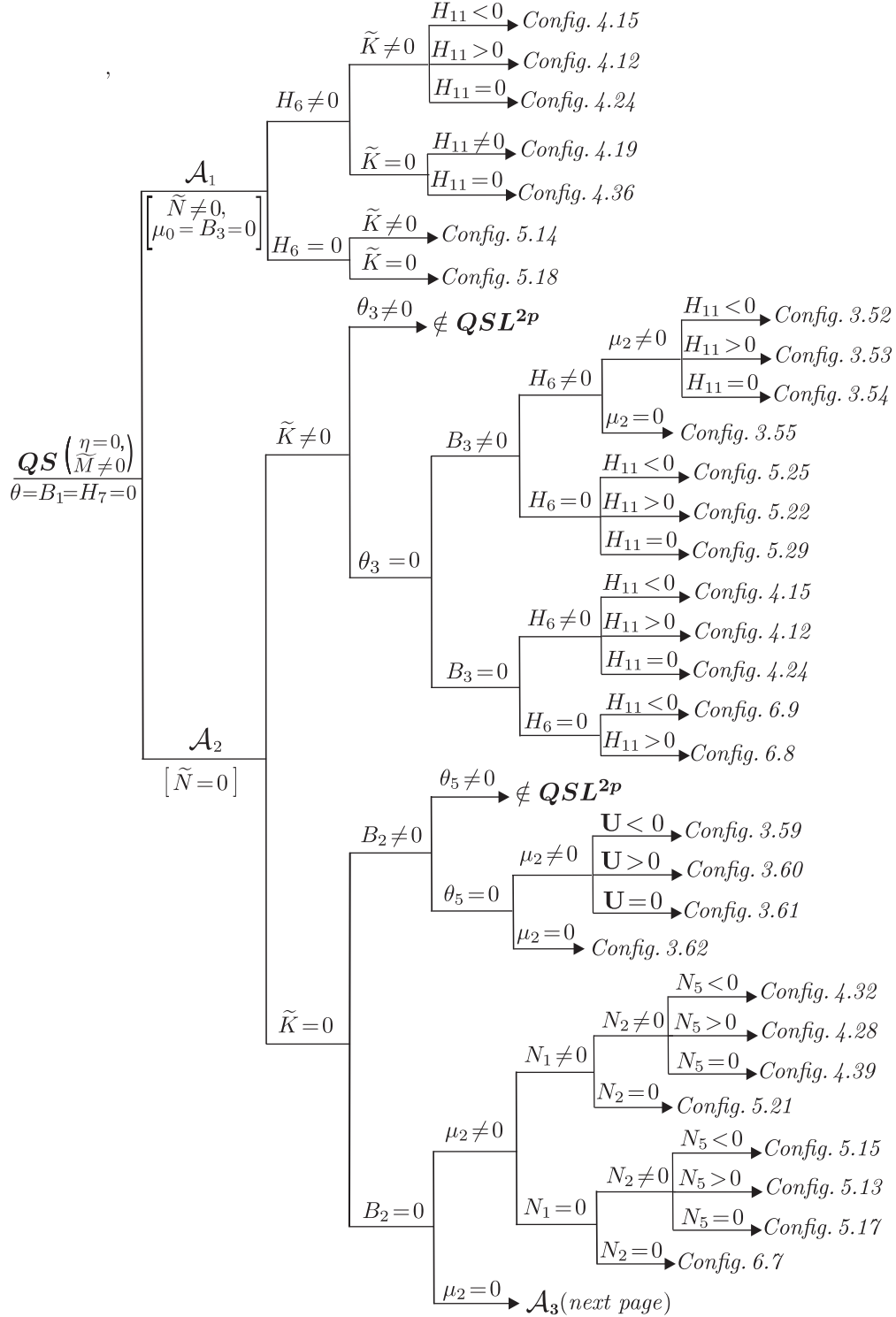


Diagram 3 (continued): The invariant criteria for configurations of systems in \mathbf{QSL}^{2p} (case $\eta = 0 \neq \tilde{M}$)

- The conditions $H_{16} < 0$, $\mathcal{G}_2 > 0$ and $H_4 > 0$ imply $\mathcal{G}_3 > 0$.
- The conditions $H_{16} > 0$ and $\mathcal{G}_2 > 0$ imply $H_4 > 0$ and $\mathcal{G}_3 < 0$.

Therefore taking into account Lemma 4.2 we can state the next remark.

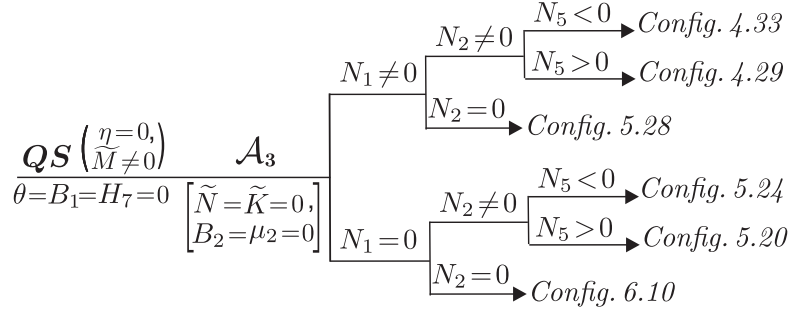


Diagram 3 (continued): The invariant criteria for configurations of systems in \mathbf{QSL}^{2p} (case $\eta = 0 \neq \widetilde{M}$)

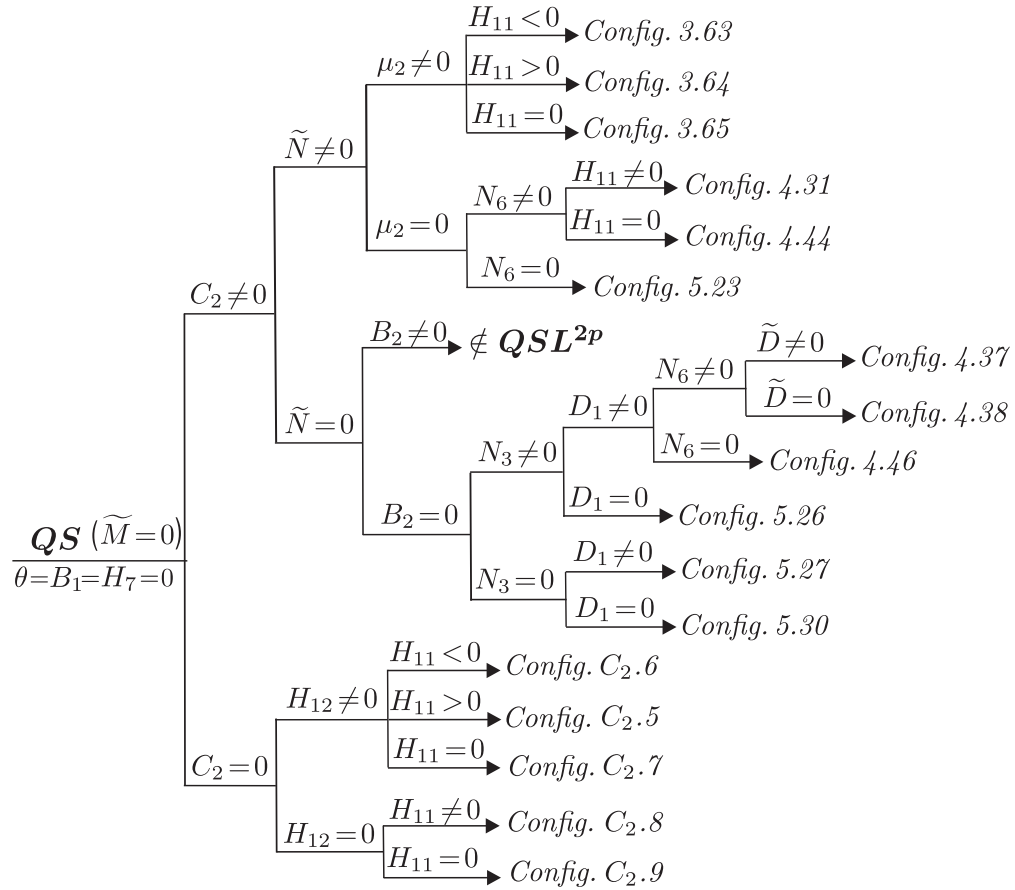


Diagram 4: The invariant criteria for configurations of systems in \mathbf{QSL}^{2p} (case $\eta = 0 = \widetilde{M}$)

Remark 4.4. (i) The configuration Config. 4.9a (i.e. $H_{16} < 0$) leads to the phase portrait Portrait 4.9(b) if and only if either $\mathcal{G}_2 < 0$, or $\mathcal{G}_2 > 0$ and $H_4 < 0$; and it leads to the phase portrait Portrait 4.9(c) if and only if $\mathcal{G}_2 > 0$ and $H_4 > 0$.

(ii) The configuration Config. 4.9 (i.e. $H_{16} > 0$) leads to the phase portrait Portrait 4.9(b) if and only if $\mathcal{G}_2 < 0$ and to the phase portrait Portrait 4.9(a) if and only if $\mathcal{G}_2 > 0$.

We denote Portrait 4.9(b), Portrait 4.9(c) and Portrait 4.9(a) by Ric. 3, Ric. 4 and Ric. 5, respectively.

3: $\mu_0 \neq 0, \widetilde{N}H_{10} > 0, H_9 = 0 \Rightarrow \text{Config. 4.10}$. Considering [21] (see Table 2) and taking

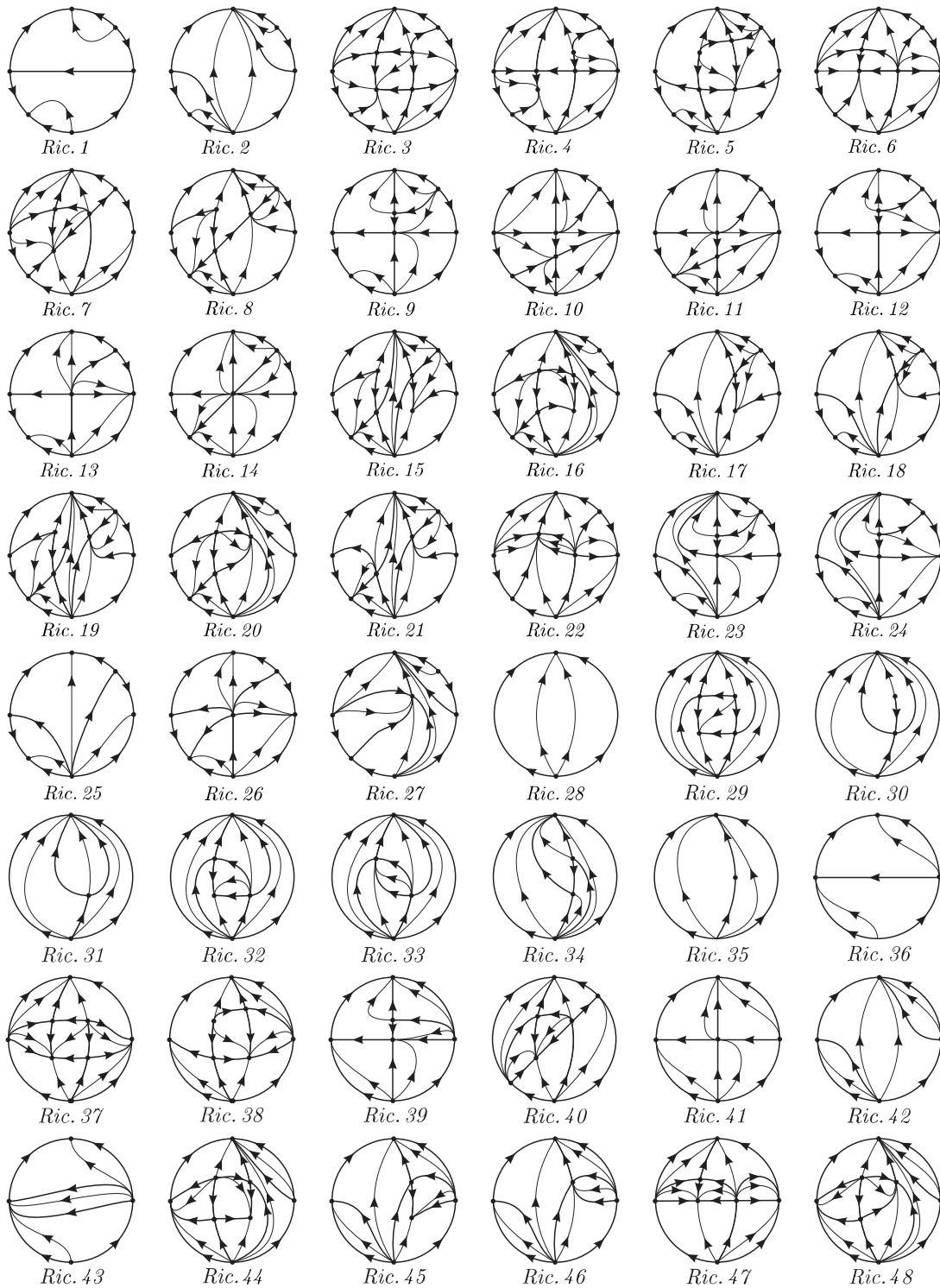


Figure 5: The phase portraits of Riccati quadratic systems

into account the condition $\tilde{N} \neq 0$ we obtain that *Config. 4.10* leads to one of the three possible phase portraits, determined by the invariant polynomials H_4 and \mathcal{G}_3 . More exactly we have the

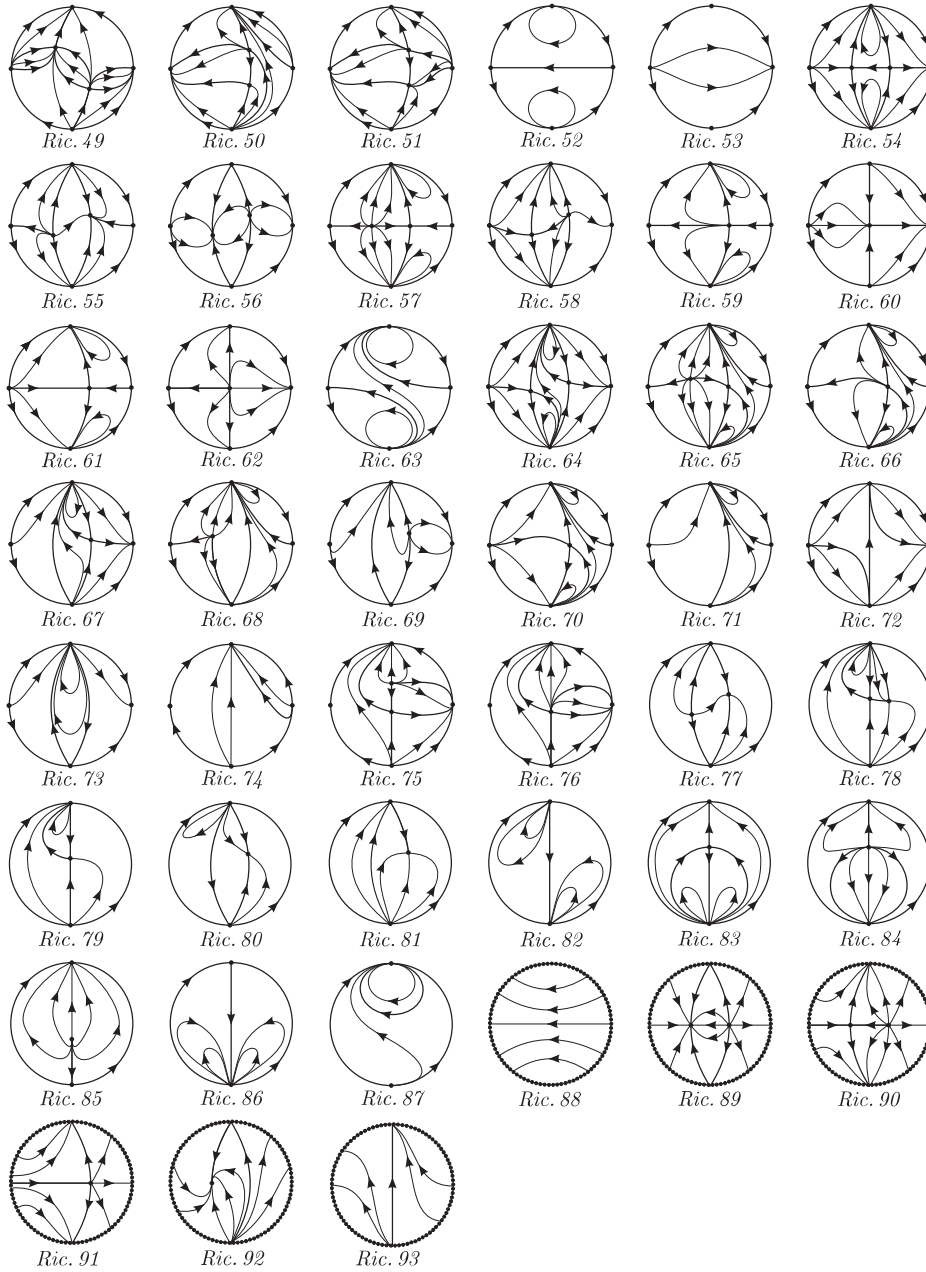


Figure 5 (*continuation*): The phase portraits of Riccati quadratic systems

following classification of the corresponding phase portraits:

$$\begin{aligned}
 \text{Portrait 4.10(a)} &\Leftrightarrow H_4 > 0, \mathcal{G}_3 > 0; \\
 \text{Portrait 4.10(b)} &\Leftrightarrow H_4 < 0; \\
 \text{Portrait 4.10(c)} &\Leftrightarrow H_4 > 0, \mathcal{G}_3 < 0.
 \end{aligned}$$

We denote *Portrait 4.10(b)*, *Portrait 4.10(c)* and *Portrait 4.10(a)* by *Ric. 6*, *Ric. 7* and *Ric. 8*, respectively.

4: $\mu_0 \neq 0, H_{10} = 0 \Rightarrow \text{Config. 4.22}$. Since $\tilde{N} \neq 0$ according to [21] we get *Portrait 4.22(a)* if $H_1 > 0$ and *Portrait 4.22(b)* if $H_1 < 0$. We denote here *Portrait 4.22(b)* by *Ric. 9* and *Portrait 4.22(a)* by *Ric. 10*.

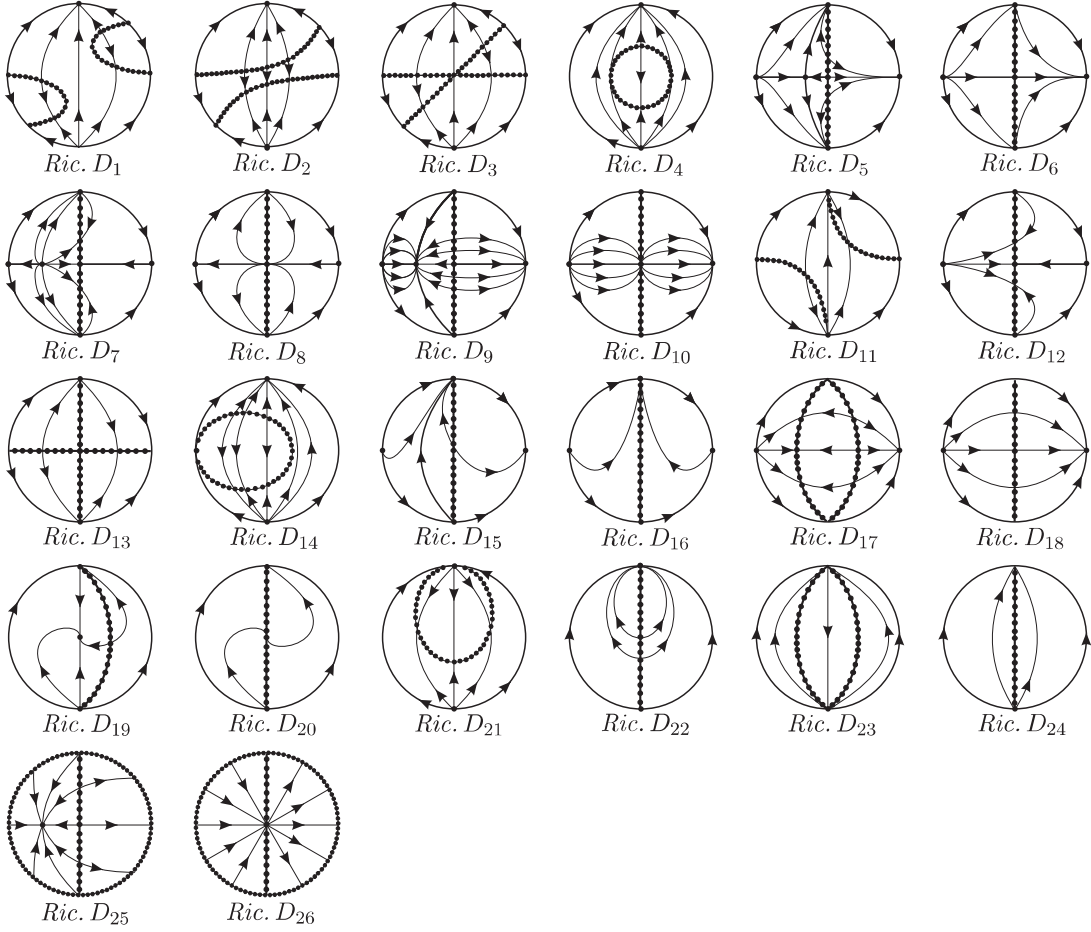


Figure 6: The phase portraits of Riccati degenerate quadratic systems

5: $\mu_0 = 0, \mu_2 \neq 0, H_9 \neq 0 \Rightarrow$ *Config. 4.16*. By [21] we get *Portrait 4.16(a)* if $\mathcal{G}_2 > 0$ and *Portrait 4.16(b)* if $\mathcal{G}_2 < 0$. We denote *Portrait 4.16(b)* and *Portrait 4.16(a)* by *Ric. 11*, and *Ric. 12*, respectively.

6: $\mu_0 = 0, \mu_2 \neq 0, H_9 = 0 \Rightarrow$ *Config. 4.17*. According to [21, Table 2] this configuration leads to the unique phase portrait which we denote by *Ric. 13*.

7: $\mu_0 = 0, \mu_2 = 0 \Rightarrow$ *Config. 4.34*. In this case according to [21] (see page 56, Table 2) we could have only two phase portraits: *Portrait 4.34(a)* and *Portrait 4.34(b)*. Moreover it is claimed that first phase portrait is defined by the condition $H_4 < 0$ and the second one by the condition $H_4 > 0$.

However we have detected an error in this paper. More precisely the next remark is valid.

Remark 4.5. *In the article [21] in Table 3(a) on page 57 there appear the phase portraits Portrait 4.34(a) with Portrait 4.34(b). In the proof for the invariant conditions for these two phase portraits each one of them appeared with the correct conditions. However in the Table these conditions were interchanged. More exactly, in the case $H_4 > 0$ (respectively $H_4 < 0$) we must have a phase portrait with a separatrix connection (respectively without separatrix connection).*

Considering this remark we deduce that in the case $H_4 < 0$ the phase portrait corresponds to *Ric. 2* (which is equivalent to *Portrait 4.34(b)*), whereas in the case $H_4 > 0$ the phase portrait corresponds to *Ric. 1* (which is equivalent to *Portrait 4.34(a)*).

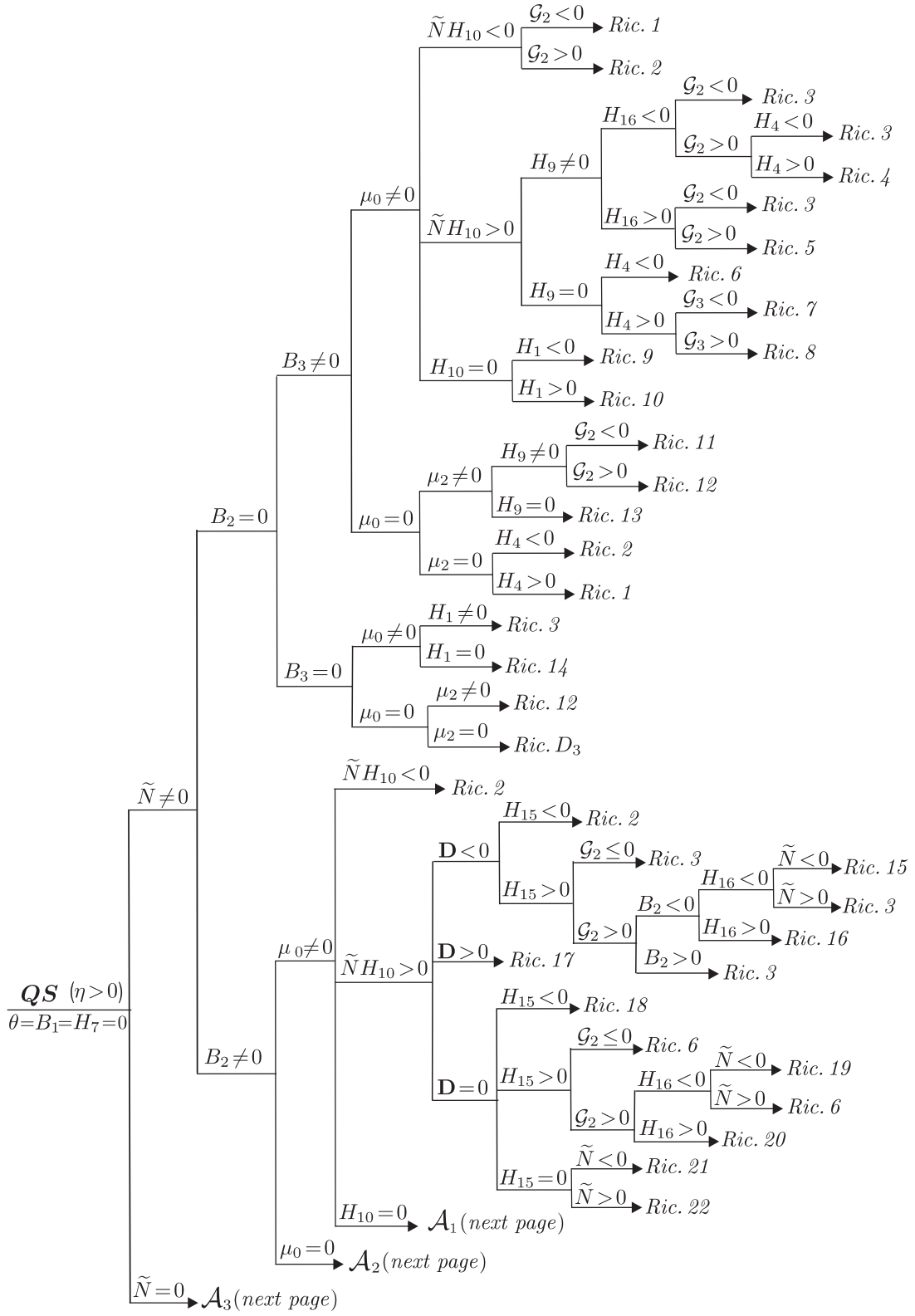


Diagram 5: The invariant criteria for phase portraits of systems in QS_{Ric} (case $\eta > 0$).

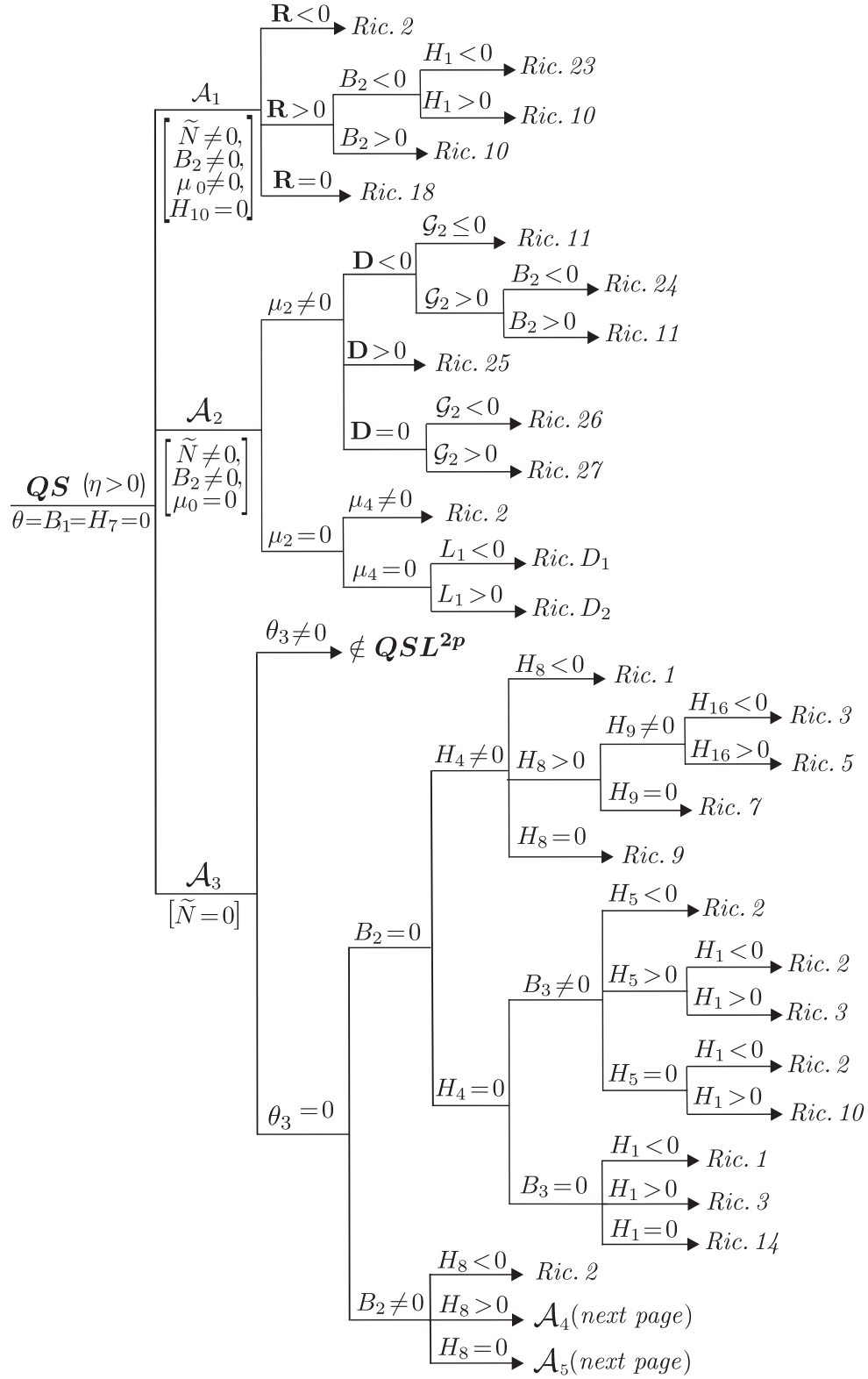


Diagram 5 (continuation): The invariant criteria for phase portraits of systems in QS_{Ric} (case $\eta > 0$).

4.1.1.1.2 The case $B_3 = 0$. Then by Lemma 3.1 we could have invariant lines in three directions. Moreover according to Diagram 1 the systems in this class possess invariant lines of

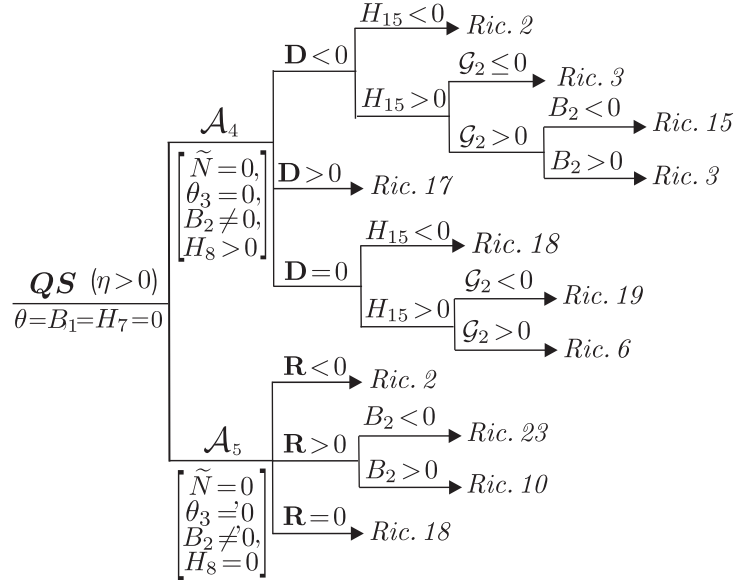


Diagram 5 (continuation): The invariant criteria for phase portraits of systems in \mathbf{QS}_{Ric} (case $\eta > 0$).

total multiplicity five. So we shall apply the classification of this family of systems given in [16]. According to Diagram 1 we have to consider the next 3 possibilities.

1: $\mu_0 \neq 0, H_1 \neq 0 \Rightarrow$ *Config. 5.1*. According to [19] (see Diagram 3) this configuration leads to the unique phase portrait given by *Picture 5.1* which is topologically equivalent to *Ric. 3*.

2: $\mu_0 \neq 0, H_1 = 0 \Rightarrow$ *Config. 5.8*. By [19] we arrive at the unique phase portrait given by *Picture 5.8* which we denote by *Ric. 14*.

3: $\mu_0 = 0 \Rightarrow$ *Config. 5.7*. According to [19] we get the unique phase portrait given by *Picture 5.7* (\simeq *Ric. 12*)

4.1.1.2 The possibility $B_2 \neq 0$. By Lemma 3.1 systems (8) could possess invariant lines only in the direction $x = 0$ and we examine the corresponding cases provided by Diagram 1.

1: $\mu_0 \neq 0, \tilde{N}H_{10} < 0$. According to Diagram 1 these conditions lead to *Config. 3.14*. We observe that due to the condition $\mu_0 \neq 0$ by Remark 4.2 at infinity there are one saddle and two nodes.

On the other hand according to [25] for quadratic systems we have the next lemma.

Lemma 4.3. *If two affine separatrices of a pair of opposite infinite saddles connect, then this separatrix connection is an invariant straight line.*

Therefore by $B_2 \neq 0$ we could not have a separatrix connection and this leads to the unique phase portrait which is topological equivalent to the one given by *Ric. 2*.

Remark 4.6. *We point out that some of the phase portraits that we will obtain for the systems with $B_2 \neq 0$ are topologically equivalent to some already obtained for the case $B_2 = 0$. This happens even if the systems with $B_2 \neq 0$ belong to the class \mathbf{QSL}_3 , whereas the systems with $B_2 = 0$ belong to the class $\mathbf{QSL}_{\geq 4}$. In drawing a phase portrait it is useful to use the invariant algebraic curves a system may possess. We may have two phase portraits appearing in different contexts drawn with the help of different configurations of algebraic invariant curves and these two phase portraits may be topologically equivalent as this equivalence disregards the algebraic properties of the systems.*

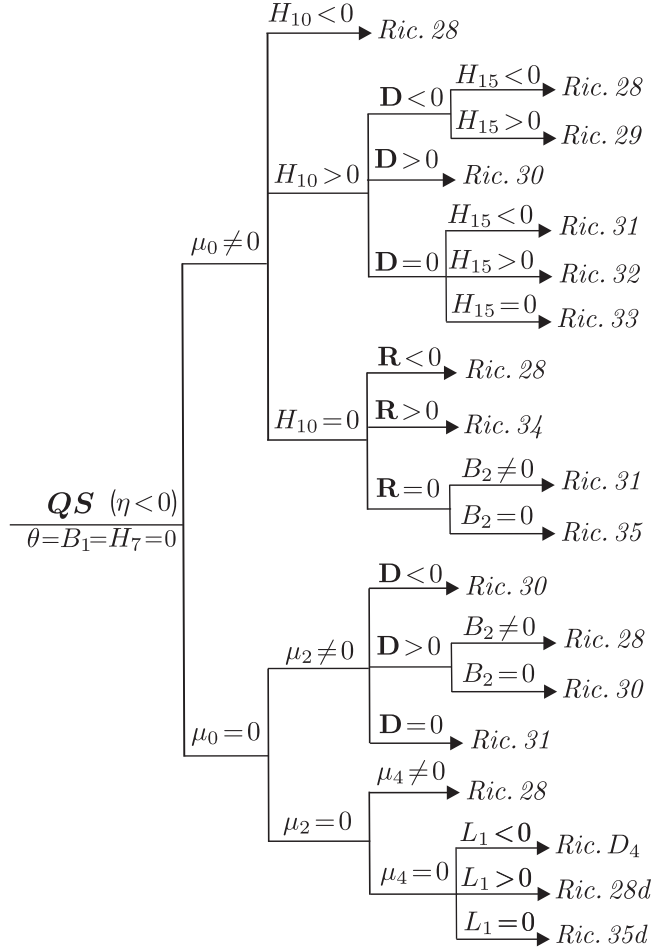


Diagram 6: The invariant criteria for phase portraits of systems in \mathbf{QS}_{Ric} (case $\eta < 0$).

2: $\mu_0 \neq 0, \tilde{N}H_{10} > 0, \mathbf{D} < 0, H_{15} < 0 \Rightarrow \text{Config. 3.15}$. We observe that the phase plane is divided by two parallel real invariant lines in three regions. And for the affine separatrices of the opposite infinite saddles there exists the unique possibility to go to the infinite node located at the intersections of invariant lines (in the corresponding direction). As a result we arrive at the unique phase portrait *Ric. 2*.

3: $\mu_0 \neq 0, \tilde{N}H_{10} > 0, \mathbf{D} < 0, H_{15} > 0 \Rightarrow \text{Config. 3.16}$. This family has four finite singularities: two saddles and two nodes and three elemental infinite singularities: two nodes and one saddle (see Remark 4.2). Similarly to the case of *Config. 3.15* the phase plane of this family is divided by two parallel real invariant lines in three regions. The finite singularities are located on these lines, more exactly a saddle and a node on each line. Clearly the singular point at infinity common to the two lines is a node. So in each one of the three regions there are two separatrices which may either connect or not.

If there is no separatrix connection, then systems (8) belong to family 10 of the structurally stable quadratic systems modulo limit cycles [2]. From the 16 possible phase portraits of this family it is easy to see that only three of them are compatible with the existence of two real parallel invariant lines. More exactly we have the phase portraits presented in Figure 7 as $\mathbb{S}_{10,14}^2$, $\mathbb{S}_{10,15}^2$ and $\mathbb{S}_{10,16}^2$.

In case when they have a connection of separatrices then according to [3] they must be either the phase portrait $\mathbb{U}_{D,44}^1$ or $\mathbb{U}_{D,60}^1$ (see Figure 7), which bifurcate in the previously mentioned

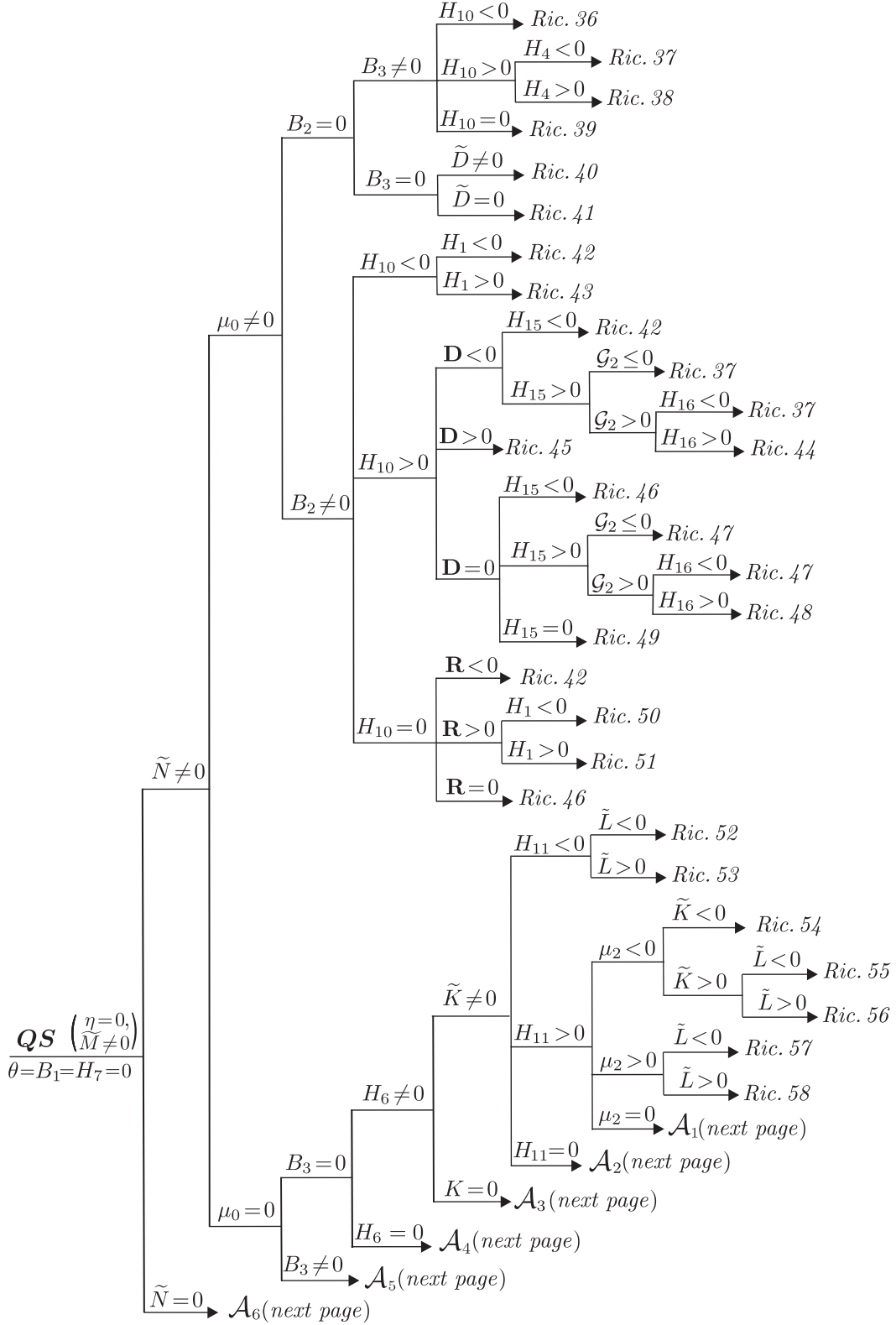


Diagram 7: The invariant criteria for phase portraits of systems in \mathbf{QS}_{Ric} (case $\eta = 0 \neq \tilde{M}$).

structurally stable systems.

According to [3, Lemma 3.5] (see also [26]) these two phase portraits force (in this family) the existence of another invariant line which contradicts the condition $B_2 \neq 0$ (see Lemma 3.1).

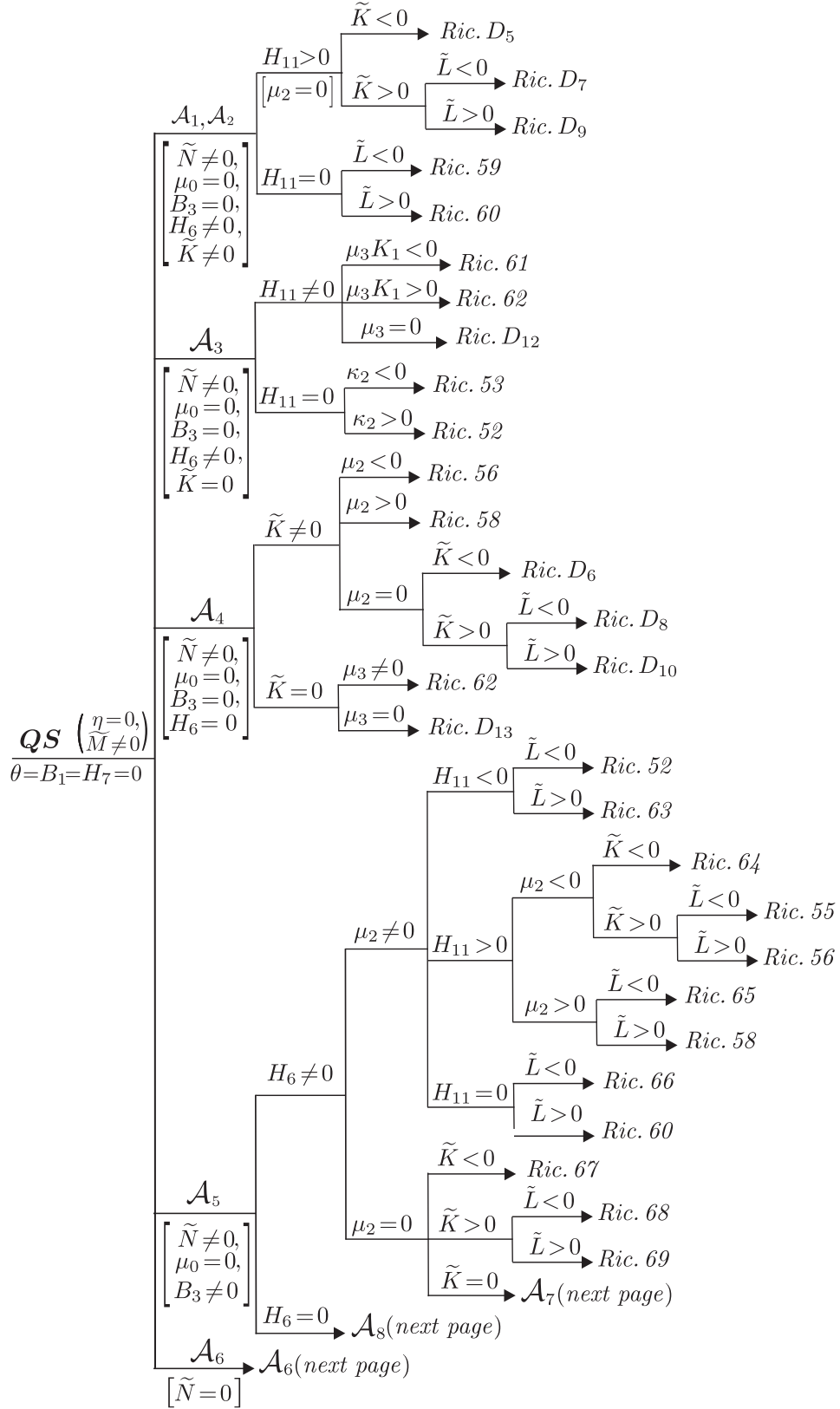


Diagram 7 (continuation): The invariant criteria for phase portraits of systems in QS_{Ric} (case $\eta = 0 \neq \tilde{M}$).

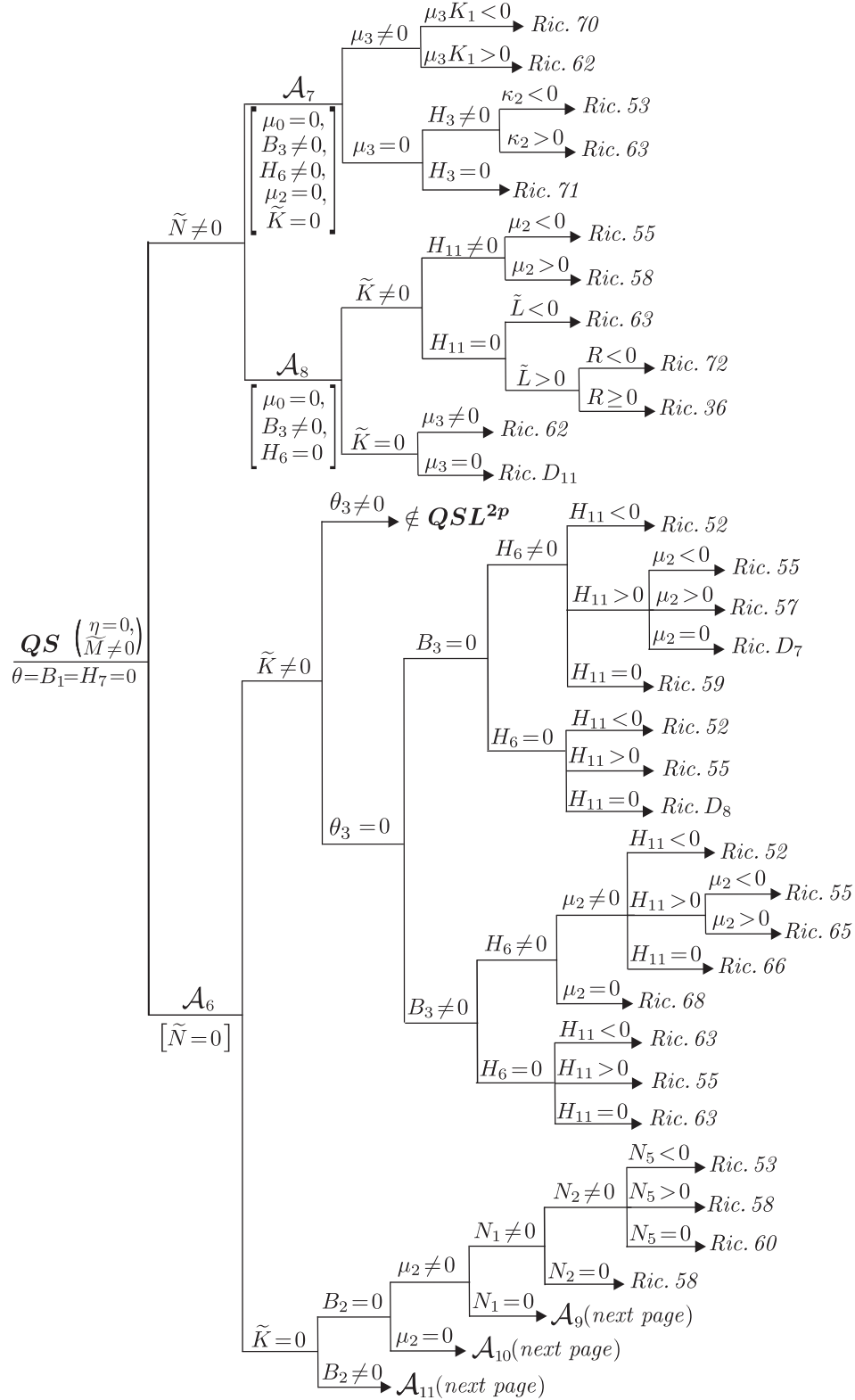


Diagram 7 (continuation): The invariant criteria for phase portraits of systems in QS_{Ric} (case $\eta = 0 \neq \tilde{M}$).

So *Config. 3.16* leads to three topologically distinct phase portraits: two of them, corresponding to $\mathbb{S}_{10,15}^2$ and $\mathbb{S}_{10,14}^2$ are new and we denote them by *Ric. 15* and *Ric. 16*, respectively.

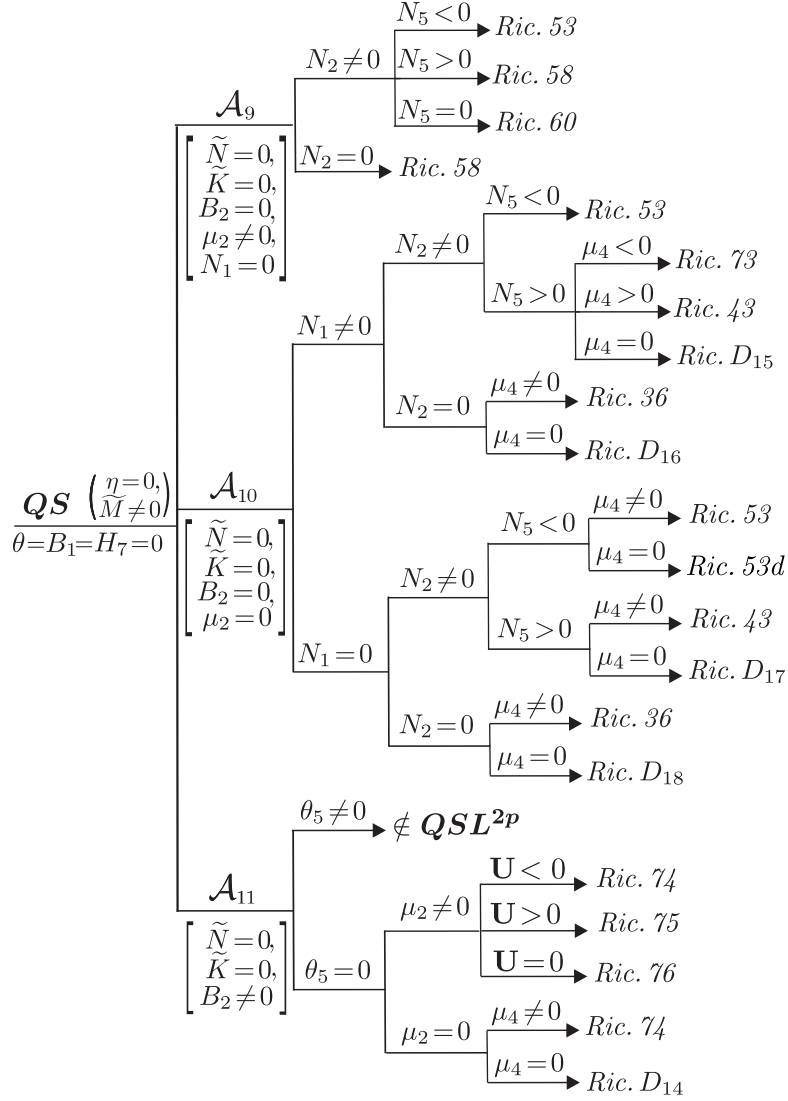


Diagram 7 (*continuation*): The invariant criteria for phase portraits of systems in QS_{Ric} (case $\eta = 0 \neq \tilde{M}$).

The remaining one which corresponds to $S_{10,16}^2$ is topologically equivalent to *Ric. 3*.

In order to construct the affine invariant conditions for distinguishing each one of the detected phase portraits we determine first the corresponding canonical form of the Riccati systems possessing *Config. 3.16*.

As it was shown in [10] if for a system (8) the conditions

$$\eta > 0, \tilde{N} \neq 0, \mu_0 \neq 0, \tilde{N}H_{10} > 0, \mathbf{D} < 0, H_{15} > 0$$

hold then this system possess *Config. 3.16* and via an affine transformation and time rescaling it could be brought to the canonical form (37) from [10], i.e. it belongs to the family of systems

$$\dot{x} = g(x^2 - 1), \quad \dot{y} = b + ex + (g - 1)xy + y^2. \quad (10)$$

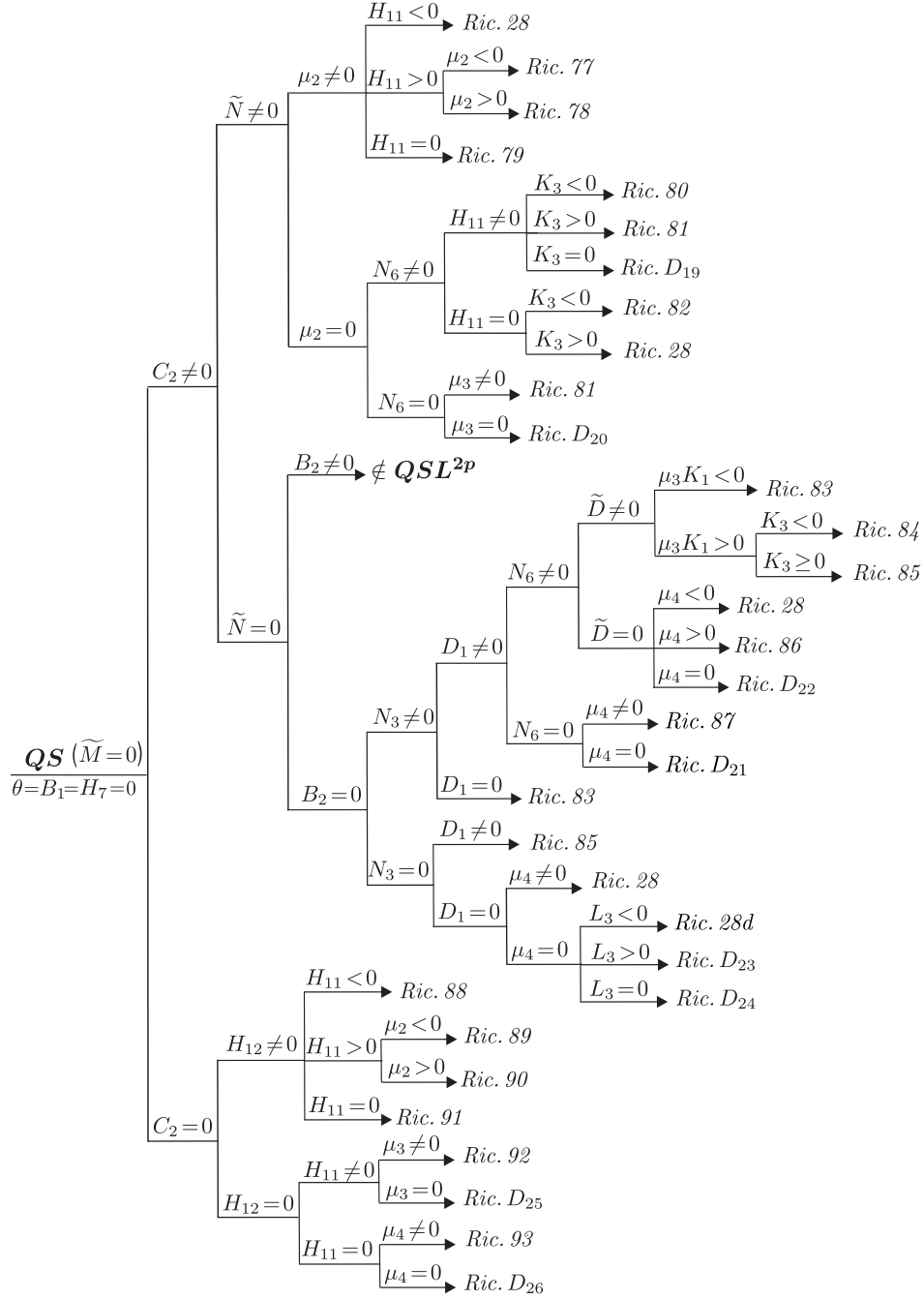


Diagram 8: The invariant criteria for phase portraits of systems in $QS Ric$ (case $\eta = 0 = \tilde{M}$).

For these systems calculations yield

$$\begin{aligned}
 B_2 &= -648[e^2 + b(g-1)^2][e^2 + (b+g)(1+g)^2]x^4 \equiv -648x^4\Phi_1\Phi_2, \\
 \mathbf{D} &= -768g^6[(g-1)^2 - 4(b+e)][(g-1)^2 - 4(b-e)] \equiv -768g^6V_1V_2, \\
 H_{15} &= 256g^4(1 - 4b - 2g + g^2) \equiv 128(V_1 + V_2), \quad \tilde{N} = (g^2 - 1)x^2, \quad \mu_0 = g^2
 \end{aligned} \tag{11}$$

and we observe that the conditions $\mathbf{D} < 0$ and $H_{15} > 0$ imply $V_1 > 0$ and $V_2 > 0$ which in addition with $\mu_0 \neq 0$ guarantee the existence of four finite real distinct singularities. We prove the following lemma.

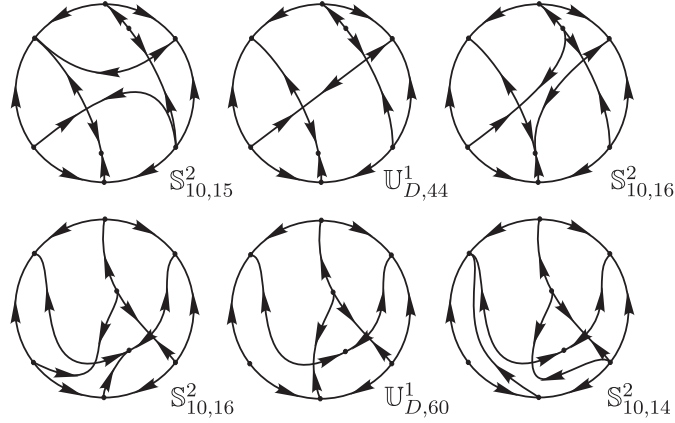


Figure 7: Potential phase portraits generated by *Config. 3.16*

Lemma 4.4. *For the 3-parameter family of systems (10) we may assume without losing the generality that the conditions $g > 0$ and $e > 0$ hold.*

Proof: Applying the linear transformation $x_1 = -x$, $y_1 = -x + y$ to systems (10) we arrive at the systems

$$\dot{x}_1 = g_1(x_1^2 - 1), \quad \dot{y}_1 = b_1 + e_1x_1 + (g_1 - 1)x_1y_1 + y_1^2 \quad (12)$$

which have exactly the form (10) but with new parameters

$$g_1 = -g, \quad b_1 = b + g, \quad e_1 = -e.$$

Thus we may assume in systems (10) $g > 0$. Then keeping the sign of this parameter via the rescaling $(x, y, t) \rightarrow (-x, -y, -t)$ we change the sign of the parameter e and this completes the proof of Lemma 4.4. ■

Next we fix the parameter $g = g_0$ obtaining a family of two parameters b and e . We point out, that due to the conditions (11) the condition $g_0(g_0^2 - 1) \neq 0$ has to be satisfied. However considering Lemma 4.4 it is clear that we could choose $g_0 \in (0, 1) \cup (1, \infty)$ and clearly these two intervals are distinguished by the invariant polynomial \tilde{N} . More exactly we could choose $g_0 \in (0, 1)$ if $\tilde{N} < 0$ and $g_0 \in (1, \infty)$ if $\tilde{N} > 0$.

In order to construct the bifurcation diagram for (10) with fixed $g = g_0$, additionally to the invariant polynomials \mathbf{D} and B_2 we consider here two other invariant polynomials: \mathcal{G}_2 and H_{16} . For systems (10) we calculate

$$\begin{aligned} \mathcal{G}_2 &= 13824g^2 [2b(1 + g^2) + 2e^2 + g(g - 1)^2], \\ H_{16} &= -180g^6 [4b + (1 + g)^2] [16b^2 + 16bg - 8e^2 + (g^2 - 1)^2]. \end{aligned}$$

In what follows we investigate the geometric locations in the plane (e, b) of the following curves, depending on the parameter g_0 :

$$\begin{aligned}
V_1(b, e, g_0) = 0 & \Rightarrow b = -e + (g_0 - 1)^2/4; & (\mathcal{V}_1) \\
V_2(b, e, g_0) = 0 & \Rightarrow b = e + (g_0 - 1)^2/4; & (\mathcal{V}_2) \\
\Phi_1(b, e, g_0) = 0 & \Rightarrow b = -\frac{e^2}{(g_0 - 1)^2}; & (\mathcal{F}_1) \\
\Phi_2(b, e, g_0) = 0 & \Rightarrow b = -\frac{e^2}{(g_0 + 1)^2} - g_0; & (\mathcal{F}_2) \\
\mathcal{G}_2(b, e, g_0) = 0 & \Rightarrow b = -\frac{e^2}{g_0^2 + 1} - \frac{(g_0 - 1)^2 g_0}{2(g_0^2 + 1)}; & (\mathcal{G}') \\
H_{16}(b, e, g_0) = 0 & \Rightarrow \begin{cases} b = -(g_0 + 1)^2/4; & (\mathcal{H}') \\ 16b^2 + 16bg_0 - 8e^2 + (g_0^2 - 1)^2 = 0. & (\mathcal{H}'') \end{cases}
\end{aligned}$$

Remark 4.7. We observe that for any value of the parameter $g_0 \neq 0, \pm 1$ the curves (\mathcal{V}_1) , (\mathcal{V}_2) and (\mathcal{H}') are lines; (\mathcal{F}_1) and (\mathcal{F}_2) are parabolas and the curve (\mathcal{H}'') is a hyperbola.

It is not too difficult to determine that in the domain $\widehat{\mathcal{D}}$ defined by the condition $0 < e \leq -b + (g_0 - 1)^2/4$ (where we have $V_1 \geq 0$ and $V_2 > 0$) there are located only the following four points of intersection of some of the above defined curves:

$$\begin{aligned}
E_1\left(\frac{1}{2}(g_0 - 1)^2, -\frac{1}{4}(g_0 - 1)^2\right) & : \text{ intersection of the curves } (\mathcal{V}_1), (\mathcal{F}_1), (\mathcal{G}'), (\mathcal{H}''); \\
E_2\left(\frac{1}{2}(g_0 + 1)^2, \frac{1}{4}(1 + 6g_0 + g_0^2)\right) & : \text{ intersection of the curves } (\mathcal{V}_1), (\mathcal{F}_2), (\mathcal{G}'), (\mathcal{H}''); \\
E_3\left(\frac{1}{2}(g_0^2 - 1), -\frac{1}{4}(g_0 + 1)^2\right) & : \text{ intersection of the curves } (\mathcal{H}'), (\mathcal{H}''), (\mathcal{F}_1), (\mathcal{F}_2); \\
E_4\left(\frac{1}{2}(g_0^2 + 1), -\frac{1}{4}(g_0 + 1)^2\right) & : \text{ intersection of the curves } (\mathcal{V}_1), (\mathcal{H}').
\end{aligned}$$

We point out that the point E_3 is located on the domain $\widehat{\mathcal{D}}$ for $g_0^2 - 1 > 0$ (i.e. $\widetilde{N} > 0$). In this case the corresponding symmetric point with respect to the axis $e = 0$ is $E'_3\left(-\frac{1}{2}(g_0^2 - 1), -\frac{1}{4}(g_0 + 1)^2\right)$. So in the case $\widetilde{N} < 0$ the point E'_3 is located on the domain $\widehat{\mathcal{D}}$. However this does not affect the number and the positions of the intersection points E_i depending on the parameter g_0 .

We point out several properties of the curves (\mathcal{V}_1) , (\mathcal{F}_1) , (\mathcal{F}_2) , (\mathcal{H}') and (\mathcal{H}'') as well as of their intersection points.

Lemma 4.5. For any value of the parameter $g_0 > 0$, $g_0 \neq 1$ the following properties are valid:

- (i) The four points E_j ($j = 1, 2, 3, 4$) are distinct, i.e. $E_j \neq E_k$, $j, k \in \{1, 2, 3, 4\}$, $j \neq k$.
- (ii) The parabolas (\mathcal{F}_1) and (\mathcal{F}_2) are located entirely in the domain $b - (g_0 - 1)^2/4 \leq e \leq -b + (g_0 - 1)^2/4$ and each one of them has a tangent point with the line (\mathcal{V}_1) .
- (iii) For $g_0 > 0$ the hyperbola (\mathcal{H}'') is reducible into two intersecting straight lines for two distinct values of g_0 : $g'_0 \in (0, 1)$ and $g''_0 \in (1, \infty)$.

Proof: The statement (i) follows directly from the comparison of the coordinates of the points $E_j(e_j, b_j)$ ($j = 1, 2, 3, 4$). We have

$$\begin{aligned}
e_1 - e_2 &= -2g_0, & e_1 - e_3 &= 1 - g_0, & e_1 - e_4 &= -g_0, \\
e_2 - e_3 &= g_0 + 1, & e_2 - e_4 &= g_0, & e_3 - e_4 &= -1
\end{aligned}$$

and evidently due to the conditions $\mu_0 \widetilde{N} \neq 0$ (i.e. $g_0(g_0^2 - 1) \neq 0$) we have $e_j - e_k \neq 0$, $j, k \in \{1, 2, 3, 4\}$, $j \neq k$. In other words all four mentioned points of intersections are distinct for any value of the parameter g_0 satisfying the condition $g_0(g_0^2 - 1) \neq 0$.

(ii) Consider now the curves (\mathcal{F}_1) (i.e. $b = -e^2/(g_0 - 1)^2$) and (\mathcal{F}_2) (i.e. $b = -e^2/(g_0 + 1)^2 - g_0$) and taking into account (11) we calculate:

$$V_{1,2}(b, e, g_0) \Big|_{(\mathcal{F}_1)} = [(g_0 - 1)^2 - 4(b \pm e)] \Big|_{(\mathcal{F}_1)} = \frac{[(g_0 - 1)^2 \mp 2e]^2}{(g_0 - 1)^2};$$

$$V_{1,2}(b, e, g_0) \Big|_{(\mathcal{F}_2)} = [(g_0 - 1)^2 - 4(b \pm e)] \Big|_{(\mathcal{F}_2)} = \frac{[(g_0 + 1)^2 \mp 2e]^2}{(g_0 + 1)^2}.$$

So we obtain that on the parabolas (\mathcal{F}_1) and (\mathcal{F}_2) we have $V_1 \geq 0$ and $V_2 \geq 0$, i.e. these curves are entirely located on the domain $b - (g_0 - 1)^2/4 \leq e \leq -b + (g_0 - 1)^2/4$. Moreover since the curve (\mathcal{F}_1) (respectively (\mathcal{F}_2)) for $e > 0$ has the unique point of intersection E_1 (respectively E_2) with the line (\mathcal{V}_1) we deduce that this point is a tangent point of the parabola (\mathcal{F}_1) (respectively (\mathcal{F}_2)) with the line (\mathcal{V}_1) . This completes the proof of the statement (ii) of the lemma.

(iii) Calculating the discriminant $\bar{\Delta}$ of the conic (\mathcal{H}'') (which is a hyperbola) we obtain:

$$\bar{\Delta} = -128 (g_0^2 - 2g_0 - 1) (g_0^2 + 2g_0 - 1).$$

Therefore for $g_0 > 0$ we have two values $g'_0 = \sqrt{2} - 1$ and $g''_0 = \sqrt{2} + 1$ of this parameter for which $\bar{\Delta} = 0$ and hence the hyperbola (\mathcal{H}'') is reducible. We observe that $g'_0 \in (0, 1)$ and $g''_0 \in (1, \infty)$. Lemma 4.5 is proved. \blacksquare

Remark 4.8. We point out that the values $g_0 = g'_0$, $g_0 = g''_0$ for which the hyperbola (\mathcal{H}'') becomes reducible are not bifurcation points for the phase portraits. Moreover we could have one of the following possibilities:

- when (\mathcal{H}'') does not intersect the axis $e = 0$ then the same branch of the hyperbola passes through both points E_1 and E_2 (as it is shown in Figure 8);
- when (\mathcal{H}'') intersects the axis $e = 0$ then one branch of the hyperbola passes through E_1 and another one through E_2 (as it is shown in Figure 9);
- when (\mathcal{H}'') is reducible then both its components (i.e. straight lines) intersect at the axis $e = 0$, one line passing through E_1 and another one through E_2 .

Considering the fact that the invariant polynomial H_{16} contains as components the line (\mathcal{H}') and the hyperbola (\mathcal{H}'') , it is clear that the sign of H_{16} is always negative (respectively positive) in the domains (\mathcal{A}) (respectively (\mathcal{B})) independently of the position of the branches of the hyperbola (see Figures 8 and 9) or if it splits into two intersecting straight lines..

Taking into account Remarks 4.7 and 4.8 as well as Lemma 4.5 we conclude that in order to detect the affine invariant conditions for the realization of each one of the phase portraits *Ric. 3*, *Ric. 15* and *Ric. 16* it is sufficient to examine the bifurcation diagram in the space (e, b) of the systems (10) with $g = g_0 > 0$ taking only two values of the parameter g_0 : one from the interval $(0, 1)$ and another from $(1, \infty)$.

In Figure 8 we have the bifurcation diagram for $g_0 \in (1, \infty)$. As it can be observed directly from this diagram the next remark follows.

Remark 4.9. Assume that for a system (10) the conditions $\mu_0 \neq 0$ and $\tilde{N} > 0$ hold. Then under one of the conditions listed below we have on its right side the corresponding phase portrait:

$$\begin{aligned} \mathcal{G}_2 \leq 0 & \Rightarrow Ric. 3; \\ \mathcal{G}_2 > 0, B_2 > 0 & \Rightarrow Ric. 3; \\ \mathcal{G}_2 > 0, B_2 < 0, H_{16} < 0 & \Rightarrow Ric. 3; \\ \mathcal{G}_2 > 0, B_2 < 0, H_{16} > 0 & \Rightarrow Ric. 16. \end{aligned}$$

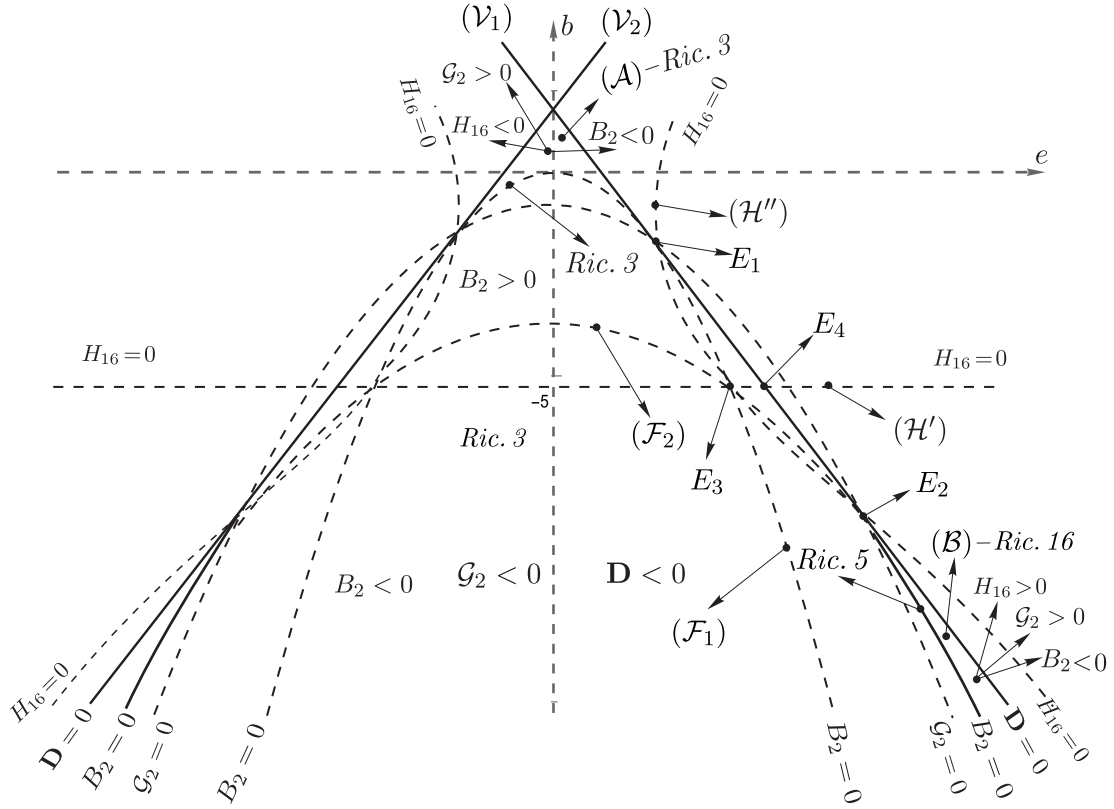


Figure 8: Bifurcation diagram for systems (10) with $g > 1$

In the case $\tilde{N} < 0$ we take a value of the parameter $g_0 \in (0, 1)$ and we arrive at the bifurcation diagram represented in Figure 9. As it can be detected directly from this diagram the next remark follows.

Remark 4.10. Assume that for a system (10) the conditions $\mu_0 \neq 0$ and $\tilde{N} < 0$ hold. Then the phase portrait of this system corresponds to the one of the indicated below if the corresponding conditions are satisfied, respectively:

$$\begin{aligned}
\mathcal{G}_2 \leq 0 &\Rightarrow Ric. 3; \\
\mathcal{G}_2 > 0, B_2 > 0 &\Rightarrow Ric. 3; \\
\mathcal{G}_2 > 0, B_2 < 0, H_{16} < 0 &\Rightarrow Ric. 15; \\
\mathcal{G}_2 > 0, B_2 < 0, H_{16} > 0 &\Rightarrow Ric. 16.
\end{aligned}$$

We observe that the conditions provided by Remarks 4.9 and 4.10 could be joined and we arrive at the next lemma.

Lemma 4.6. Assume that for a system (10) the condition $\mu_0 \tilde{N} \neq 0$ holds. Then under the conditions given below on the left we obtain the corresponding phase portrait on the right.

$$\begin{aligned}
\mathcal{G}_2 \leq 0 &\Rightarrow Ric. 3; \\
\mathcal{G}_2 > 0, B_2 > 0 &\Rightarrow Ric. 3; \\
\mathcal{G}_2 > 0, B_2 < 0, H_{16} < 0, \tilde{N} < 0 &\Rightarrow Ric. 15; \\
\mathcal{G}_2 > 0, B_2 < 0, H_{16} < 0, \tilde{N} > 0 &\Rightarrow Ric. 3; \\
\mathcal{G}_2 > 0, B_2 < 0, H_{16} > 0 &\Rightarrow Ric. 16.
\end{aligned}$$

4: $\mu_0 \neq 0, \tilde{N} H_{10} > 0, \mathbf{D} > 0 \Rightarrow Config. 3.17$. Considering this configuration it is easy to detect that it leads to the three potential topologically distinct phase portraits: $\mathbb{S}_{9,1}^2, \mathbb{U}_{1,18}^1$ and $\mathbb{I}_{9,1}$ (see Figure 10).

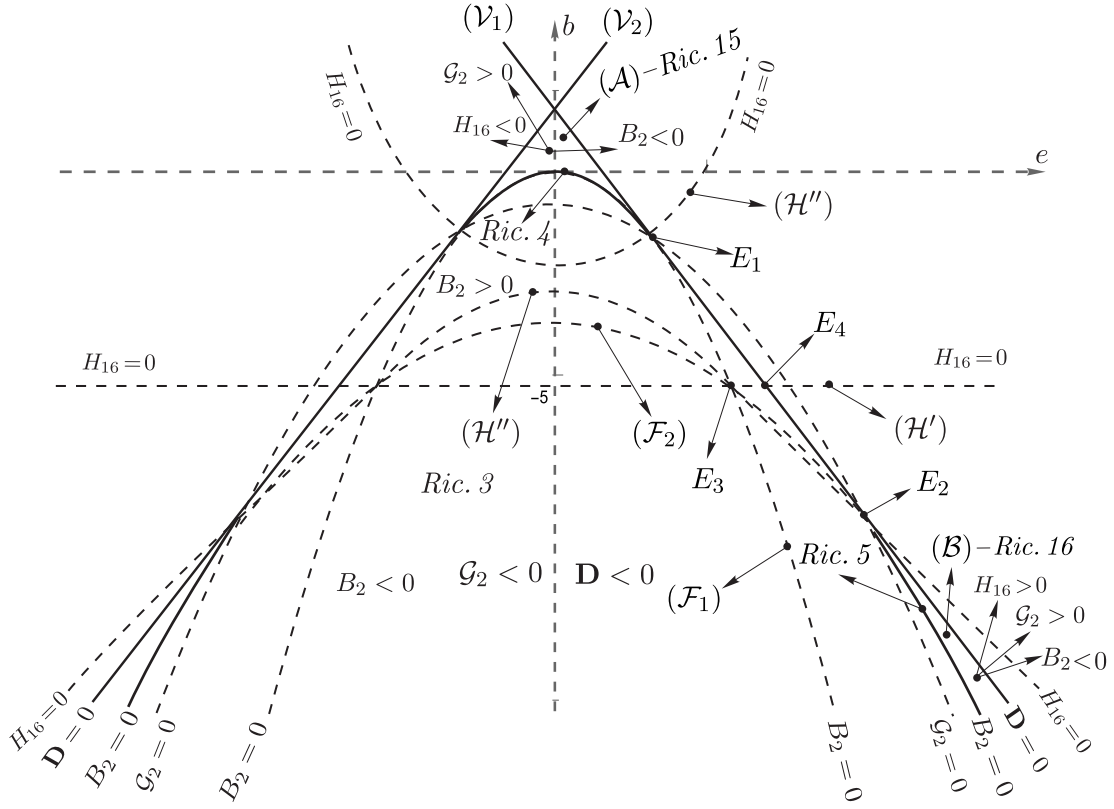


Figure 9: Bifurcation diagram for systems (10) with $0 < g < 1$

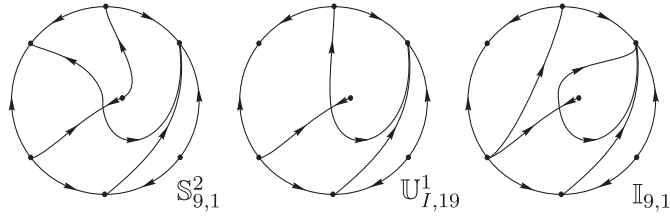


Figure 10: Potential phase portraits generated by *Config. 3.17*

These phase portraits are given in [3, Figure 5.133] where it is shown that the last two are not realizable. Thus there remains only the phase portrait $\mathbb{S}^2_{9,1}$ which we denote by *Ric. 17*.

5: $\mu_0 \neq 0, \tilde{N}H_{10} > 0, \mathbf{D} = 0, H_{15} < 0 \Rightarrow \text{Config. 3.18}$. We observe that this configuration is obtained from *Config. 3.17* by coalescing the two singularities (a node and a saddle) on the invariant line. As a consequence by continuity we obtain the unique phase portrait which we denote by *Ric. 18*.

6: $\mu_0 \neq 0, \tilde{N}H_{10} > 0, \mathbf{D} = 0, H_{15} > 0 \Rightarrow \text{Config. 3.19}$. It is evident that this configuration could be obtained from *Config. 3.16* by coalescing the two singularities (a node and a saddle) on one of the invariant lines. We recall that *Config. 3.16* leads to the phase portraits *Ric. 3*, *Ric. 15* and *Ric. 16*. From *Ric. 3* as well as from *Ric. 15* (due to the symmetry that they have) only one phase portrait is possible to obtain from each of them and they are respectively *Ric. 6* and a new phase portrait which we denote by *Ric. 19*.

However in *Ric. 16* we have 2 possibilities to produce the coalescence, but from [3] it follows that only one is realizable ($\mathbb{U}^1_{A,52}$) which is denoted here by *Ric. 20*.

We point out that the conditions for distinguishing these three phase portraits can be obtained from Lemma 4.6 and Figures 8 and 9 because the bifurcation surface $\mathbf{D} = 0$ borders the generic regions where *Config. 3.16* is given.

On the other hand for systems (10) for $\mathbf{D} = 0$ (we can take $V_1 = 0$ due to $e > 0$) we have $b = \frac{1}{4} [(g-1)^2 - 4e]$ and this gives us

$$B_2 = -\frac{81}{2} [(g-1)^2 + 2e]^2 [(g-1)^2 - 2e]^2 x^4 < 0.$$

Therefore considering Lemma 4.6 and Figures 8 and 9 the next lemma follows.

Lemma 4.7. *Assume that for a system (10) the conditions $\mu_0 \tilde{N} \neq 0$ and $\mathbf{D} = 0$ hold. Then under the conditions given below on the left we obtain the corresponding phase portrait on the right.*

$$\begin{aligned} \mathcal{G}_2 \leq 0 & \Rightarrow Ric. 6; \\ \mathcal{G}_2 > 0, H_{16} < 0, \tilde{N} < 0 & \Rightarrow Ric. 19; \\ \mathcal{G}_2 > 0, H_{16} < 0, \tilde{N} > 0 & \Rightarrow Ric. 6; \\ \mathcal{G}_2 > 0, H_{16} > 0 & \Rightarrow Ric. 20. \end{aligned}$$

7: $\mu_0 \neq 0, \tilde{N} H_{10} > 0, \mathbf{D} = 0, H_{15} = 0 \Rightarrow Config. 3.20$. We observe that this configuration could be obtained from *Config. 3.19* by coalescing the elemental singularities (a node and a saddle). Then from *Ric. 19* and *Ric. 6* we produce new phase portraits which we denote respectively by *Ric. 21* and *Ric. 22*. These pictures are topologically equivalent to the phase portraits given in Table 9 on page 37 in [8] under the names $AA_{19}^{sn sn}$ and $AA_{20}^{sn sn}$ (see Remark 4.11 below).

However it is not possible to do the same from *Ric. 20* (as from *Ric. 19* and *Ric. 6*) because as we have shown earlier for *Config. 3.19* only one of the couples of elemental singularities from *Ric. 16* can coalesce. As a result we arrive at two topologically distinct phase portraits in the case of *Config. 3.20*.

We determine that the conditions $\mathbf{D} = H_{16} = 0$ define the point of intersection of the lines \mathcal{V}_1 and \mathcal{V}_2 on both diagrams in Figures 8 and 9. We observe that in the interior of the region (\mathcal{A}) in Figure 8 corresponding to the condition $\tilde{N} > 0$ we have *Ric. 3* and on the line \mathcal{V}_1 (border of (\mathcal{A})) we have *Ric. 6*. Therefore as it was mentioned above we get *Ric. 22* at the point of intersection of the lines \mathcal{V}_1 and \mathcal{V}_2 .

Similarly if $\tilde{N} < 0$ considering Figure 9 we have respectively *Ric. 15*, *Ric. 19* and *Ric. 21*.

Thus we get *Ric. 21* for $\tilde{N} < 0$ and *Ric. 22* for $\tilde{N} > 0$.

Remark 4.11. *A final enumeration of phase portraits determined in the article [8] is given in Table 9. However there exists a gap in this enumeration namely the notation $\mathbb{U}_{AA,32}^2$ is skip. So in the last three cases from the Table 9 must be $\mathbb{U}_{AA,32}^2$, $\mathbb{U}_{AA,33}^2$ and $\mathbb{U}_{AA,34}^2$ instead of notations $\mathbb{U}_{AA,33}^2$, $\mathbb{U}_{AA,34}^2$ and $\mathbb{U}_{AA,35}^2$, respectively.*

8: $\mu_0 \neq 0, H_{10} = 0, \mathbf{R} < 0 \Rightarrow Config. 3.21$. Since we do not have real finite singularities and there is an invariant (double) straight line it is clear that we get a unique phase portrait which is topologically equivalent to *Ric. 2*.

9: $\mu_0 \neq 0, H_{10} = 0, \mathbf{R} > 0 \Rightarrow Config. 3.22$. We have two saddle-nodes on the double invariant lines. It is clear that a perturbation of this configuration could lead to *Config. 3.16* which has saddles and nodes in a convex quadrilateral. Then when we pass from *Config. 3.16* to *Config. 3.22* the parabolic sectors of the saddle-nodes must be on the opposite sides of the semi-planes defined by the double invariant line. Therefore there are two possibilities: (a) the separatrices of the saddle-nodes in every semi-plane have the same stability as the separatrix of the infinite saddle or (b) they have opposite stabilities (see Figure 11).

In the first case both separatrices (finite and infinite) in every semi-plane must come/go from/to the infinite node $N_3[0 : 1 : 0]$. However this phase portrait (see Figure 11 (a_1)) is impossible because by a perturbation, it leads to the phase portrait $\mathbb{I}_{10,20}$ from [3] (see Figure 11 (a_2)) which was proved to be impossible in [2].

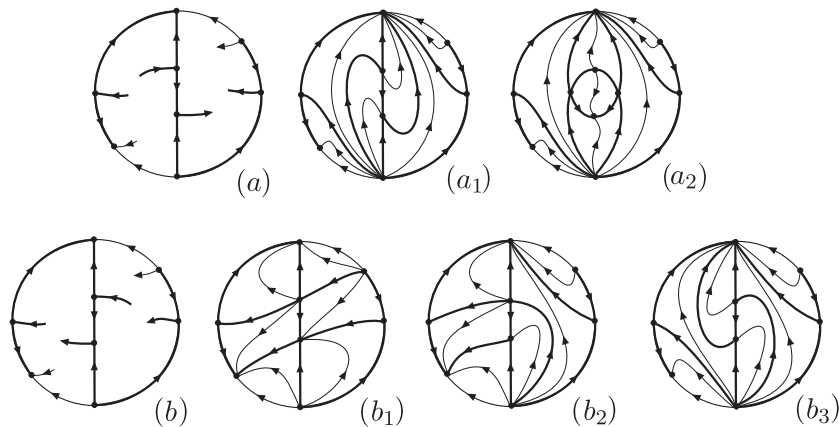


Figure 11: Generic potential phase portraits generated by *Config. 3.22*

In the case (b) we have three generic potential phase portraits (b_1)–(b_3) given in Figure 11 and two that have a separatrix connection. The cases (b_1) and (b_2) are realizable whereas (b_3) is impossible because a perturbation of it may lead to the phase portrait (a_2) ($\simeq \mathbb{I}_{10,20}$ from [2]) which is impossible as it is mentioned above. Moreover the phase portrait (b_1) is topologically equivalent to *Ric. 10* whereas (b_2) is new and we denote it by *Ric. 23*.

Next we claim that if there is any separatrix connection then either this connection is part of an invariant straight line or the phase portrait is impossible. Indeed there are two potential ways to produce a separatrix connection. One leads to a phase portrait topologically equivalent to *Ric. 9* which by Lemma 3.5 of [3], this separatrix connection must be part of an invariant straight line which contradicts $B_2 \neq 0$. We observe that *Ric. 9* may bifurcate in *Ric. 10* or *Ric. 23*. The phase portrait with the second potential connection would bifurcate into *Ric. 23* or the phase portrait (b_3) of Figure 11. Since the latter has already been proved to be impossible we deduce that the connection is also impossible.

As it was shown in [10] if for a system (8) the conditions

$$\eta > 0, \tilde{N} \neq 0, \mu_0 \neq 0, H_{10} = 0, \mathbf{R} > 0$$

hold then this system possesses *Config. 3.22* and via an affine transformation and time rescaling it could be brought to the canonical form (39) from [10], i.e. it belongs to the family of systems

$$\dot{x} = gx^2, \quad \dot{y} = b + ex + (g-1)xy + y^2.$$

For these systems we have $\mu_0 = g^2$, $\mathbf{R} = -16bg^4x^2$ and due to $\mu_0 \neq 0$ the condition $\mathbf{R} > 0$ implies $b < 0$. Then we may assume $b = -1$ due to the rescaling $(x, y, t) \mapsto (\sqrt{-b}x, \sqrt{-b}y, t/\sqrt{-b})$. Then we arrive at the 2-parameter family of systems

$$\dot{x} = gx^2, \quad \dot{y} = -1 + ex + (g-1)xy + y^2 \tag{13}$$

for which we may assume $g > 0$ and $e \geq 0$ because this can be achieved via the transformation $(x, y, t) \rightarrow \xi(-x, y-x, t)$, where $\xi = -\text{sign}(e)$ (see also the proof of Lemma 4.4).

Next we construct the bifurcation diagram in the space (e, g) of systems (13) (see Figure 12).

As it can be detected directly from this diagram we have the next remark.

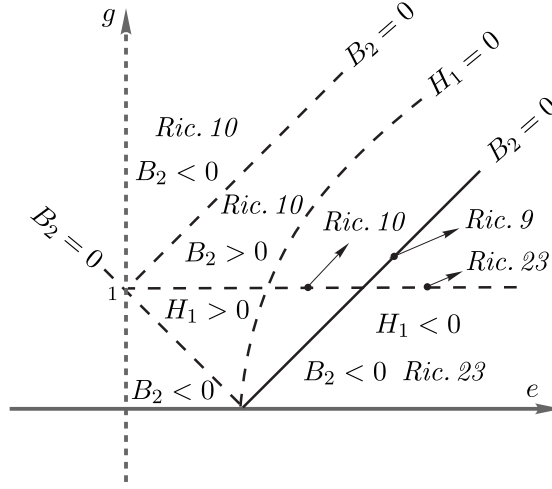


Figure 12: Bifurcation diagram of systems (13) for $g \neq 0$

Remark 4.12. The phase portraits of systems (13) with $\mu_0 \tilde{N} \neq 0$ correspond to the ones indicated below if the corresponding conditions on the left are satisfied, respectively:

$$\begin{aligned} B_2 > 0 &\Rightarrow Ric. 10; \\ B_2 < 0, H_1 < 0 &\Rightarrow Ric. 23; \\ B_2 < 0, H_1 > 0 &\Rightarrow Ric. 10. \end{aligned}$$

10: $\mu_0 \neq 0, H_{10} = 0, \mathbf{R} = 0 \Rightarrow Config. 3.23$. It is not so difficult to determine that the unique finite singularity of multiplicity four is a nilpotent saddle-node. More precisely two separatrices of this singular point form the invariant line $x = 0$ and the third one lies on one of the semi-planes divided by invariant line. As a result we arrive at the unique phase portrait which is equivalent to *Ric. 18*.

11: $\mu_0 = 0, \mu_2 \neq 0, \mathbf{D} < 0 \Rightarrow Config. 3.24$. According to [10] a system (8) possessing this configuration could be brought via an affine transformation and time rescaling to the canonical form (41) from [10], i.e. we consider the family of systems

$$\dot{x} = a + x, \quad \dot{y} = b - xy + y^2. \quad (14)$$

We observe that for $B_2 = -648b(1 - a + b)x^4 = 0$ the above systems gain an invariant straight line: $y = 0$ if $b = 0$ and $y = x + 1$ if $b = a - 1$. In the case $B_2 = 0$ we obtain *Config. 4.16* and as it was shown earlier (see page 26, p. 5:) this configuration generates two phase portraits: *Ric. 11* if $\mathcal{G}_2 < 0$ and *Ric. 12* if $\mathcal{G}_2 > 0$.

Since *Ric. 11* contains no separatrix connection it is clear that after breaking the non-vertical invariant line then we get the same phase portrait *Ric. 11*.

On the other hand *Ric. 12* contains a separatrix connection (which is part of the invariant line) and after breaking this connection we get either *Ric. 11* or *Ric. 24*. In order to determine the conditions for distinguishing these two phase portraits we construct the bifurcation diagram in the parameter space (a, b) of systems (14) (see Figure 13).

As it can be detected directly from this diagram we have the next remark.

Remark 4.13. A phase portrait of systems (14) with $\mathbf{D} < 0$ under one of the conditions indicated below on the left side is the portrait indicated on the right side.

$$\begin{aligned} \mathcal{G}_2 \leq 0 &\Rightarrow Ric. 11; \\ \mathcal{G}_2 > 0, B_2 < 0 &\Rightarrow Ric. 24; \\ \mathcal{G}_2 > 0, B_2 > 0 &\Rightarrow Ric. 11. \end{aligned}$$

transformation and time rescaling to the form (14) (from [10]), i.e. we arrive at the subfamily of the Riccati systems

$$\dot{x} = a + x^2, \quad \dot{y} = b + ex + y^2. \quad (15)$$

We observe that for these systems $\mu_0 = 1 > 0$ and since $\eta > 0$ we conclude that Remark 4.2 also is valid for the above systems. So systems (15) possess at infinity one saddle and two nodes, all elemental.

According to Diagram 1 we examine again two possibilities: $B_2 = 0$ and $B_2 \neq 0$.

4.1.2.1 The possibility $B_2 = 0$. Following Diagram 1 we examine the next cases considering the topological classifications of systems in the families $QSL_{\geq 4}$ given in the articles [19] and [21].

1: $H_4 \neq 0, H_8 < 0 \Rightarrow$ *Config. 4.13*. Since the condition $\tilde{N} = 0$ holds, according to [21] (see Table 2) we get the unique phase portrait *Portrait 4.13(b)* which is topologically equivalent to *Ric. 1*.

2: $H_4 \neq 0, H_8 > 0, H_9 \neq 0$ and either (i) $H_{16} < 0 \Rightarrow$ *Config. 4.9a* or (ii) $H_{16} > 0 \Rightarrow$ *Config. 4.9*. We examine these two cases together due to the inexactitude in [21] (as well as in [18]) concerning the configuration *Config. 4.9* (see Lemma 4.2). As it was shown earlier in the case $\tilde{N} \neq 0$ (see Remark 4.4) we distinguished which of the phase portraits *Portrait 4.9(a)*, *Portrait 4.9(b)* and *Portrait 4.9(c)* are generated by *Config. 4.9a* and which by *Config. 4.9*.

So we have to do the same in the case $\tilde{N} = 0$. First of all we give here the next lemma which is analog to Lemma 4.2 and the proof of which follows directly from [10] (see Lemma 6.2) and from [21] (see Table 2).

Lemma 4.8. *Assume that for an arbitrary quadratic system the conditions $\eta > 0, \theta = H_7 = B_2 = 0, \mu_0 B_3 H_4 H_9 \neq 0, \tilde{N} = 0$ and $H_8 > 0$ are satisfied. Then the configuration of the invariant lines of this system corresponds to *Config. 4.9a* if $H_{16} < 0$ and to *Config. 4.9* if $H_{16} > 0$. Moreover the phase portrait of this system corresponds to one of the portraits given below if and only if the corresponding set of the conditions hold, respectively:*

$$\begin{aligned} \text{Portrait 4.9(a)} &\Leftrightarrow \mathcal{G}_2 > 0, H_4 > 0, \mathcal{G}_3 < 0; \\ \text{Portrait 4.9(b)} &\Leftrightarrow \text{either } \mathcal{G}_2 > 0, H_4 < 0 \text{ or } \mathcal{G}_2 < 0; \\ \text{Portrait 4.9(c)} &\Leftrightarrow \mathcal{G}_2 > 0, H_4 > 0, \mathcal{G}_3 > 0. \end{aligned}$$

Next we would like to distinguish which of these three phase portraits is generated by the configuration *Config. 4.9a* and which by *Config. 4.9*.

Assume that for an arbitrary quadratic system (2) the conditions provided by Lemma 4.8 are satisfied. Then as it was shown in [10] (see the proof of Lemma 6.2), this system could be brought via an affine transformation and time rescaling to the 1-parameter family of systems

$$\dot{x} = x^2 - 1, \quad \dot{y} = -1 - e^2/4 + ex + y^2. \quad (16)$$

For these systems we calculate

$$H_4 = 96e^2, \quad H_{16} = 180(-2 + e)e^4(2 + e), \quad \mathcal{G}_2 = 13824(-2 + e)(2 + e), \quad \mathcal{G}_3 = -576e^2.$$

Since for the above systems the condition $H_4 \neq 0$ holds we obtain $H_4 > 0, \mathcal{G}_3 < 0$ and $\text{sign}(\mathcal{G}_2) = \text{sign}(H_{16})$. Therefore considering Lemma 4.8 we evidently arrive at the next remark.

Remark 4.14. *If for a quadratic system the conditions provided by Lemma 4.8 are satisfied then this system possesses the phase portrait *Portrait 4.9(b)* (i.e. *Ric. 3*) if $H_{16} < 0$ and *Portrait 4.9(a)* (i.e. *Ric. 5*) if $H_{16} > 0$.*

Observation 4.1. According to the above remark we conclude that in the case $\tilde{N} = 0$ the phase portrait *Portrait 4.9(c)* is not realizable.

3: $H_4 \neq 0, H_8 > 0, H_9 = 0 \Rightarrow$ *Config. 4.10*. According to [21] (see Table 2) due to the condition $\tilde{N} = 0$ we get the unique phase portrait *Portrait 4.10(c)* (\simeq *Ric. 7*).

4: $H_4 \neq 0, H_8 = 0 \Rightarrow$ *Config. 4.22*. By [21, Table 2] \Rightarrow *Portrait 4.22(b)* (\simeq *Ric. 9*).

5: $H_4 = 0, B_3 \neq 0, H_5 < 0 \Rightarrow$ *Config. 5.4*. By [19, Diagram 3] \Rightarrow *Picture 5.4* (\simeq *Ric. 2*).

6: $H_4 = 0, B_3 \neq 0, H_5 > 0, H_1 < 0 \Rightarrow$ *Config. 5.5*. By [19, Diagram 3] \Rightarrow *Picture 5.5* (\simeq *Ric. 2*).

7: $H_4 = 0, B_3 \neq 0, H_5 > 0, H_1 > 0 \Rightarrow$ *Config. 5.3*. By [19, Diagram 3] \Rightarrow *Picture 5.3* (\simeq *Ric. 3*).

8: $H_4 = 0, B_3 \neq 0, H_5 = 0, H_1 < 0 \Rightarrow$ *Config. 5.16*. By [19, Diagram 3] \Rightarrow *Picture 5.16* (\simeq *Ric. 2*).

9: $H_4 = 0, B_3 \neq 0, H_5 = 0, H_1 > 0 \Rightarrow$ *Config. 5.12*. By [19, Diagram 3] \Rightarrow *Picture 5.12* (\simeq *Ric. 10*).

10: $H_4 = 0, B_3 = 0, H_1 < 0 \Rightarrow$ *Config. 6.2*. By [19, Diagram 1] \Rightarrow *Picture 6.2* (\simeq *Ric. 1*).

11: $H_4 = 0, B_3 = 0, H_1 > 0 \Rightarrow$ *Config. 6.1*. By [19, Diagram 1] \Rightarrow *Picture 6.1* (\simeq *Ric. 3*).

12: $H_4 = 0, B_3 = 0, H_1 = 0 \Rightarrow$ *Config. 6.5*. By [19, Diagram 1] \Rightarrow *Picture 6.5* (\simeq *Ric. 14*).

4.1.2.2 The possibility $B_2 \neq 0$. By Lemma 3.1 systems (15) could possess invariant lines only in the direction $x = 0$.

In what follows we consider one by one all the configurations provided by Diagram 1 and we determine the corresponding phase portraits.

1: $H_8 < 0 \Rightarrow$ *Config. 3.14*. As it was shown in the case $\tilde{N} \neq 0$ this configuration leads to the unique phase portrait *Ric. 2*.

2: $H_8 > 0, \mathbf{D} < 0, H_{15} < 0 \Rightarrow$ *Config. 3.15*. We have exactly the same situation as in the previous case and so we arrive at the same phase portrait *Ric. 2*.

3: $H_8 > 0, \mathbf{D} < 0, H_{15} > 0 \Rightarrow$ *Config. 3.16*. Since for systems (15) we have

$$H_8 = -3456ae^2, \quad H_{15} = 1024ab, \quad B_2 = -648e^2(-4a + 4b + e^2)x^4$$

the conditions $B_2 \neq 0, H_8 > 0$ and $H_{15} > 0$ imply $e \neq 0, a < 0$ and $b < 0$. Therefore via the rescaling $(x, y, t) \mapsto (\sqrt{-a}x, \sqrt{-a}y, t/\sqrt{-a})$ we may assume $a = -1$ and we get the 2-parameter family of systems

$$\dot{x} = x^2 - 1, \quad \dot{y} = b + ex + y^2. \quad (17)$$

For these systems we calculate

$$\begin{aligned} H_{15} &= -1024b > 0, \quad B_2 = -648e^2(4 + 4b + e^2)x^4 \neq 0, \\ \mathbf{D} &= -12288(b - e)(b + e) < 0, \quad \mathcal{G}_2 = 27648(2b + e^2). \end{aligned}$$

Taking into account the curves defined by the equations $B_2 = 0, \mathbf{D} = 0$ and $\mathcal{G}_2 = 0$ we arrive at the bifurcation diagram for the phase portraits of systems (17) with the conditions $H_{15} > 0$ and $\mathbf{D} < 0$ (see Figure 14).

From this diagram it follows that under the provided conditions we get the phase portrait *Ric. 3* if $\mathcal{G}_2 \leq 0$. If $\mathcal{G}_2 > 0$ then we obtain *Ric. 15* for $B_2 < 0$ and *Ric. 3* for $B_2 > 0$.

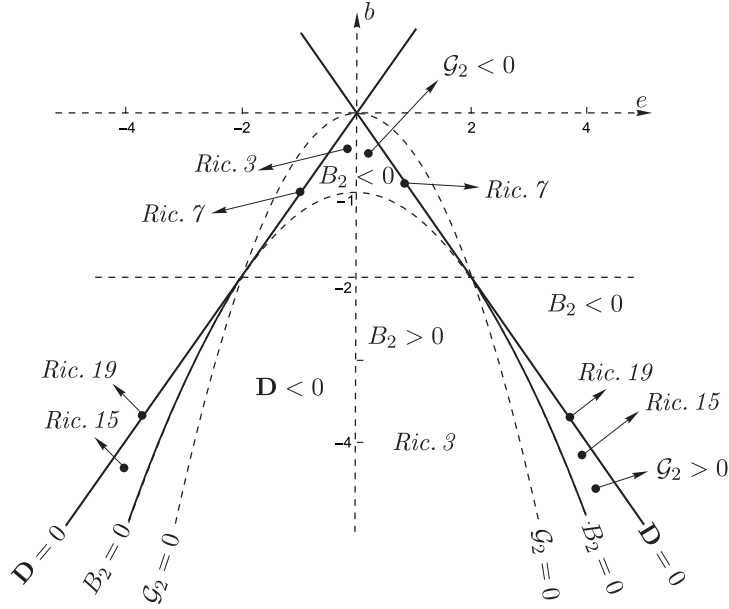


Figure 14: Bifurcation diagram for systems (17) with $b < 0$ and $b^2 - e^2 > 0$

4: $H_8 > 0, \mathbf{D} > 0 \Rightarrow \text{Config. 3.17}$. It was proved earlier (see page 39) that this configuration leads to the unique phase portrait *Ric. 17*.

5: $H_8 > 0, \mathbf{D} = 0, H_{15} < 0 \Rightarrow \text{Config. 3.18}$. As it was shown earlier (see page 40) *Config. 3.18* leads to the unique phase portrait *Ric. 18*.

6: $H_8 > 0, \mathbf{D} = 0, H_{15} > 0 \Rightarrow \text{Config. 3.19}$. We examined this configuration earlier (see page 40) and have shown that this configuration could only lead to the two phase portraits: *Ric. 19* and *Ric. 6*. More exactly, by coalescing the two singularities (a node and a saddle) on one of the invariant lines (i.e. when $\mathbf{D} \rightarrow 0$) from *Ric. 15* we obtain *Ric. 19*, whereas from *Ric. 3* we obtain *Ric. 6*.

Therefore considering diagram in Figure 14 we conclude that the phase portrait corresponds to *Ric. 19* for $\mathcal{G}_2 < 0$ and *Ric. 6* for $\mathcal{G}_2 > 0$.

7: $H_8 = 0, \mathbf{R} < 0 \Rightarrow \text{Config. 3.21}$. This configurations was investigated earlier in the case $\tilde{N} \neq 0$ and it was shown the existence of the unique phase portrait *Ric. 2* which also is realizable for $\tilde{N} = 0$.

8: $H_8 = 0, \mathbf{R} > 0 \Rightarrow \text{Config. 3.22}$. The condition $H_8 = -3456ae^2 = 0$ due to $B_2 \neq 0$ (i.e. $e \neq 0$) gives us $a = 0$ for systems (15) and then $\mathbf{R} = -16bx^2 > 0$ implies $b < 0$. Then we may assume $b = -1$ due to the rescaling $(x, y, t) \mapsto (\sqrt{-b}x, \sqrt{-b}y, t/\sqrt{-b})$ and we observe that in this case we get a subfamily of systems (13) defined by the condition $g = 1$.

So from the bifurcation diagram of systems (13) given in Figure 12, for systems (15) we obtain *Ric. 23* if $B_2 < 0$ and *Ric. 10* if $B_2 > 0$.

9: $H_8 = 0, \mathbf{R} = 0 \Rightarrow \text{Config. 3.23}$. As in the generic case $\tilde{N} \neq 0$ examined before we get the unique phase portrait *Ric. 18*.

4.2 The case $\eta < 0$

Following Diagram 2 we consider each one of the configurations of invariant lines in order to determine how many topological phase portraits could be obtained from each one of the configurations in the case when at infinity we have one real and two complex singularities.

1: $\mu_0 \neq 0, H_{10} < 0 \Rightarrow \text{Config. } 3.28$. Since we have only one real singularity at infinity which is a node (more precisely, a star node) we arrive at the unique phase portrait which we denote by *Ric. 28*.

2: $\mu_0 \neq 0, H_{10} > 0, \mathbf{D} < 0, H_{15} < 0 \Rightarrow \text{Config. } 3.29$. For the same arguments as in the previous paragraph we get the same phase portrait *Ric. 28*.

3: $\mu_0 \neq 0, H_{10} > 0, \mathbf{D} < 0, H_{15} > 0 \Rightarrow \text{Config. } 3.30$. This family has four finite singularities: two saddles and two nodes and one elemental infinite singularity which is a star node. Since there is no separatrix connection, systems having this configuration belong to family 3 of the structurally stable quadratic systems modulo limit cycles [2]. From the 5 possible phase portraits of this family it is easy to see that two of them ($\mathbb{S}_{3,1}^2$ and $\mathbb{S}_{3,5}^2$) are incompatible with the existence of two real parallel invariant lines. The other three, in the form they are presented in [2], seem to be compatible with the existence of two parallel real invariant lines. However the pictures given in [2] are topologically valid but not geometrically. The real pictures are much more twisted than the presented ones (see Figure 15). Here we will prove that the phase portraits $\mathbb{S}_{3,2}^2$ and $\mathbb{S}_{3,3}^2$ are impossible in the Riccati family.

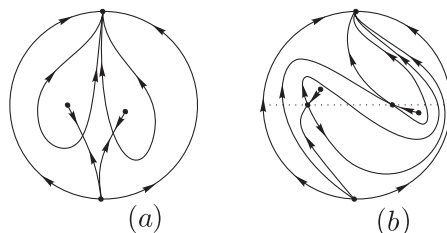


Figure 15: Example of phase portrait (a): $\mathbb{S}_{3,2}^2$ as given in [2] versus (b): real one

Suppose that we have a system possessing the configuration *Config. 3.30* and consider a straight line L passing through two finite saddles, located on the vertical invariant lines. Then by a time change we may assume that the flow on both unbounded segments of this line goes up. According to [3, Lemma 3.4] in the bounded segment the flow goes down. Then the other two points (which are nodes) are located on different parallel invariant lines and on different parts with respect to L (see Figure 16).

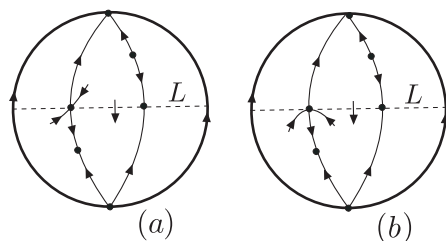


Figure 16: Impossibility of the phase portraits $\mathbb{S}_{3,2}^2$ and $\mathbb{S}_{3,3}^2$ from [2] in Riccati systems

What we see in Figure 16 is that we cannot send the two separatrices of the same finite saddle to the same infinite node. In the case (a) because one of the separatrices could not intersect the line L and in the case (b) because the flow on the line L is in contradiction with the position of the separatrices. This voids the possible existence of the phase portraits $\mathbb{S}_{3,2}^2$ and $\mathbb{S}_{3,3}^2$ from [2] in Riccati systems.

From the scheme given in Figure 16 it easily can be seen that it is impossible to force the two separatrices of one saddle to go to the same infinite singularity due to the direction of the flow on the line L .

Thus the configuration *Config. 3.30* leads to a unique phase portrait $\mathbb{S}_{3,4}^2$ from [2] which we denote by *Ric. 29*.

4: $\mu_0 \neq 0, H_{10} > 0, \mathbf{D} > 0, B_2 \neq 0 \Rightarrow$ *Config. 3.31*. Since we have only one saddle and one node located on the same vertical invariant straight line we arrive at the phase portrait which we denote by *Ric. 30*.

5: $\mu_0 \neq 0, H_{10} > 0, \mathbf{D} > 0, B_2 = 0 \Rightarrow$ *Config. 5.2*. By [19, Diagram 3] we obtain *Picture 5.2* (\simeq *Ric. 30*).

6: $\mu_0 \neq 0, H_{10} > 0, \mathbf{D} = 0, H_{15} < 0 \Rightarrow$ *Config. 3.32*. In this case the node and the saddle coalesced and the only possible phase portrait is $\mathbb{U}_{A,1}^1$ from [3] which we denote here by *Ric. 31*.

7: $\mu_0 \neq 0, H_{10} > 0, \mathbf{D} = 0, H_{15} > 0 \Rightarrow$ *Config. 3.33*. This configuration is obtained from *Config. 3.30* when a saddle and a node coalesced. Therefore we have to coalesce a saddle and a node from *Ric. 29* obtaining the phase portrait $\mathbb{U}_{A,7}^1$ from [3]. We denote here this phase portrait by *Ric. 32*.

8: $\mu_0 \neq 0, H_{10} > 0, \mathbf{D} = 0, H_{15} = 0 \Rightarrow$ *Config. 3.34*. This configuration could be obtained from *Config. 3.33* when the other couple of a saddle and a node coalesced. So we need to coalesce the saddle and the node from *Ric. 32* obtaining the phase portrait $\mathbb{U}_{AA,19}^2$ from [8]. We denote here this phase portrait by *Ric. 33*.

9: $\mu_0 \neq 0, H_{10} = 0, \mathbf{R} < 0 \Rightarrow$ *Config. 3.35*. Since there are no real finite singularities we get the unique phase portrait which is equivalent to *Ric. 28*.

10: $\mu_0 \neq 0, H_{10} = 0, \mathbf{R} > 0 \Rightarrow$ *Config. 3.36*. This configuration could be obtained from *Config. 3.30* by coalescing the two lines and moreover, the saddle (respectively the node) located on one line coalesced with the node (respectively the saddle) located on the other line. Then we get one separatrix of a saddle-node on each semi-plane and they both must go to the infinite singularities (in different directions). As a result we obtain a new phase portrait which we denote by *Ric. 34*.

11: $\mu_0 \neq 0, H_{10} = 0, \mathbf{R} = 0, B_2 \neq 0 \Rightarrow$ *Config. 3.37*. In these conditions we have a double line and a unique finite singularity which is of multiplicity four. We observe that the systems possessing *Config. 3.37* are not homogeneous, otherwise we must have invariant lines of total multiplicity at least four. So this singularity is nilpotent with index 0 and it must be a saddle-node. Therefore we get a phase portrait which is topologically equivalent to *Ric. 31*.

12: $\mu_0 \neq 0, H_{10} = 0, \mathbf{R} = 0, B_2 = 0 \Rightarrow$ *Config. 5.10*. According to [19, Diagram 3] we obtain *Picture 5.10* which is denoted here by *Ric. 35*.

13: $\mu_0 = 0, \mu_2 \neq 0, \mathbf{D} < 0 \Rightarrow$ *Config. 3.38*. This configuration can be obtained from *Config. 3.31* by coalescing the finite invariant line without real singularities with infinite line. As a result we obtain the same phase portrait *Ric. 30*.

14: $\mu_0 = 0, \mu_2 \neq 0, \mathbf{D} > 0, B_2 \neq 0 \Rightarrow$ *Config. 3.39*. This configuration can be obtained from *Config. 3.29* by coalescing one of the finite invariant lines with the infinite line. So we arrive at the phase portrait *Ric. 28*.

15: $\mu_0 = 0, \mu_2 \neq 0, \mathbf{D} > 0, B_2 = 0 \Rightarrow$ *Config. 5.9*. By [19, Diagram 3] we obtain *Picture 5.9* (\simeq *Ric. 30*).

16: $\mu_0 = 0, \mu_2 \neq 0, \mathbf{D} = 0 \Rightarrow$ *Config. 3.40*. This configuration can be obtained from *Config. 3.32* by coalescing the finite invariant line without real singularities with the infinite line. So the unique phase portrait is given by *Ric. 31*.

17: $\mu_0 = 0, \mu_2 = 0 \Rightarrow$ *Config. 3.41*. This configuration can be obtained from *Config. 3.39* by coalescing the finite invariant line with the infinite one. In this case we arrive at the phase portrait *Ric. 28*.

4.3 The case $\eta = 0, \widetilde{M} \neq 0$

According to the Diagram 3 we examine two subcases: $\widetilde{N} \neq 0$ and $\widetilde{N} = 0$.

4.3.1 The subcase $\widetilde{N} \neq 0$

Since $\eta = 0$ and $\widetilde{M} \neq 0$, according to Lemma 3.4 we consider the following canonical form:

$$\begin{aligned} \dot{x} &= a + cx + dy + gx^2 + hxy, \\ \dot{y} &= b + ex + fy + (g-1)xy + hy^2, \end{aligned} \quad (18)$$

for which by Lemma 3.7 the conditions $\theta = B_1 = H_7 = 0$ have to be fulfilled. As it was shown in [10] forcing these conditions in the case $\mu_0 \neq 0$ we arrive at the family of systems

$$\dot{x} = a + cx + x^2, \quad \dot{y} = b + xy + y^2 \quad (\mu_0 \neq 0) \quad (19)$$

and in the case $\mu_0 = 0$ we get the family of systems

$$\dot{x} = a + cx + gx^2, \quad \dot{y} = b + (g-1)xy \quad (\mu_0 = 0). \quad (20)$$

So in what follows we consider two possibilities: $\mu_0 \neq 0$ and $\mu_0 = 0$.

4.3.1.1 The possibility $\mu_0 \neq 0$. In this case we consider systems (19) for which the following remark is valid.

Remark 4.15. *The singular point $N_1[1 : 0 : 0]$ of systems (19) is a saddle-node of the type $\binom{0}{2}SN$, because it is a double singularity obtained by coalescence of two infinite singularities. The elemental singular point $N_2[0 : 1 : 0]$ is a star node, because the corresponding Jacobian matrix is of the form $\begin{pmatrix} 1 & 0 \\ 0 & 1 \end{pmatrix}$.*

According to Diagram 3 we have to examine two cases: $B_2 \neq 0$ and $B_2 = 0$. However as it was pointed out earlier in the case $\eta > 0$, we begin with $B_2 = 0$ because in this case the systems belong to a higher codimension subfamilies and these subfamilies form a skeleton from which systems will bifurcate into systems with $B_2 \neq 0$.

4.3.1.1.1 The case $B_2 = 0$. Following Diagram 3 we examine one by one the corresponding cases.

1: $B_3 \neq 0, H_{10} < 0 \Rightarrow$ *Config. 4.14*. Since we are in the class of quadratic systems possessing invariant lines of total multiplicity ≥ 4 we use the classifications given in [21] and [19].

According to this classification (see [21, Table 2]) the configuration *Config. 4.14* leads to the unique phase portrait *Portrait 4.14* which we denote here by *Ric. 36*.

2: $B_3 \neq 0, H_{10} > 0$ and either (i) $H_4 < 0 \Rightarrow$ *Config. 4.11* or (ii) $H_4 > 0 \Rightarrow$ *Config. 4.11a*. We examine these two cases together in the paper [21] (as well as in [18]) there is omitted the configuration *Config. 4.11a*. This mistake was corrected in [10] (see Remark 6.6 and Lemma 6.4) where it was proved that the invariant polynomial H_4 distinguishes these two configurations as it is indicated above. Moreover as it was proved in [21] (see Table 2) that this invariant polynomial distinguishes also the phase portraits *Portrait 4.11(b)* and *Portrait 4.11(a)*. We denote them here by *Ric. 37* and *Ric. 38*, respectively.

Thus according to [21, Table 2] we get *Ric. 37* if $H_4 < 0$ and *Ric. 38* if $H_4 > 0$.

3: $B_3 \neq 0, H_{10} = 0 \Rightarrow \text{Config. 4.23}$. By [21, Table 2] this configuration gives us only the phase portrait *Portrait 4.23* which we denote by *Ric. 39*.

4: $B_3 = 0, \tilde{D} \neq 0 \Rightarrow \text{Config. 5.11}$. According to [19, Diagram 3] we obtain *Picture 5.11* which is denoted here by *Ric. 40*.

5: $B_3 = 0, \tilde{D} = 0 \Rightarrow \text{Config. 5.19}$. By [19, Diagram 3] we get *Picture 5.19* which we denote by *Ric. 41*.

4.3.1.1.2 The case $B_2 \neq 0$. According to Diagram 3 we consider the next cases as follows.

1: $H_{10} < 0 \Rightarrow \text{Config. 3.42}$. This configuration can be derived from *Config. 4.14* by breaking the separatrix connection which is the straight line defined by the condition $b = 0$ in the systems (19). More exactly, if we perturb these systems, making $0 < |b| \ll 1$ then we detect that taking perturbation $b > 0$ we get a new phase portrait which we denote by *Ric. 42*. In the case $b < 0$ we also obtain a new phase portrait which we denote by *Ric. 43*.

On the other hand for systems (19) we calculate $H_1 = -576b$, i.e. $\text{sign}(H_1) = -\text{sign}(b)$. So we get *Ric. 42* if $H_1 < 0$ and *Ric. 43* if $H_1 > 0$.

2: $H_{10} > 0, \mathbf{D} < 0, H_{15} < 0 \Rightarrow \text{Config. 3.43}$. The singularities in this configuration are exactly the same as in *Config. 3.42*. However the existence of real invariant parallel lines makes impossible to obtain it from a perturbation of *Config. 4.14*. Therefore in this case we obtain the unique phase portrait which is topologically equivalent to *Ric. 42*.

3: $H_{10} > 0, \mathbf{D} < 0, H_{15} > 0 \Rightarrow \text{Config. 3.44}$. This configuration can be obtained from *Config. 3.16* by coalescing of the infinite singularity $N_2[1 : 1 : 0]$ with $N_1[1 : 0 : 0]$ obtaining a double singular point. As it was proved earlier (see page 34) the configuration *Config. 3.16* generates three phase portraits: *Ric. 3*, *Ric. 15* and *Ric. 16*. Moreover Lemma 4.6 provides the necessary and sufficient conditions for the realization of each one of the three phase portraits.

We determine that for systems (19) we have $\tilde{N} = x^2 > 0$. On the other hand according to Lemma 4.6 the condition $\tilde{N} < 0$ is necessary for the existence of the phase portrait *Ric. 15*. So we deduce that after any perturbation from a phase portrait generated by *Config. 3.44* we cannot obtain *Ric. 15*. This means that by coalescing the two infinite singularities (as it is described above) we could obtain only two phase portraits: one from *Ric. 3* which is topologically equivalent to *Ric. 37* and one from *Ric. 16* which is new and we denote it by *Ric. 44*.

On the other hand for systems (19) we have $B_2 = -648b^2x^4 < 0$. Therefore considering the conditions for distinguishing the phase portraits *Ric. 3* and *Ric. 16* provided by Lemma 4.6 we conclude that we have *Ric. 37* if either $\mathcal{G}_2 \leq 0$ or $\mathcal{G}_2 > 0$ and $H_{16} < 0$. In the case $\mathcal{G}_2 > 0$ and $H_{16} > 0$ we have the phase portrait *Ric. 44*.

4: $H_{10} > 0, \mathbf{D} > 0 \Rightarrow \text{Config. 3.45}$. This configuration can be obtained from *Config. 3.17* by coalescing the infinite singularity $N_2[1 : 1 : 0]$ with $N_1[1 : 0 : 0]$. Since *Config. 3.17* generates a single phase portrait then in this case we also obtain the unique phase portrait which is new and we denote by *Ric. 45*.

5: $H_{10} > 0, \mathbf{D} = 0, H_{15} < 0 \Rightarrow \text{Config. 3.46}$. This configuration can be obtained from *Config. 3.18* by coalescing the infinite singularity $N_2[1 : 1 : 0]$ with $N_1[1 : 0 : 0]$. Since *Config. 3.18* generates a single phase portrait then in this case we also obtain the unique phase portrait which is new and we denote it by *Ric. 46*.

6: $H_{10} > 0, \mathbf{D} = 0, H_{15} > 0 \Rightarrow \text{Config. 3.47}$. This configuration can be obtained from *Config. 3.19* by coalescing the infinite singularity $N_2[1 : 1 : 0]$ with $N_1[1 : 0 : 0]$ in the same way as

Config. 3.44 came from *Config. 3.16*. Therefore we obtain two new phase portraits: one from *Ric. 37* which we denote by *Ric. 47* and one from *Ric. 44* which we denote by *Ric. 48*.

Thus considering the conditions for distinguishing the phase portraits *Ric. 37* and *Ric. 44* we conclude that we have *Ric. 47* if either $\mathcal{G}_2 \leq 0$ or $\mathcal{G}_2 > 0$ and $H_{16} < 0$. In the case $\mathcal{G}_2 > 0$ and $H_{16} > 0$ we have the phase portrait *Ric. 48*.

7: $H_{10} > 0, \mathbf{D} = 0, H_{15} = 0 \Rightarrow$ *Config. 3.48*. This configuration can be obtained from *Config. 3.47* by coalescing the elemental finite singularities along the invariant line on which they are located.

For systems (19) we calculate

$$\begin{aligned} H_{10} &= -8(4a - c^2), & H_{15} &= 32(4a - c^2)(2a + 8b - c^2), \\ \mathbf{D} &= -48(4a - c^2)^2[(a + 4b)^2 - 4bc^2]. \end{aligned}$$

Since $H_{10} > 0$ the condition $H_{15} = 0$ yields $a = \frac{1}{2}(c^2 - 8b)$. Then the last factor in \mathbf{D} (which must be zero) gives $-c^2(16b - c^2)/4 = 0$ and due to $H_{10} \neq 0$ we get $c = 0$. Then $a = -4b$ and for these values of the parameters a and c for (19) we have:

$$H_{16} = -184320b^4, \quad H_{10} = 128b.$$

So since $H_{10} \neq 0$ we get $H_{16} < 0$ and considering the conditions for the realization of the phase portraits *Ric. 47* and *Ric. 48* we conclude that *Ric. 48* could not produce any phase portrait by coalescing the elemental finite singularities. So *Config. 3.48* generates only one phase portrait which we denote by *Ric. 49*.

8: $H_{10} = 0, \mathbf{R} < 0 \Rightarrow$ *Config. 3.49*. This configuration can be obtained from *Config. 3.43* by coalescing the two real invariant lines obtaining one double without real finite singularities. Since *Config. 3.43* generates only the phase portrait *Ric. 42* we also obtain here the unique phase portrait which is topologically equivalent to *Ric. 42*.

9: $H_{10} = 0, \mathbf{R} > 0 \Rightarrow$ *Config. 3.50*. This configuration can be obtained from *Config. 4.23* which implies the phase portrait *Ric. 39*. We observe that by breaking the separatrix connection between the infinite saddle-node and a finite one we can produce two different phase portraits which are new and we denote them by *Ric. 50* and *Ric. 51*.

We observe that for the systems (19) the condition $H_{10} = -8(4a - c^2) = 0$ yields $a = c^2/4$ and this leads to the family of systems

$$\dot{x} = (x + c/2)^2, \quad \dot{y} = b + xy + y^2.$$

So for $b = 0$ these systems possess the invariant line $y = 0$. Therefore the parameter b governs the breaking of the separatrix connection and the invariant polynomial which is responsible for the sign of this parameter is $H_1 = -576b$. Thus we have $\text{sign}(H_1) = -\text{sign}(b)$ and we arrive at the phase portrait *Ric. 50* if $H_1 < 0$ and at *Ric. 51* if $H_1 > 0$.

10: $H_{10} = 0, \mathbf{R} = 0 \Rightarrow$ *Config. 3.51*. This configuration can be obtained from *Config. 3.23* by coalescing the infinite singularity $N_2[1 : 1 : 0]$ with $N_1[1 : 0 : 0]$. Since *Config. 3.23* generates a single phase portrait (*Ric. 18*) then in this case we also obtain the unique phase portrait which is topologically equivalent to *Ric. 46*.

4.3.1.2 The possibility $\mu_0 = 0$. In this case we consider systems (20) for which we calculate:

$$\begin{aligned} \mu_0 = \mu_1 = B_2 &= 0, & \mu_2 &= ag(g - 1)^2x^2, & B_3 &= -3b(g - 1)^2, \\ \tilde{N} &= (g^2 - 1)x^2, & \tilde{K} &= 2g(g - 1)x^3. \end{aligned} \tag{21}$$

So we examine two cases: $B_3 = 0$ and $B_3 \neq 0$.

4.3.1.2.1 The case $B_3 = 0$. Due to $\tilde{N} \neq 0$ we get $b = 0$ and hence systems (20) have an additional invariant line $y = 0$. This means that these systems belong to the class $\mathbf{QSL}_{\geq 4}$ and we shall use the classifications given in [21] and [19].

We point out that in the case $\tilde{K} \neq 0$ and $B_3 = 0$ (i.e. $b = 0$) the condition $\mu_2 = 0$ leads to degenerate systems because considering (21) these conditions give us $a = 0$ (due to $\tilde{K} \neq 0$) and then the right hand sides of systems (20) have the common factor x .

So considering Remark 4.1 in the case $\tilde{K} \neq 0$ we assume $\mu_2 \neq 0$.

We follow step by step the branch of the Diagram 3 corresponding to the case $B_3 = 0$.

1: $H_6 \neq 0, \tilde{K} \neq 0, H_{11} < 0 \Rightarrow$ *Config. 4.15*. According to [21, Table 2]) the configuration *Config. 4.15* generates two distinct phase portraits *Portrait 4.15(a)* and *Portrait 4.15(b)*. They are new and we denoted the second one by *Ric. 52* and the first one *Ric. 53*.

According to [21, Table 2] the phase portrait *Ric. 52* is realizable for $\tilde{L} < 0$ whereas *Ric. 53* for $\tilde{L} > 0$.

2: $H_6 \neq 0, \tilde{K} \neq 0, H_{11} > 0 \Rightarrow$ *Config. 4.12*. By [21, Table 2]) this configuration generates 5 topologically distinct phase portraits *Portrait 4.12(a)* - *Portrait 4.12(e)*. Moreover in [21, Table 2]) there are determined necessary and sufficient affine invariant conditions for the realization of each one of the indicated phase portraits. More exactly we have the next remark.

Remark 4.16. For $\mu_2 \neq 0$ *Config. 4.12* generates the following five phase portraits indicated below if the corresponding conditions are satisfied (we denote them respectively as it is indicated):

$$\begin{aligned} \mu_2 < 0, \tilde{K} < 0 &\Rightarrow \text{Portrait 4.12(c)} \Rightarrow \text{Ric. 54;} \\ \mu_2 < 0, \tilde{K} > 0, \tilde{L} < 0 &\Rightarrow \text{Portrait 4.12(e)} \Rightarrow \text{Ric. 55;} \\ \mu_2 < 0, \tilde{K} > 0, \tilde{L} > 0 &\Rightarrow \text{Portrait 4.12(d)} \Rightarrow \text{Ric. 56;} \\ \mu_2 > 0, \tilde{L} < 0 &\Rightarrow \text{Portrait 4.12(b)} \Rightarrow \text{Ric. 57;} \\ \mu_2 > 0, \tilde{L} > 0 &\Rightarrow \text{Portrait 4.12(a)} \Rightarrow \text{Ric. 58.} \end{aligned}$$

3: $H_6 \neq 0, \tilde{K} \neq 0, H_{11} = 0 \Rightarrow$ *Config. 4.24*. According to [21, Table 2]) this configuration generates two topologically distinct phase portraits: *Portrait 4.24(a)* and *Portrait 4.24(b)*. Furthermore in the case $\tilde{L} < 0$ we have *Portrait 4.24(b)* (we denote it by *Ric. 59*) whereas for $\tilde{L} > 0$ we obtain *Portrait 4.24(a)* (which we denote by *Ric. 60*).

4: $H_6 \neq 0, \tilde{K} = 0, H_{11} \neq 0 \Rightarrow$ *Config. 4.19*. By [21, Table 2]) we arrive at two topologically distinct phase portraits: *Portrait 4.19(a)* and *Portrait 4.19(b)*. Moreover as it was proved in [21] (see Table 2) in the case $\mu_3 K_1 < 0$ we have *Portrait 4.19(a)* (we denote it by *Ric. 61*) and for $\mu_3 K_1 > 0$ we obtain *Portrait 4.19(b)* (which we denote by *Ric. 62*).

5: $H_6 \neq 0, \tilde{K} = 0, H_{11} = 0 \Rightarrow$ *Config. 4.36*. According to [21, Table 2]) this configuration generates two topologically distinct phase portraits: *Portrait 4.36(a)* and *Portrait 4.36(b)*. Furthermore in the case $\kappa_2 < 0$ we have *Portrait 4.36(a)* (which is topologically equivalent to *Ric. 53*) whereas for $\kappa_2 > 0$ we obtain *Portrait 4.36(b)* (which is topologically equivalent to *Ric. 52*).

6: $H_6 = 0, \tilde{K} \neq 0 \Rightarrow$ *Config. 5.14*. So we are in the class of systems possessing invariant lines of total multiplicity five. According to [19] (see Diagram 3) this configuration leads to the two phase portraits: *Picture 5.14(a)* (which is equivalent to *Ric. 58*) and *Picture 5.14(b)* (which is equivalent to *Ric. 56*). Considering [19] (see page 2053) we deduce that in this case *Ric. 56* is realizable for $\mu_2 < 0$, whereas we get *Ric. 58* for $\mu_2 > 0$.

6: $H_6 = 0, \tilde{K} = 0 \Rightarrow$ *Config. 5.18*. According to [19] (see Diagram 3) this configuration leads to the unique phase portrait *Picture 5.18* (\simeq *Ric. 62*).

4.3.1.2.2 The case $B_3 \neq 0$. According to Diagram 3 we examine the next possibilities.

1: $H_6 \neq 0, \mu_2 \neq 0, H_{11} < 0 \Rightarrow \text{Config. 3.52}$. This configuration can be obtained from *Config. 4.15* by breaking the real invariant line. As it was shown earlier (see point **1**: in the case $B_3 = 0$ above) *Config. 4.15* leads to the two phase portraits: *Ric. 52* (for $\tilde{L} < 0$) and *Ric. 53* (for $\tilde{L} > 0$).

We observe that *Ric. 52* has no affine separatrix connection and by breaking the line we could not produce a new phase portrait. At the same time *Ric. 53* has a separatrix which is the line itself. So breaking it we can produce two phase portraits which due to symmetry are topologically equivalent getting a unique new phase portrait which we denote by *Ric. 63*.

Thus we obtain *Ric. 52* for $\tilde{L} < 0$ and *Ric. 63* for $\tilde{L} > 0$.

2: $H_6 \neq 0, \mu_2 \neq 0, H_{11} > 0 \Rightarrow \text{Config. 3.53}$. Similarly as in the previous case this configuration is related with *Config. 4.12*, which generates 5 phase portraits: *Ric. 54 - Ric. 58* (see Remark 4.16).

As in the previous case phase portraits *Ric. 55, Ric. 56* and *Ric. 58* do not have separatrix connections and so the breaking of the horizontal invariant line we obtain the same phase portrait, correspondingly.

On the other hand each one of the phase portraits *Ric. 54* and *Ric. 57* after breaking the invariant line (which is a separatrix connection) produces only one new phase portrait because of the symmetry. We denote them by *Ric. 64* and *Ric. 65*, respectively.

Considering Remark 4.16 we get the following affine invariant criteria for the realization of each one of the phase portraits mentioned above.

Remark 4.17. *The configuration Config. 3.53 generates the following five phase portraits indicated below if the corresponding conditions are satisfied:*

$$\begin{aligned} \mu_2 < 0, \tilde{K} < 0 &\Rightarrow \text{Ric. 64;} \\ \mu_2 < 0, \tilde{K} > 0, \tilde{L} < 0 &\Rightarrow \text{Ric. 55;} \\ \mu_2 < 0, \tilde{K} > 0, \tilde{L} > 0 &\Rightarrow \text{Ric. 56;} \\ \mu_2 > 0, \tilde{L} < 0 &\Rightarrow \text{Ric. 65;} \\ \mu_2 > 0, \tilde{L} > 0 &\Rightarrow \text{Ric. 58.} \end{aligned}$$

3: $H_6 \neq 0, \mu_2 \neq 0, H_{11} = 0 \Rightarrow \text{Config. 3.54}$. This configuration can be obtained from *Config. 4.24* by breaking the real simple invariant line. As it was shown earlier (see point **3**: in the case $B_3 = 0$ above) *Config. 4.24* leads to the two phase portraits: *Ric. 59* (for $\tilde{L} < 0$) and *Ric. 60* (for $\tilde{L} > 0$). We observe that *Ric. 60* does not have separatrix connection outside the double vertical line and hence we could not produce new phase portraits by breaking the horizontal invariant line. The phase portrait *Ric. 59* has a separatrix connection (being a part of the horizontal invariant line) and breaking this invariant line due to the symmetry we get a single phase portrait. It is new and we denote it by *Ric. 66*.

4: $H_6 \neq 0, \mu_2 = 0, \tilde{K} \neq 0 \Rightarrow \text{Config. 3.55}$. Since $\tilde{K} \neq 0$, according to (21) the condition $\mu_2 = 0$ gives us $a = 0$ and the systems (20) have the form

$$\dot{x} = x(c + gx), \quad \dot{y} = b + (g - 1)xy. \quad (22)$$

For these systems we have

$$\begin{aligned} \eta = 0, \tilde{M} = -8x^2, \mu_0 = \mu_1 = \mu_2 = 0, \mu_3 = -bcg(g - 1)x^3, B_3 = -3b(g - 1)^2x^4, \\ \tilde{N} = (g^2 - 1)x^2, \tilde{K} = 2g(g - 1)x^3, \tilde{L} = 8gx^2, H_6 = -128c^2(g - 1)^4x^6 \end{aligned}$$

and due to $B_3\tilde{K}H_6 \neq 0$ we get $\mu_3\tilde{L} \neq 0$. So according to [17, Table 4] (see also [5, Diagram 6.3]) we conclude that the behavior of the trajectories in the vicinity of infinity corresponds to three

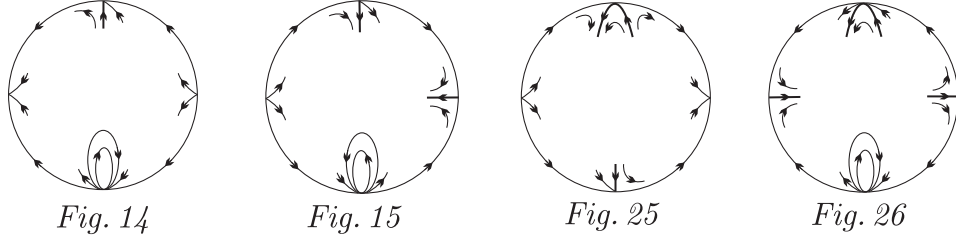


Figure 17: Some configurations of infinite singularities for systems (20)

of those presented in Figure 17 and are governed by the invariant polynomials \tilde{K} and \tilde{L} . More exactly, according to [17, Table 4] we have *Fig. 14* if $\tilde{K} < 0$; *Fig. 26* if $\tilde{K} > 0$ and $\tilde{L} < 0$ and we have *Fig. 25* if $\tilde{K} > 0$ and $\tilde{L} > 0$.

Taking into consideration that systems (22) possess two real parallel invariant lines intersecting at infinity at the intricate singular point $N_2[0 : 1 : 0]$ it is not too difficult to determine that we arrive at three new phase portraits which we denote as following: *Ric. 67* if $\tilde{K} < 0$; *Ric. 68* if $\tilde{K} > 0$ and $\tilde{L} < 0$ and *Ric. 69* if $\tilde{K} > 0$ and $\tilde{L} > 0$.

5: $H_6 \neq 0, \mu_2 = 0, \tilde{K} = 0, \mu_3 \neq 0 \Rightarrow$ *Config. 3.56*. This configuration can be obtained from *Config. 4.19* by breaking the real horizontal invariant line. As it was shown earlier (see point **4**: in the case $B_3 = 0$ above) *Config. 4.19* leads to the two phase portraits: *Ric. 61* (for $\mu_3 K_1 < 0$) and *Ric. 62* (for $\mu_3 K_1 > 0$).

We observe that in the case of *Ric. 62* the invariant line under discussion is not a separatrix connection and hence, by breaking this line we obtain the same phase portrait.

On the other hand in *Ric. 61* this line is a separatrix connection and considering Corollary 4.1 we deduce that by breaking the horizontal invariant line the separatrix connection disappears. Therefore due to a symmetry we obtain a single phase portrait which is new and we denote it by *Ric. 70*. Therefore for $\mu_3 K_1 < 0$ we get *Ric. 70* and for $\mu_3 K_1 > 0$ we get *Ric. 62*.

6: $H_6 \neq 0, \mu_2 = 0, \tilde{K} = 0, \mu_3 = 0, H_3 \neq 0 \Rightarrow$ *Config. 3.57*. This configuration can be obtained from *Config. 4.36* by breaking the real invariant line. As it was shown earlier (see point **5**: in the case $B_3 = 0$ above) *Config. 4.36* generates two phase portraits: *Ric. 53* (for $\kappa_2 < 0$) and *Ric. 52* (for $\kappa_2 > 0$).

We observe that in the case of *Ric. 53* the invariant line under discussion is not a separatrix connection and hence, by breaking this line we obtain the same phase portrait.

On the other hand in *Ric. 52* this line is a separatrix connection and considering Corollary 4.1 we deduce that by breaking the horizontal invariant line the separatrix connection disappears. Therefore due to a symmetry we obtain a single phase portrait which is topologically equivalent to *Ric. 63*. So for $\kappa_2 < 0$ we obtain and *Ric. 53* and for $\kappa_2 > 0$ we obtain *Ric. 63*.

7: $H_6 \neq 0, \mu_2 = 0, \tilde{K} = 0, \mu_3 = 0, H_3 = 0 \Rightarrow$ *Config. 3.58*. Considering (21) we observe that for systems (20) the conditions $\tilde{K} = 0$ and $B_2 \neq 0$ yield $g = 0$ and this implies $\mu_2 = 0$. Then for systems (20) we calculate $H_3 = 8ax^2$ and therefore the condition $H_3 = 0$ gives $a = 0$. As a result we arrive at the family of systems

$$\dot{x} = cx, \quad \dot{y} = b - xy. \quad (23)$$

for which we calculate:

$$\begin{aligned} \eta = 0, \quad \tilde{M} = -8x^2, \quad \mu_0 = \mu_1 = \mu_2 = \mu_3 = 0, \quad \mu_4 = -bc^2x^3y, \\ \kappa = \kappa_1 = \tilde{L} = 0, \quad K_1 = -cx^2y, \quad H_6 = -128c^2x^6. \end{aligned}$$

The condition $H_6 \neq 0$ implies $\mu_4 K_1 \neq 0$ and according to [17, Table 4] (see also [5, Diagram 6.3]) we conclude that the behavior of the trajectories in the vicinity of infinity corresponds to *Fig. 15* in Figure 17.

Taking into consideration the invariant line passing through intricate infinite singularity it is not too difficult to determine that we get a new phase portrait denoted here by *Ric. 71*.

8: $H_6 = 0, \tilde{K} \neq 0, H_{11} \neq 0 \Rightarrow$ *Config. 4.30*. According to [21, Table 2] this configuration generates two topologically distinct phase portraits: *Portrait 4.30(a)* if $\mu_2 > 0$ and *Portrait 4.30(b)* if $\mu_2 < 0$. We observe that the first phase portrait is topologically equivalent to *Ric. 58* and the second to *Ric. 55*.

9: $H_6 = 0, \tilde{K} \neq 0, H_{11} = 0 \Rightarrow$ *Config. 3.43*. By [21, Table 2] this configuration generates three phase portraits: *Portrait 4.43(a)* if $\tilde{L} < 0$; *Portrait 4.43(b)* if $\tilde{L} > 0$ and $R \geq 0$ and *Portrait 4.43(c)* if $\tilde{L} > 0$ and $R < 0$. We determine that *Portrait 4.43(a)* \simeq *Ric. 63* and *Portrait 4.43(b)* \simeq *Ric. 36* whereas *Portrait 4.43(c)* is new and we denote it by *Ric. 72*.

10: $H_6 = 0, \tilde{K} = 0 \Rightarrow$ *Config. 4.40*. According to [21, Table 2] this configuration leads to the unique phase portrait *Picture 4.40* (\simeq *Ric. 62*).

4.3.2 The subcase $\tilde{N} = 0$

According to Diagram 3 we have to consider two possibilities: $\tilde{K} \neq 0$ and $\tilde{K} = 0$.

4.3.2.1 The possibility $\tilde{K} \neq 0$. As it was shown in [10] in this case a quadratic system with $\theta_3 \neq 0$ could not belong to the class \mathbf{QSL}^{2p} and hence, it could neither belong to the family \mathbf{QS}_{Ric} .

On the other hand according to [10] for $\theta_3 = 0$ this system could be brought via an affine transformation and time rescaling to the form (24) (from [10]), i.e. we arrive at the subfamily of the Riccati systems

$$\dot{x} = a + cx - x^2, \quad \dot{y} = b - 2xy. \quad (24)$$

For these systems we have $B_3 = -12bx^4$ and we consider two cases: $B_3 = 0$ and $B_3 \neq 0$.

4.3.2.1.1 The case $B_3 = 0$. Then we have $b = 0$ and hence systems (24) have an additional invariant line $y = 0$. This means that these systems belong to the class $\mathbf{QSL}_{\geq 4}$ and we shall use the classifications given in [21] and [19] for the systems in this class.

We follow step by step the branch of the Diagram 3 corresponding to the case $B_3 = 0$.

1: $H_6 \neq 0, H_{11} < 0 \Rightarrow$ *Config. 4.15*. As it was shown earlier (see page 53) this configuration leads to the phase portrait *Ric. 52* if $\tilde{L} < 0$ and to *Ric. 53* for $\tilde{L} > 0$. However for systems (24) with $b = 0$ we have $\tilde{L} = -8x^2 < 0$ and hence only the phase portrait *Ric. 52* is realizable in this case.

2: $H_6 \neq 0, H_{11} > 0 \Rightarrow$ *Config. 4.12*. In the generic case $\tilde{N} \neq 0$ this configuration generates five topologically distinct phase portraits (see Remark 4.16). However in the case $\tilde{N} = 0$ only two of them are realizable. Indeed, for systems (24) we calculate:

$$\mu_2 = -4ax^2, \quad \tilde{K} = 4x^2, \quad \tilde{L} = -8x^2 \quad (25)$$

and hence the conditions $\tilde{K} > 0$ and $\tilde{L} < 0$ hold. Therefore considering Remark 4.16 we get *Ric. 55* if $\mu_2 < 0$ and *Ric. 57* if $\mu_2 > 0$.

3: $H_6 \neq 0, H_{11} = 0 \Rightarrow$ *Config. 4.24*. As it was shown earlier (see page 53) the configuration *Config. 4.24* generates two phase portraits: *Ric. 59* if $\tilde{L} < 0$ and *Ric. 60* for $\tilde{L} > 0$. However as

it is mentioned in previous case the condition $\tilde{L} < 0$ holds for systems (24) with $b = 0$. Therefore we obtain the unique phase portrait *Ric. 59*.

4: $H_6 = 0, H_{11} < 0 \Rightarrow$ *Config. 6.9*. According to [19] (see Diagram 1) this configuration leads to the unique phase portrait *Picture 6.9* (\simeq *Ric. 52*).

5: $H_6 = 0, H_{11} > 0 \Rightarrow$ *Config. 6.8*. By [19] (see Diagram 1) this configuration leads to the unique phase portrait *Picture 6.8* (\simeq *Ric. 55*).

4.3.2.1.2 The case $B_3 \neq 0$. Then $b \neq 0$ and the line $y = 0$ is not invariant for systems (24). According to Diagram 3 we examine the next possibilities.

1: $H_6 \neq 0, \mu_2 \neq 0, H_{11} < 0 \Rightarrow$ *Config. 3.52*. We have examined this configuration in the generic case $\tilde{N} \neq 0$ and we obtained two phase portraits: *Ric. 52* (for $\tilde{L} < 0$) and *Ric. 63* (for $\tilde{L} > 0$). Since for systems (24) we have $\tilde{L} = -8x^2 < 0$ it follows that only *Ric. 52* is realizable in the case considered.

2: $H_6 \neq 0, \mu_2 \neq 0, H_{11} > 0 \Rightarrow$ *Config. 3.53*. In the generic case $\tilde{N} \neq 0$ we proved (see Remark 4.17) that the configuration *Config. 3.53* generates five topologically distinct phase portraits. Considering (25) for systems (24) the conditions $\tilde{K} > 0$ and $\tilde{L} < 0$ hold. Therefore considering Remark 4.17 we get *Ric. 55* if $\mu_2 < 0$ and *Ric. 65* if $\mu_2 > 0$.

3: $H_6 \neq 0, \mu_2 \neq 0, H_{11} = 0 \Rightarrow$ *Config. 3.54*. As it was shown in the generic case $\tilde{N} \neq 0$ this configuration leads to the two phase portraits: *Ric. 66* (for $\tilde{L} < 0$) and *Ric. 60* (for $\tilde{L} > 0$). Since for systems (24) we have $\tilde{L} < 0$ (see the previous case) we conclude that in this case we have the unique phase portrait *Ric. 66*.

4: $H_6 \neq 0, \mu_2 = 0 \Rightarrow$ *Config. 3.55*. We have examined this configuration in the generic case $\tilde{N} \neq 0$ and we obtained three phase portraits: *Ric. 67* if $\tilde{K} < 0$; *Ric. 68* if $\tilde{K} > 0$ and $\tilde{L} < 0$ and *Ric. 69* if $\tilde{K} > 0$ and $\tilde{L} > 0$. Since from (25) for systems (24) we have $\tilde{K} > 0$ and $\tilde{L} < 0$, we conclude that in the considered case only *Ric. 68* is realizable.

5: $H_6 = 0, H_{11} < 0 \Rightarrow$ *Config. 5.25*. According to [19] (see Diagram 3) this configuration leads to the unique phase portrait *Picture 5.25* (\simeq *Ric. 63*).

6: $H_6 = 0, H_{11} > 0 \Rightarrow$ *Config. 5.22*. By [19] (see Diagram 3) this configuration leads to the unique phase portrait *Picture 5.22* (\simeq *Ric. 55*).

7: $H_6 = 0, H_{11} = 0 \Rightarrow$ *Config. 5.29*. According to [19] (see Diagram 3) this configuration leads to the unique phase portrait *Picture 5.29* (\simeq *Ric. 63*).

4.3.2.2 The possibility $\tilde{K} = 0$. According to Diagram 3 we have to consider two cases: $B_2 = 0$ and $B_2 \neq 0$.

4.3.2.2.1 The case $B_2 = 0$. Following Diagram 3 we examine the next possibilities.

1: $\mu_2 \neq 0, N_1 \neq 0, N_2 \neq 0, N_5 < 0 \Rightarrow$ *Config. 4.32*. According to [21, Table 2]) this configuration leads to a single phase portrait *Portrait 4.32* (\simeq *Ric. 53*).

2: $\mu_2 \neq 0, N_1 \neq 0, N_2 \neq 0, N_5 > 0 \Rightarrow$ *Config. 4.28*. By [21, Table 2]) this configuration leads to a single phase portrait *Portrait 4.28* (\simeq *Ric. 58*).

3: $\mu_2 \neq 0, N_1 \neq 0, N_2 \neq 0, N_5 = 0 \Rightarrow$ *Config. 4.39*. According to [21, Table 2]) this configuration leads to a single phase portrait *Portrait 4.39* (\simeq *Ric. 60*).

4: $\mu_2 \neq 0, N_1 \neq 0, N_2 = 0 \Rightarrow$ *Config. 5.21*. By [19] (see Diagram 3) this configuration leads to the unique phase portrait *Picture 5.21* (\simeq *Ric. 58*).

5: $\mu_2 \neq 0, N_1 = 0, N_2 \neq 0, N_5 < 0 \Rightarrow \text{Config. 5.15}$. According to [19] (see Diagram 3) this configuration generates the unique phase portrait *Picture 5.15* ($\simeq \text{Ric. 53}$).

6: $\mu_2 \neq 0, N_1 = 0, N_2 \neq 0, N_5 > 0 \Rightarrow \text{Config. 5.13}$. By [19] (see Diagram 3) this configuration leads to the unique phase portrait *Picture 5.13* ($\simeq \text{Ric. 58}$).

7: $\mu_2 \neq 0, N_1 = 0, N_2 \neq 0, N_5 = 0 \Rightarrow \text{Config. 5.17}$. According to [19] (see Diagram 3) this configuration generates the unique phase portrait *Picture 5.17* ($\simeq \text{Ric. 60}$).

8: $\mu_2 \neq 0, N_1 = 0, N_2 = 0 \Rightarrow \text{Config. 6.7}$. By [19, Diagram 1] $\Rightarrow \text{Picture 6.7}$ ($\simeq \text{Ric. 58}$).

9: $\mu_2 = 0, N_1 \neq 0, N_2 \neq 0, N_5 < 0 \Rightarrow \text{Config. 4.33}$. According to [21, Table 2]) this configuration leads to a single phase portrait *Portrait 4.33* ($\simeq \text{Ric. 53}$).

10: $\mu_2 = 0, N_1 \neq 0, N_2 \neq 0, N_5 > 0 \Rightarrow \text{Config. 4.29}$. According to [21, Table 2]) this configuration generates two phase portraits: *Portrait 4.29(b)* for $\mu_4 < 0$ and *Portrait 4.29(a)* for $\mu_4 > 0$. The first phase portrait is new and we denote it by *Ric. 73*. The second one is topologically equivalent to *Ric. 43*. So we get *Ric. 73* for $\mu_4 < 0$ and *Ric. 43* for $\mu_4 > 0$.

11: $\mu_2 = 0, N_1 \neq 0, N_2 = 0 \Rightarrow \text{Config. 5.28}$. According to [19] (see Diagram 3) this configuration generates the unique phase portrait *Picture 5.28* ($\simeq \text{Ric. 36}$).

12: $\mu_2 = 0, N_1 = 0, N_2 \neq 0, N_5 < 0 \Rightarrow \text{Config. 5.24}$. By [19] (see Diagram 3) this configuration leads to the unique phase portrait *Picture 5.24* ($\simeq \text{Ric. 53}$).

13: $\mu_2 = 0, N_1 = 0, N_2 \neq 0, N_5 > 0 \Rightarrow \text{Config. 5.20}$. According to [19] (see Diagram 3) this configuration generates the unique phase portrait *Picture 5.20* ($\simeq \text{Ric. 43}$).

14: $\mu_2 = 0, N_1 = 0, N_2 = 0 \Rightarrow \text{Config. 6.10}$. By [19] (see Diagram 1) this configuration leads to the unique phase portrait *Picture 6.10* ($\simeq \text{Ric. 36}$).

4.3.2.2 The case $B_2 \neq 0$. According to Lemma 3.7 in this case a quadratic system with $\theta_5 \neq 0$ could not belong to the class \mathbf{QSL}^{2P} and hence, it could neither belong to the family \mathbf{QS}_{Ric} .

On the other hand according to [10] for $\theta_5 = 0$ this system could be brought via an affine transformation and time rescaling to the form (26) (from [10]), i.e. we arrive at the subfamily of the Riccati systems

$$\dot{x} = a + cx, \quad \dot{y} = b + ex + y^2. \quad (26)$$

Following [6, Diagram 3] we evaluate for systems (26) the following invariant polynomials:

$$\begin{aligned} \eta = \mu_0 = \mu_1 = 0, \quad \widetilde{M} = -8y^2, \quad \mu_2 = c^2y^2, \quad \kappa = 0, \quad \kappa_1 = 32e, \\ \mathbf{U} = -4c^3(bc - ae)x^2y^4, \quad \widetilde{K} = 0, \quad \widetilde{L} = 8y^2, \quad B_2 = -648e^4x^4. \end{aligned} \quad (27)$$

We examine the possibilities given by Diagram 3.

1: $\mu_2 \neq 0, \mathbf{U} < 0 \Rightarrow \text{Config. 3.59}$. By (27) we have $\mu_2 > 0$ and $\kappa_1 \neq 0$ due to $B_2 \neq 0$. Then considering the conditions $\kappa = \widetilde{K} = 0$ and $\mu_2 \widetilde{L} > 0$, according to [6, Diagram 3] the global topological configuration of the singularities (finite and infinite) corresponds to (142): $\binom{2}{2}PH - H, N$. Since we do not have real finite singularities and only one finite separatrix belonging to the multiple infinite singularity, we conclude that this separatrix must go to the infinite node which is adjacent to the parabolic part of the non-elemental singularity. This leads to a unique phase portrait which is new and we denote it here by *Ric. 74*.

2: $\mu_2 \neq 0, \mathbf{U} > 0 \Rightarrow \text{Config. 3.60}$. In this case considering (27) according to [6, Diagram 3] the global topological configuration of the singularities corresponds to (135): $s, a; \binom{2}{2}PH - H, N$.

Since we have an invariant straight line passing through both finite singularities (a saddle and a node) and tending to the infinite node $N[0 : 1 : 0]$, this splits the plane in two semi-planes. By a vertical symmetry, we may assume the saddle is located below the node, and by a time change we may assume the node being repeller. We have a nilpotent singularity at $N[1 : 0 : 0]$ being a saddle-node which has only one finite separatrix, which by a symmetry we may assume it on the right semi-plane.

The unstable separatrix of the finite saddle on the left semi-plane can only go to the infinite attractor node $N[0 : 1 : 0]$. On the right semi-plane there are several possibilities depending on the stability of the finite separatrix of the infinite singularity and the relative position of the two separatrices in that semi-plane (see (b) in Figure 18). However, we must notice first that the separatrix of the finite saddle cannot go to the same infinite node since that would contradict Proposition 3.34 from [3] (see (b_1) in Figure 18). This proposition says that if a phase portrait has at least two pairs of infinite singularities and a finite saddle sends two separatrices to the same infinite point, the opposite infinite point cannot receive a separatrix from this finite saddle. So the separatrix of the finite saddle must go the nodal part of the nilpotent singularity, or coincide with its separatrix. However, if the connection were possible, by means of small perturbation, we could arrive to the previous situation which contradicts Proposition 3.34 of [3]. So, the connection is not possible.

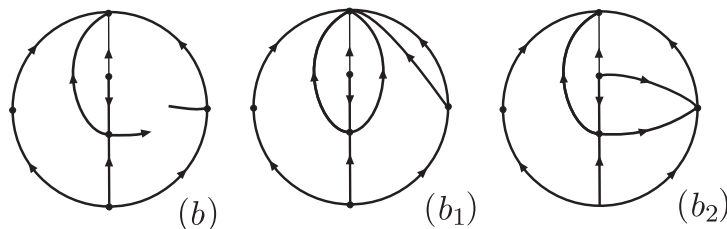


Figure 18: Scheme of the proof to obtain *Ric. 75*.

So, it remains (see (b) in Figure 18) to determine the position and stability of the finite separatrix of the infinite singularity. Since the surrounding of the singularity must have a parabolic and an hyperbolic sectors the only possibility is that the separatrix go to infinity and come from the finite node producing a unique phase portrait that we denote by *Ric. 75* (see (b_2) in Figure 18).

3: $\mu_2 \neq 0, \mathbf{U} = 0 \Rightarrow$ *Config. 3.61*. This configuration could be obtained from *Config. 3.60* by coalescing the two finite singularities. This means that we can produce a single phase portrait denoted here by *Ric. 76*.

4: $\mu_2 = 0 \Rightarrow$ *Config. 3.62*. Considering (27) the condition $\mu_2 = 0$ gives us $c = 0$ and then for systems (26) we obtain $\mu_3 = 0$ and $\mu_4 = a^2 y^4 \neq 0$, otherwise we get degenerate systems. Then considering (27) according to [6, Diagram 3, page 15] the global topological configuration of the singularities corresponds to $\{142\}$: $\binom{4}{2}PH - H, N$ which topologically is equivalent with the configuration $\binom{2}{2}PH - H, N$ examined above (see case **1**). Thus we arrive at the same phase portrait *Ric. 74*.

4.4 The case $\eta = 0 = \widetilde{M}$

According to the Diagram 4 we examine two subcases: $C_2 \neq 0$ and $C_2 = 0$.

4.4.1 The subcase $C_2 \neq 0$

Since $\eta = 0 = \widetilde{M}$ and $C_2 \neq 0$, according to [24] (see also [17]) we consider the following canonical form:

$$\begin{aligned}\dot{x} &= a + cx + dy + gx^2 + hxy, \\ \dot{y} &= b + ex + fy - x^2 + gxy + hy^2.\end{aligned}\tag{28}$$

for which by Lemma 3.7 the conditions $\theta = B_1 = H_7 = 0$ have to be fulfilled. As it was shown in [10] forcing these conditions to be satisfied, in the case $\widetilde{N} \neq 0$ we arrive at the family of systems (95) from [10], i.e. we consider the family of systems

$$\dot{x} = a + cx + gx^2, \quad \dot{y} = b - x^2 + gxy.\tag{29}$$

On the other hand for $\widetilde{N} = 0$ we obtain the family of systems (98) from [10], i.e. in this case we consider the family of systems

$$\dot{x} = a + cx, \quad \dot{y} = b + fy - x^2.\tag{30}$$

Thus as in the previous cases we have to examine two possibilities: $\widetilde{N} \neq 0$ and $\widetilde{N} = 0$.

4.4.1.1 The possibility $\widetilde{N} \neq 0$. Following [6, Diagram 3] we evaluate for systems (29) the following invariant polynomials:

$$\begin{aligned}C_2 &= x^3, \quad \widetilde{N} = g^2x^2, \quad \mu_2 = ag^3x^2, \quad \mathbf{U} = g^2(c^2 - 4ag)x^4[(a + bg)x - agy]^2, \\ H_{11} &= 48g^4(c^2 - 4ag)x^4, \quad \widetilde{K} = 2g^2x^2, \quad \kappa = 0, \quad \widetilde{L} = 0.\end{aligned}\tag{31}$$

We observe that if $H_{11} \neq 0$ then $\text{sign}(H_{11}) = \text{sign}(\mathbf{U})$.

According to the Diagram 4 we consider the next cases.

1: $\mu_2 \neq 0, H_{11} < 0 \Rightarrow \text{Config. 3.63}$. The condition $H_{11} < 0$ implies $\mathbf{U} < 0$ and due to $\widetilde{N} \neq 0$ we have $\widetilde{K} \neq 0$. Then considering the condition $\kappa = \widetilde{L} = 0$, according to [6, Diagram 3] the global topological configuration of the singularities corresponds to (12): $\binom{2}{3}P - P$. So this is topologically equivalent with an elemental node and thus the only possible phase portrait is *Ric. 28*.

2: $\mu_2 \neq 0, H_{11} > 0 \Rightarrow \text{Config. 3.64}$. By (31) this implies $\mathbf{U} > 0$ and we consider two cases: $\mu_2 < 0$ and $\mu_2 > 0$.

2.1: If $\mu_2 < 0$ then taking into consideration (31) by [6, Diagram 3] we obtain that the global topological configuration of the singularities corresponds to (127): $a, a; \binom{2}{3}HHP - PHH$.

Since $H_{11} = 48g^4(c^2 - 4ag)x^4 > 0$ we have $c^2 - 4ag > 0$ and the phase portrait has two parallel vertical invariant straight lines. We also have one node located on each invariant line. This leads to a unique phase portrait which is new and we denote it here by *Ric. 77*.

2.2: Assuming $\mu_2 > 0$ according to [6, Diagram 3] we obtain that the global topological configuration of the singularities corresponds to (130): $s, a; \binom{2}{3}HE - P$.

Since $H_{11} > 0$, as it was mentioned above we have two parallel vertical invariant lines and on each one of them there is a singular point. As one of the finite singularities is a saddle we conclude that one separatrix of this saddle is located between the two parallel invariant lines. Without loss of generality we may assume that the parabolic sector of the infinite intricate singularity is located on the semi-plane $y > 0$ and that it is an attractor. This forces the direction of the flow on every separatrix. Therefore the separatrix between the invariant lines must come from the finite node and the other separatrix must border the infinite elliptic sector. Thus we obtain a unique phase portrait which is new and we denote it here by *Ric. 78*.

3: $\mu_2 \neq 0, H_{11} = 0 \Rightarrow \text{Config. } 3.65$. The condition $H_{11} = 0$ implies $\mathbf{U} = 0$ and by [6, Diagram 3] we get the global topological configuration of the singularities (146): $sn; \binom{2}{3}HE - P$. We observe that in this case systems under consideration possess a vertical invariant line (of multiplicity at least two) and a semi-elemental saddle-node of multiplicity 2 is located on this line. Moreover both semi-lines of this invariant line are the separatrices of the saddle-node and the separatrices can be considered repeller due to a time rescaling. We have another separatrix in one of the semi-planes defined by the invariant line. Without loss of generality we may consider that the parabolic sector of the infinite singularity is located in the semi-plane $y > 0$. Therefore the finite separatrix can only come from the opposite region formed by parabolic sector. As a result we obtain the elliptic sector and this leads to a unique phase portrait which is new and we denote it here by *Ric. 79*.

4: $\mu_2 = 0, N_6 \neq 0, H_{11} \neq 0 \Rightarrow \text{Config. } 4.31$. According to [21, Table 2]) this configuration leads to the phase portrait *Portrait 4.31(a)* if $K_3 > 0$ and *Portrait 4.31(b)* if $K_3 < 0$. These phase portraits are new for the Riccati family and we denote *Portrait 4.31(b)* by *Ric. 80* and *Portrait 4.31(a)* by *Ric. 81*. Thus we get *Ric. 80* for $K_3 < 0$ and *Ric. 81* for $K_3 > 0$.

5: $\mu_2 = 0, N_6 \neq 0, H_{11} = 0 \Rightarrow \text{Config. } 4.44$. By [21, Table 2]) this configuration generates two phase portraits: *Portrait 4.44(a)* if $K_3 > 0$ and *Portrait 4.44(b)* if $K_3 < 0$. The first phase portrait is topologically equivalent to *Ric. 28*, whereas *Portrait 4.44(b)* is new and we denote it by *Ric. 82*.

6: $\mu_2 = 0, N_6 = 0 \Rightarrow \text{Config. } 5.23$. According to [19] (see Diagram 3) this configuration generates the unique phase portrait *Picture 5.23* (\simeq *Ric. 81*).

4.4.1.2 The possibility $\tilde{N} = 0$. Following the branch of Diagram 4 defined by this condition we consider the next cases.

1: $N_3 \neq 0, D_1 \neq 0, N_6 \neq 0, \tilde{D} \neq 0 \Rightarrow \text{Config. } 4.37$. By [21, Table 2]) this configuration generates three phase portraits: *Portrait 4.37(a)* if $\mu_3 K_1 > 0$ and $K_3 \geq 0$; *Portrait 4.37(b)* if $\mu_3 K_1 > 0$ and $K_3 < 0$ and *Portrait 4.37(c)* if $\mu_3 K_1 < 0$. All these phase portraits are new for the Riccati family and we denote *Portrait 4.37(c)* (respectively, *Portrait 4.37(b)*; *Portrait 4.37(a)*) by *Ric. 83* (respectively *Ric. 84*; *Ric. 85*).

2: $N_3 \neq 0, D_1 \neq 0, N_6 \neq 0, \tilde{D} = 0 \Rightarrow \text{Config. } 4.38$. According to [21, Table 2]) this configuration generates two phase portraits: *Portrait 4.38(a)* if $\mu_4 > 0$ and *Portrait 4.38(b)* if $\mu_4 < 0$. We observe that the second phase portrait is topologically equivalent to *Ric. 28*, whereas *Portrait 4.38(a)* is new and we denote it by *Ric. 86*.

3: $N_3 \neq 0, D_1 \neq 0, N_6 = 0 \Rightarrow \text{Config. } 4.46$. According to [21, Table 2]) this configuration leads to the unique phase portrait *Portrait 4.46* which is new and we denote by *Ric. 87*.

4: $N_3 \neq 0, D_1 = 0 \Rightarrow \text{Config. } 5.26$. According to [19] (see Diagram 3) this configuration generates the unique phase portrait *Picture 5.26* (\simeq *Ric. 83*).

5: $N_3 = 0, D_1 \neq 0 \Rightarrow \text{Config. } 5.27$. By [19] (see Diagram 3) this configuration leads to the unique phase portrait *Picture 5.27* (\simeq *Ric. 85*).

6: $N_3 = 0, D_1 = 0 \Rightarrow \text{Config. } 5.30$. According to [19] (see Diagram 3) this configuration generates the unique phase portrait *Picture 5.30* (\simeq *Ric. 28*).

4.4.2 The subcase $C_2 = 0$

In this case the invariant line at infinity of a quadratic system is filled up with singularities. This class of systems was classified in [20], where all the phase portraits as well as the affine invariant

criteria for their realization are detected. Following Diagram 4 we present here below the phase portraits in the Riccati family for which $C_2 = 0$ together with the corresponding conditions.

$$\begin{aligned}
H_{12} \neq 0, H_{11} < 0 &\Leftrightarrow \text{Config. } C_{2.6} \Rightarrow \text{Picture } C_{2.6} &&\Rightarrow \text{Ric. } 88; \\
H_{12} \neq 0, H_{11} > 0 &\Leftrightarrow \text{Config. } C_{2.5} \Rightarrow \begin{cases} \text{Picture } C_{2.5(a)} \text{ if } \mu_2 < 0 \\ \text{Picture } C_{2.5(b)} \text{ if } \mu_2 > 0 \end{cases} &&\Rightarrow \text{Ric. } 89; \\
&&&\hspace{10em} \Rightarrow \text{Ric. } 90; \\
H_{12} \neq 0, H_{11} = 0 &\Leftrightarrow \text{Config. } C_{2.7} \Rightarrow \text{Picture } C_{2.7} &&\Rightarrow \text{Ric. } 91; \\
H_{12} = 0, H_{11} \neq 0 &\Leftrightarrow \text{Config. } C_{2.8} \Rightarrow \text{Picture } C_{2.8} &&\Rightarrow \text{Ric. } 92; \\
H_{12} = 0, H_{11} = 0 &\Leftrightarrow \text{Config. } C_{2.9} \Rightarrow \text{Picture } C_{2.9} &&\Rightarrow \text{Ric. } 93.
\end{aligned}$$

4.5 The degenerate Riccati systems

We split this class of quadratic systems in sub-classes defined by the invariant polynomials η , \widetilde{M} and C_2 according to the number and the kind of infinite singularities.

4.5.1 The case $\eta > 0$

According to Lemma 3.4 we consider the family of systems (\mathbf{S}_I) . We claim that if for a system belonging to this family the condition $\widetilde{N} = 0$ holds then this system could not be degenerate.

Indeed for systems (\mathbf{S}_I) we calculate

$$\mu_0 = gh(g+h-1), \quad \widetilde{N} = (g^2-1)x^2 + 2(g-1)(h-1)xy + (h^2-1)y^2$$

and therefore $\widetilde{N} = 0$ if and only if $(g, h) \in \{(1, 1), (1, -1), (-1, 1)\}$. However evidently in all these cases we get $\mu_0 \neq 0$ and by Lemma 3.3 the systems could not be degenerate.

Thus we assume that for systems (\mathbf{S}_I) the condition $\widetilde{N} \neq 0$ is fulfilled. As it was shown earlier (see Subsection 4.1.1) in this case a system in \mathbf{QS}_{Ric} via an affine transformation and time rescaling can be brought to the canonical form

$$\dot{x} = a + cx + gx^2, \quad \dot{y} = b + ey + fy + (g-1)xy + y^2. \quad (32)$$

According to Lemma 3.3 in order to obtain degenerate systems we have to impose the conditions $\mu_i = 0$ for all $i \in \{0, 1, \dots, 4\}$.

For the above systems we have $\mu_0 = g^2 = 0$ which implies $g = 0$. Then $\mu_1 = 0$ and $\mu_2 = -c^2(x-y)y$. So the condition $\mu_2 = 0$ gives $c = 0$ and then we calculate

$$\mu_3 = 0, \quad \mu_4 = a^2y^2(-x+y)^2.$$

Therefore $\mu_4 = 0$ yields $a = 0$ and after the translation $(x, y) \mapsto (x + 2e + f, y + e)$ (forcing $e = f = 0$) we arrive at the family of degenerate systems

$$\dot{x} = 0, \quad \dot{y} = b - xy + y^2. \quad (33)$$

It is clear that in the case $b \neq 0$ the conic $b - xy + y^2 = 0$ is a hyperbola which becomes reducible if $b = 0$.

On the other hand for the above systems we calculate $L_1 = -12bx^2$. Since $\text{sign}(L_1) = -\text{sign}(b)$ we arrive at the phase portrait *Ric. D₁* if $L_1 < 0$; *Ric. D₂* if $L_1 > 0$ and at the phase portrait *Ric. D₃* if $L_1 = 0$.

It remains to observe that for systems (33) we have $B_2 = -648b^2x^4$ and hence the condition $L_1 = 0$ is equivalent with $B_2 = 0$. So for $B_2 \neq 0$ we arrive at the conditions given in Diagram 5 for *Ric. D₁* and *Ric. D₂*.

We examine the case of the phase portrait *Ric. D₃*. We claim that for systems (32) the conditions $\mu_0 = \mu_2 = 0$ and $B_3 = 0$ lead to degenerate systems. Indeed, as it is mentioned above

the conditions $\mu_0 = \mu_2 = 0$ for (32) give us $g = c = 0$ and this implies $\mu_3 = 0$. Moreover we may assume $e = f = 0$ due a translation and then for these systems we calculate

$$B_3 = -3x^2(bx^2 - 2bxy + ay^2).$$

Evidently the condition $B_3 = 0$ yields $b = a = 0$ (which gives $B_2 = 0$) and this implies $\mu_4 = 0$ which leads to degenerate systems and this proves our claim.

In such a way we determine exactly the branches in the Diagram 5 on which are located the phase portraits *Ric. D₁*, *Ric. D₂* and *Ric. D₃*, correspondingly.

4.5.2 The case $\eta < 0$

In this case we have to consider the family of systems (\mathbf{S}_{II}). As in the case $\eta > 0$ we claim that if for a system belonging to this family the condition $\tilde{N} = 0$ holds then this system could not be degenerate.

Indeed for systems (\mathbf{S}_{II}) we calculate

$$\mu_0 = -h(g^2 + (h+1)^2), \quad \tilde{N} = x^2(g^2 - 2h + 2) + 2g(h+1)xy + (h^2 - 1)y^2$$

and we determine that the condition $\tilde{N} = 0$ holds if and only if $g = 0$ and $h = 1$. However in this case we get $\mu_0 = -4 \neq 0$ and this complete the proof of our claim.

So we assume $\tilde{N} \neq 0$. Then according to [10] a quadratic system satisfying the conditions $\eta < 0$ and $\theta = B_1 = H_7 = 0$ could be brought via an affine transformation and time rescaling to the form

$$\dot{x} = a + cx + gx^2, \quad \dot{y} = b + ex - x^2 + gxy - y^2. \quad (34)$$

For these systems we have $\mu_0 = g^2 = 0$, i.e. $g = 0$. Then we get $\mu_1 = 0$ and $\mu_2 = c^2(x^2 + y^2)$. Therefore the condition $\mu_2 = 0$ gives us $c = 0$ and this implies $\mu_3 = 0$ and $\mu_4 = a^2(x^2 + y^2)^2$. Clearly the condition $\mu_4 = 0$ yields $a = 0$ and after the translation $(x, y) \mapsto (x + e/2, y)$ (forcing $e = 0$) we arrive at the family of degenerate systems

$$\dot{x} = 0, \quad \dot{y} = b - x^2 - y^2. \quad (35)$$

It is clear that in the case $b \neq 0$ the conic $b - xy + y^2 = 0$ is an ellipse which becomes reducible if $b = 0$.

On the other hand for the above systems we calculate $L_1 = -12bx^2$. Since $\text{sign}(L_1) = -\text{sign}(b)$ we arrive at the phase portrait *Ric. D₄* if $L_1 < 0$.

There are some cases with degenerate systems that produce phase portraits which are topologically equivalent to non-degenerate systems. We have the followin remark

Remark 4.18. *In the case $L_1 > 0$ we have a phase portrait which is topologically equivalent to Ric. 28 (the complex ellipse is not visible). Even more interesting is the case $L_1 = 0$ (i.e. $b = 0$) where we have a flow formed by vertical straight lines plus a finite singularity $(0, 0)$ which comes from the intersection of two complex lines. In this case we obtain a phase portrait which is topologically equivalent to Ric. 35 (where the singular point is an intricate singularity with two hyperbolic sectors). For this reason we will denote by Ric. 28d if $L_1 > 0$ and Ric. 35d if $L_1 = 0$ in Diagram 6. However we do not add these phase portraits in the lists of phase portraits given in Figures 5 and 6.*

4.5.3 The case $\eta = 0, \tilde{M} \neq 0$

In this case we have to consider the family of systems (\mathbf{S}_{III}) and we examine two subcases: $\tilde{N} \neq 0$ and $\tilde{N} = 0$.

4.5.3.1 The subcase $\tilde{N} \neq 0$. Since we are interested in degenerate systems the condition $\mu_0 = 0$ is necessary. As it was mentioned earlier (see Subsection 4.3.1) in this case a Riccati system could be brought via an affine transformation to the canonical form (20), i.e. we consider the family of systems

$$\dot{x} = a + cx + gx^2, \quad \dot{y} = b + (g-1)xy. \quad (36)$$

For these systems we have

$$\mu_0 = \mu_1 = 0, \quad \mu_2 = ag(g-1)^2x^2, \quad \tilde{N} = (g^2-1)x^2, \quad \tilde{K} = 2(g-1)gx^2$$

and we consider two possibilities: $\tilde{K} \neq 0$ and $\tilde{K} = 0$.

4.5.3.1.1 The possibility $\tilde{K} \neq 0$. Then $g(g-1) \neq 0$ and hence the condition $\mu_2 = 0$ implies $a = 0$. In this case we calculate

$$\mu_3 = -bc(g-1)gx^3, \quad \mu_4 = bx^3 [bg^2x + c^2(g-1)y] \quad (37)$$

and evidently due to $\tilde{K} \neq 0$ the condition $\mu_3 = \mu_4 = 0$ implies $b = 0$. So we arrive at the family of degenerate systems

$$\dot{x} = x(c+gx), \quad \dot{y} = (g-1)xy. \quad (38)$$

which possess the invariant line $x = 0$ filled with singularities. For the above systems we have

$$\tilde{K} = 2g(g-1)x^2 \neq 0, \quad \tilde{L} = 8gx, \quad K_2 = 48c^2(2-g+g^2)x^2.$$

We observe that the underlying linear systems:

$$\dot{x} = c + gx, \quad \dot{y} = (g-1)y,$$

due to $\tilde{K} \neq 0$ (i.e. $g(g-1) \neq 0$) possess the finite singular point $M_1(-c/g, 0)$. Moreover this singularity is isolated if $c \neq 0$ and lies on the singular line $x = 0$ if $c = 0$. We observe that these possibilities are governed by the invariant polynomial K_2 (see its value above).

For the finite singularity $M_1(-c/g, 0)$ we obtain $\lambda_1\lambda_2 = g(g-1) \neq 0$ and hence $\text{sign}(\lambda_1\lambda_2) = \text{sign}(\tilde{K})$. So we get a saddle if $\tilde{K} < 0$ and a node if $\tilde{K} > 0$.

Moreover in the second case we have that the orbits are all (except one) tangent to the direction given by the eigenvector of the eigenvalue that is smaller in absolute value. Therefore if $g < 0$ (respectively $g > 0$) the orbits are tangent to the x -axis (respectively y -axis). Since $\text{sign}(g) = \text{sign}(\tilde{L})$ we arrive at the following phase portraits defined by the corresponding conditions:

$$\begin{aligned} \tilde{K} < 0, K_2 \neq 0 &\Rightarrow Ric. D_5; \\ \tilde{K} < 0, K_2 = 0 &\Rightarrow Ric. D_6; \\ \tilde{K} > 0, \tilde{L} < 0 \neq K_2 &\Rightarrow Ric. D_7; \\ \tilde{K} > 0, \tilde{L} < 0 = K_2 &\Rightarrow Ric. D_8; \\ \tilde{K} > 0, \tilde{L} > 0 \neq K_2 &\Rightarrow Ric. D_9; \\ \tilde{K} > 0, \tilde{L} > 0 = K_2 &\Rightarrow Ric. D_{10}. \end{aligned}$$

In order to determine the exact places of the above degenerated phase portraits in the branches of Diagram 7 we prove the following lemma.

Lemma 4.9. *In the case $\tilde{K} \neq 0$ the conditions $\mu_2 = \mu_3 = \mu_4 = 0$ for systems (36) are equivalent to $\mu_2 = B_3 = 0$. Moreover for systems (38) the conditions $H_6 \neq 0$ and $K_2 \neq 0$ are equivalent and the condition $H_6 = 0$ implies $H_{11} = 0$.*

Proof: As it was shown above the condition $\mu_2 = 0$ implies $a = 0$ for systems (36) and then $B_3 = -3b(g-1)^2x^4$. Therefore considering (37) due to $\tilde{K} \neq 0$ the condition $B_3 = 0$ is equivalent to $\mu_3 = \mu_4 = 0$. It remains to observe that for systems (38) we have

$$H_6 = -128c^2(g-1)^4x^6, \quad H_{11} = 48c^2(g-1)^4x^4$$

and considering the value of the invariant polynomial K_2 given above we deduce that the condition $H_6 \neq 0$ is equivalent to $K_2 \neq 0$ and that $H_6 = 0$ implies $H_{11} = 0$. This completes the proof of the lemma. \blacksquare

4.5.3.1.2 The possibility $\tilde{K} = 0$. Then $g(g-1) = 0$ and due to $\tilde{N} \neq 0$ we get $g = 0$ and we get the family of systems

$$\dot{x} = a + cx, \quad \dot{y} = b - xy \quad (39)$$

for which we have

$$\mu_0 = \mu_1 = \mu_2 = 0, \quad \mu_3 = -acx^2y, \quad \mu_4 = x^2y(-bc^2x + a^2y), \quad B_3 = -3bx^4. \quad (40)$$

Clearly the conditions $\mu_3 = \mu_4 = 0$ imply $a = 0$ and then $\mu_3 = 0$ and $\mu_4 = -bc^2x^3y$. So we examine two cases: $B_3 \neq 0$ and $B_3 = 0$.

1: If $B_3 \neq 0$ (i.e. $b \neq 0$) we get $c = 0$ and we obtain the family of systems

$$\dot{x} = 0, \quad \dot{y} = b - xy.$$

It is clear that in the case $b \neq 0$ the conic $b - xy = 0$ is a hyperbola which is irreducible due to $b \neq 0$. As a result, due to symmetry, we get the unique phase portrait $Ric. D_{11}$.

2: For $B_3 = 0$ we get $b = 0$ and we obtain the systems

$$\dot{x} = cx, \quad \dot{y} = -xy, \quad (41)$$

possessing the singular invariant line $x = 0$. Clearly we have to distinguish the possibilities $c \neq 0$ and $c = 0$.

2.1: In the case $c \neq 0$ we have the underlying linear systems:

$$\dot{x} = c, \quad \dot{y} = -y$$

which do not have finite singularities due to $c \neq 0$. It is not difficult to determine that in this case we obtain the phase portrait given by $Ric. D_{12}$.

2.2: For $c = 0$ we obtain the degenerate systems

$$\dot{x} = 0, \quad \dot{y} = -xy$$

and it is easy to determine that the phase portrait of the above systems is $Ric. D_{13}$.

On the other hand for systems (41) we have $K_1 = -cx^2y$ and considering the above discussion we arrive at the phase portrait $Ric. D_{12}$ if $K_1 \neq 0$ and $Ric. D_{13}$ if $K_1 = 0$.

Now we have to determine the exact places of the phase portraits $Ric. D_{11}$ – $Ric. D_{13}$ in the Diagram 7 the branches of which are defined by other invariant polynomials in the case $\tilde{K} = 0$. We prove the next lemma.

Lemma 4.10. *The phase portrait of a system (39) corresponds to one of the portraits $Ric. D_{11}$ – $Ric. D_{13}$ if the corresponding conditions are satisfied, respectively:*

$$\begin{aligned} B_3 \neq 0, \mu_3 = H_6 = 0 &\Rightarrow Ric. D_{11}; \\ B_3 = 0, \mu_3 = H_6 = 0 &\Rightarrow Ric. D_{13}; \\ B_3 = 0, \mu_3 = 0, H_{11} \neq 0 &\Rightarrow Ric. D_{12}. \end{aligned}$$

Proof: Assume first $B_3 \neq 0$, i.e. $b \neq 0$. For systems (39) we have $H_6 = 128(a - c^2)x^6$ and since $b \neq 0$ considering (40) we deduce that the conditions $\mu_3 = \mu_4 = 0$ are equivalent to $\mu_3 = H_6 = 0$ and we arrive at *Ric. D*₁₁.

Suppose now $B_3 = 0$. Then $b = 0$ and for systems (39) in this case we have

$$\mu_3 = -acx^2y, \mu_4 = a^2x^2y^2, H_{11} = 48c^2x^4, H_6 = 128(a - c^2)x^6, K_1 = -cx^2y$$

So if $\mu_3 = H_6 = 0$ then we get $a = c = 0$ which implies $\mu_3 = \mu_4 = K_1 = 0$ and this leads to *Ric. D*₁₃.

Assume now $B_3 = \mu_3 = 0$, $H_{11} \neq 0$. Then considering the above expressions for these invariant polynomials we obtain $a = 0$ (which implies $\mu_4 = 0$) and $c \neq 0$ and then $K_1 \neq 0$. So we get *Ric. D*₁₂ and this completes the proof of the lemma.

4.5.3.2 The subcase $\tilde{N} = 0$. According to Diagram 3 we have to distinguish two possibilities: $\tilde{K} \neq 0$ and $\tilde{K} = 0$.

4.5.3.2.1 The possibility $\tilde{K} \neq 0$. In this case, in order for a system to be a Riccati system the condition $\theta_3 = 0$ must be satisfied. Moreover as it was shown in [10] in this case a Riccati system could be brought via an affine transformation to the canonical form (24) from [10], i.e. we consider the family of systems

$$\dot{x} = a + cx - x^2, \quad \dot{y} = b - 2xy. \quad (42)$$

For these systems we have

$$\tilde{N} = B_2 = 0, \quad \tilde{K} = 4x^2 \neq 0, \quad \mu_0 = \mu_1 = 0, \quad \mu_2 = -4ax^2$$

and clearly the condition $\mu_2 = 0$ implies $a = 0$ and then we have

$$\mu_3 = -2bcx^3, \quad \mu_4 = bx^3(bx - 2c^2y).$$

Evidently the conditions $\mu_3 = \mu_4 = 0$ give us $b = 0$ and we arrive at the degenerate systems

$$\dot{x} = x(c - x), \quad \dot{y} = -2xy. \quad (43)$$

which possess the invariant singular line $x = 0$ and the underlying linear systems are:

$$\dot{x} = c - x, \quad \dot{y} = -2y.$$

It is easy to detect that we get the phase portrait *Ric. D*₇ in the case $c \neq 0$ and *Ric. D*₈ if $c = 0$.

On the other hand for systems (43) we have $H_6 = -2048c^2x^6$ and therefore we get *Ric. D*₇ if $H_6 \neq 0$ and *Ric. D*₈ if $H_6 = 0$.

Next in order to determine the exact places of the above degenerate phase portraits in the branches of Diagram 7 we have to take into consideration the next remark.

Remark 4.19. A system (42) possesses the phase portrait *Ric. D*₇ if $B_3 = \mu_2 = 0$ and $H_6 \neq 0$ (which implies $H_{11} > 0$) and it possess the phase portrait *Ric. D*₈ if $B_3 = H_6 = H_{11} = 0$.

Indeed for systems (42) we calculate

$$H_6 = -2048c^2x^6, \quad H_{11} = 768(4a + c^2)x^4, \quad B_3 = -12bx^4, \quad \mu_2 = -4ax^2$$

and clearly in the case $H_6 \neq 0$ (i.e. $c \neq 0$) the conditions $B_3 = \mu_2 = 0$ imply $a = b = 0$. So we get degenerate systems (43) with $c \neq 0$ and we arrive at *Ric. D*₇.

If $H_6 = 0$ we get $c = 0$ and then the conditions $B_3 = \mu_2 = 0$ are equivalent to $B_3 = H_{11} = 0$ and in this case we get *Ric. D*₈.

4.5.3.2.2 The possibility $\tilde{K} = 0$. We consider two cases: $B_2 \neq 0$ and $B_2 = 0$.

1: *The case $B_2 \neq 0$.* As it was shown in [10] in this case a Riccati system could be brought via an affine transformation to the canonical form (90) from [10], i.e. we consider the family of systems

$$\dot{x} = a + cx, \quad \dot{y} = b + ex + y^2.$$

for which we have

$$\mu_0 = \mu_1 = 0, \quad \mu_2 = c^2 y^2, \quad B_2 = -648e^4 x^4.$$

So the condition $\mu_2 = 0$ gives us $c = 0$ and then we have $\mu_3 = 0$ and $\mu_4 = a^2 x^2$. Therefore the condition $\mu_4 = 0$ implies $a = 0$ and since $e \neq 0$ we may assume $e = 1$ and $b = 0$ due to the transformation $(x, y) \mapsto (-(x+b)/e, y)$. Thus we get a degenerate system

$$\dot{x} = 0, \quad \dot{y} = x + y^2$$

possessing the phase portrait *Ric. D₁₄*.

2: *The case $B_2 = 0$.* According to [10] in this case a Riccati system could be brought via an affine transformation to the canonical form (92) from [10], i.e. we consider the family of systems

$$\dot{x} = a + x^2, \quad \dot{y} = b + ex + fy,$$

for which we have

$$\mu_0 = \mu_1 = 0, \quad \mu_2 = f^2 x^2.$$

Therefore the condition $\mu_2 = 0$ yields $f = 0$ and then we have

$$\mu_0 = \mu_1 = \mu_2 = \mu_3 = 0, \quad \mu_4 = (b^2 + ae^2)x^4, \quad N_1 = 8ex^4, \quad N_2 = 16ax, \quad N_5 = -64ax^2$$

and we consider two possibilities: $N_1 \neq 0$ and $N_1 = 0$.

2.1: If $N_1 \neq 0$ then $e \neq 0$ and we may assume $e = 1$ due to a rescaling. Then the condition $\mu_4 = 0$ gives us $a = -b^2$ (which implies $N_5 > 0$) and then we arrive at the degenerate systems

$$\dot{x} = (x-b)(b+x), \quad \dot{y} = b+x.$$

These systems possess the singular invariant line $x = -b$ and the underlying linear systems are:

$$\dot{x} = x - b, \quad \dot{y} = 1.$$

We observe that these systems have at infinity a node and a saddle-node having the invariant line $x = b$ as a separatrix. Therefore for the initial systems we get two phase portraits: *Ric. D₁₅* if $b \neq 0$ and *Ric. D₁₆* if $b = 0$. It remains to mention that in the case considered we have $N_2 = -16b^2x$ and hence this invariant polynomial distinguishes the phase portraits we obtained.

2.2: Assume $N_1 = 0$, i.e. $e = 0$. Then the condition $\mu_4 = b^2 x^4 = 0$ implies $b = 0$ and we get the degenerate systems

$$\dot{x} = a + x^2, \quad \dot{y} = 0,$$

which possess two singular invariant lines $x^2 + a = 0$. Clearly these lines could be either real (if $a < 0$) or complex (if $a > 0$) or they could coincide (if $a = 0$).

On the other hand for these systems we have $N_5 = -64ax^2$ and therefore we get *Ric. D₁₇* if $N_5 > 0$ and *Ric. D₁₈* if $N_5 = 0$. In the case $N_5 < 0$, for similar reason as given in Remark 4.18 we get *Ric. 53d*.

In order to fit this case with the conditions inside the corresponding branch of Diagram 7 we point out that the condition $N_5 = -64ax^2 = 0$ is equivalent to $N_2 = 16ax = 0$.

4.5.4 The case $\eta = \widetilde{M} = 0$

According to Diagram 4 we have to consider two possibilities: $C_2 \neq 0$ and $C_2 = 0$.

4.5.4.1 The possibility $C_2 \neq 0$. According to the Diagram 4 we have to examine two cases: $\widetilde{N} \neq 0$ and $\widetilde{N} = 0$.

1: If $\widetilde{N} \neq 0$ it was shown earlier (see Section 4.4.1) we must consider the canonical form (29), i.e. the following systems

$$\dot{x} = a + cx + gx^2, \quad \dot{y} = b - x^2 + gxy. \quad (44)$$

For these systems we calculate

$$\mu_0 = \mu_1 = 0, \quad \mu_2 = ag^3x^2, \quad \widetilde{N} = g^2x^2.$$

So $g \neq 0$ and the condition $\mu_2 = 0$ implies $a = 0$. In this case we have

$$\mu_3 = -bcg^2x^3, \quad \mu_4 = bx^3(bg^2x + c^2gy - c^2x)$$

and evidently the conditions $\mu_3 = \mu_4 = 0$ imply $b = 0$. So since $g \neq 0$ after the rescaling $(x, y) \mapsto (x/g, y/g^2)$ we arrive at the family of degenerate systems

$$\dot{x} = x(c + x), \quad \dot{y} = -x(x - y) \quad (45)$$

possessing the singular invariant line $x = 0$ and the underlying linear systems are

$$\dot{x} = c + x, \quad \dot{y} = -x + y.$$

We observe that the finite singularity of these systems $M_1(-c, -c)$ is an one-direction node and considering the fact that the invariant line $x = -c$ coincides with the singular line $x = 0$ we arrive at the phase portrait *Ric. D₁₉* if $c \neq 0$ and at *Ric. D₂₀* if $c = 0$. It remains to observe that for the systems (45) we have $N_6 = 8c^2x^3$, i.e. this invariant polynomial is responsible for the condition $c = 0$.

In order to fit this case with the conditions inside the corresponding branch of Diagram 8 we point out that for systems (44) with $a = 0$ (i.e. $\mu_2 = 0$) we have

$$N_6 = 8(b + c^2)x^3, \quad H_{11} = 48c^2x^4, \quad K_3 = -6bx^6.$$

So $K_3 = 0$ yields $b = 0$ and this implies $\mu_3 = \mu_4 = 0$ and in this case $N_6 \neq 0$ implies $H_{11} \neq 0$. So we arrive at the next remark.

Remark 4.20. *The phase portrait of a system (44) corresponds to one of the portraits Ric. D₁₉ or Ric. D₂₀ if the corresponding conditions are satisfied, respectively:*

$$\begin{aligned} N_6 \neq 0, \mu_2 = K_3 = 0 &\Rightarrow Ric. D_{19}; \\ N_6 = \mu_2 = \mu_3 = 0 &\Rightarrow Ric. D_{20}. \end{aligned}$$

2: Assume now $\widetilde{N} = 0$. As it was shown earlier (see Section 4.4.1) we have to examine the canonical form (30), i.e. the following systems

$$\dot{x} = a + cx, \quad \dot{y} = b + fy - x^2, \quad (46)$$

for which we calculate

$$\mu_0 = \mu_1 = \mu_2 = 0, \quad \mu_3 = -c^2fx^3, \quad \widetilde{D} = -f^2x^3.$$

So we consider two possibilities: $\tilde{D} \neq 0$ and $\tilde{D} = 0$.

2.1: Suppose first $\tilde{D} \neq 0$. Then $f \neq 0$ and the condition $\mu_3 = 0$ implies $c = 0$. In this case we obtain $\mu_4 = a^2x^4 = 0$ which yields $a = 0$. As a result we get the family of degenerate systems

$$\dot{x} = 0, \quad \dot{y} = b + fy - x^2, \quad (47)$$

and since $f \neq 0$ we can assume $b = 0$ and $f = 1$ due to the rescaling $(x, y, t) \mapsto (x, (y-b)y/f, t/f)$. It is not difficult to detect that we obtain the unique phase portrait *Ric. D₂₁*.

2.2: Assume now $\tilde{D} = 0$. Then $f = 0$ and this implies

$$\mu_0 = \mu_1 = \mu_2 = \mu_3 = 0, \quad \mu_4 = (a^2 - bc^2)x^4, \quad N_6 = 8c^2x^3.$$

If $N_6 \neq 0$ then $c \neq 0$ and we may assume $c = 1$ due to the rescaling $(x, y, t) \mapsto (cx, cy, t/c)$. Therefore the condition $\mu_4 = 0$ implies $b = a^2$ and we arrive at the family of degenerate systems

$$\dot{x} = a + x, \quad \dot{y} = (a - x)(a + x), \quad (48)$$

which possess the singular invariant lines $x = -a$. Since the underlying linear systems are:

$$\dot{x} = 1, \quad \dot{y} = a - x$$

it is easy to determine that we get the unique phase portrait *Ric. D₂₂*.

Suppose now $N_6 = 0$, i.e. $c = 0$. Then the condition $\mu_4 = a^2x^4 = 0$ implies $a = 0$ and we obtain the degenerate systems

$$\dot{x} = 0, \quad \dot{y} = b - x^2. \quad (49)$$

It is clear that we get the phase portrait *Ric. 28d* if $b < 0$; *Ric. D₂₃* if $b > 0$ and *Ric. D₂₄* if $b = 0$. It remains to observe that for the above systems we have $L_3 = 4bx^4$, i.e. $\text{sign}(b) = \text{sign}(L_3)$ and hence this invariant polynomial distinguishes the phase portraits obtained.

In order to fit the case $\tilde{N} = 0$ with the conditions inside the corresponding branch of Diagram 8 we prove the next lemma.

Lemma 4.11. *The phase portrait of a system (46) corresponds to one of the portraits *Ric. D₂₁* – *Ric. D₂₄* or *Ric. 28d* if the corresponding conditions are satisfied, respectively:*

$$\begin{aligned} N_3 \neq 0, N_6 = \mu_4 = 0 &\Rightarrow Ric. D_{21}; \\ N_6 \neq 0, \tilde{D} = \mu_4 = 0 &\Rightarrow Ric. D_{22}; \\ N_3 = D_1 = \mu_4 = 0, L_3 > 0 &\Rightarrow Ric. D_{23}; \\ N_3 = D_1 = \mu_4 = 0, L_3 = 0 &\Rightarrow Ric. D_{24}; \\ N_3 = D_1 = \mu_4 = 0, L_3 < 0 &\Leftrightarrow Ric. 28d. \end{aligned}$$

Proof: For systems (46) calculations yield

$$N_3 = 3(c - f)x^3, \quad N_6 = 8c(c - f)x^3, \quad D_1 = c + f, \quad \tilde{D} = -f^2x^3, \quad \mu_3 = -c^2fx^3$$

and clearly the condition $N_6 = 0$ and $N_3 \neq 0$ implies $c = 0$. Then $\mu_3 = 0$ and the condition $\mu_4 = a^2x^4 = 0$ gives $a = 0$. So we get the degenerate systems (47) which possess the phase portrait *Ric. D₂₁*. It remains to point out that in this case we have $\tilde{D}D_1 \neq 0$ due to $N_3 = -3fx^3 \neq 0$.

Assume now $N_6 \neq 0$ and $\tilde{D} = 0$. Then $f = 0$, $c \neq 0$ and since $\mu_4 = 0$ we arrive at the degenerate systems (48) which possess the phase portrait *Ric. D₂₂*. We observe that in this case due to $N_6 \neq 0$ the condition $N_3D_1 \neq 0$.

Suppose finally $N_3 = D_1 = 0$. This implies $c = f = 0$ and considering the condition $\mu_4 = 0$ we get the degenerate systems (49) possessing three phase portraits: *Ric. 28d* (if $L_3 < 0$); *Ric. D₂₃* (if $L_3 > 0$) and *Ric. D₂₄* (if $L_3 = 0$). It remains to underline that these conditions are exactly those provided by Diagram 8 for these phase portraits.

4.5.4.2 The possibility $C_2 = 0$. According to Lemma 3.4 we have to examine the family of systems (\mathbf{S}_V) for which the necessary condition $H_7 = 4d = 0$ to belong to the class \mathbf{QS}_{Ric} implies $d = 0$. Then due to a translation we can assume $e = f = 0$ and we get the systems

$$\dot{x} = a + cx + x^2, \quad \dot{y} = b + xy, \quad (50)$$

for which we calculate

$$\mu_0 = \mu_1 = 0, \quad \mu_2 = ax^2.$$

So the condition $\mu_2 = 0$ implies $a = 0$ and we obtain

$$\mu_3 = -bcx^3, \quad \mu_4 = bx^3(bx + c^2y)$$

and evidently the conditions $\mu_3 = \mu_4 = 0$ imply $b = 0$. Therefore we arrive at the family of degenerate systems

$$\dot{x} = x(c + x), \quad \dot{y} = xy,$$

which possess the invariant singular line $x = 0$. The underlying linear systems are

$$\dot{x} = c + x, \quad \dot{y} = y$$

and it is easy to determine that we get the phase portrait *Ric. D₂₅* if $c \neq 0$ and *Ric. D₂₆* if $c = 0$. On the other hand for the above degenerate systems we have $H_{11} = 48c^2x^4$ and hence this invariant polynomial distinguishes the two detected phase portraits.

Considering the block of Diagram 8 defined by the condition $C_2 = 0$, for systems (50) we calculate

$$H_{12} = -8a^2x^2, \quad \mu_2 = ax^2, \quad H_{11} = -48(4a - c^2)x^4.$$

Therefore the condition $\mu_2 = 0$ is equivalent to $H_{12} = 0$ and this yields $a = 0$. Then we obtain

$$H_{11} = 48c^2x^4, \quad \mu_3 = -bcx^3, \quad \mu_4 = bx^3(bx + c^2y)$$

and hence the conditions $H_{11} \neq 0$ (i.e. $c \neq 0$) and $\mu_3 = 0$ imply $b = 0$ (then $\mu_4 = 0$) and we get *Ric. D₂₅*.

Assuming $H_{11} = 0$ we have $c = 0$ and this implies $\mu_3 = 0$. Then in order to obtain degenerate systems we must force $\mu_4 = 0$ getting $b = 0$ and this leads to the phase portrait *Ric. D₂₆*.

Wu thus determined exactly the branches of the Diagram 8 that provide these two phase portraits. This completes the examination of the degenerate Riccati systems.

5 Topological invariants and the proof of the non-equivalence of the 119 phase portraits

In order to complete the proof of Main Theorem we prove in this section that all the phase portraits given in Figures 5 and 6 are topologically non-equivalent. For this goal a simple visual comparison two by two of the phase portraits (which may imply thousands of comparisons) does not guarantee the success.

So here we define a set of topological invariants associated to the phase portraits *Ric. 1* to *Ric. 93* and *Ric. D₁* to *Ric. D₂₆* which completely distinguish these phase portraits.

These invariants yield a classification which is easier to grasp. In this study we will start by using a new strong invariant which condenses and substitutes other invariants used in previous papers. This invariant is related with [7], where a list of all topologically different configurations of singularities (finite and infinite) containing 208 possibilities is given.

Definition 5.1. We denote by $I_1(S)$ the code from [7] which describes the topological configuration of singularities (finite and infinite). This is a code ranging from (1) to (208) and for example we have that (8) stands for $s, s, a, a; N$ meaning that the system has two finite saddles and two finite anti-saddles, plus an infinite node, or (41) stands for $phph; N, \binom{0}{2}SN$ and means that we have a finite intricate singularity with sectors (parabolic-hyperbolic-parabolic-hyperbolic) and at infinity we have a node plus a saddle-node formed by the coalescence of an infinite saddle plus an infinite node.

For a given infinite singularity s of a system S , let l_s be the number of global or local separatrices beginning or ending at s and which do not lie on the line at infinity. We have $0 \leq l_s \leq 3$.

Definition 5.2. We denote by $I_2(S)$ the sequence of all such l_s when s moves in the set of infinite singular points of the system S . We start the sequence at the infinite singular point which receives/sends the greatest number of separatrices and take the direction which yields the greatest absolute value. For example, the values 2110 and 2011 for this invariant are symmetrical (and, therefore, they are the same), so we consider $I_2(S) = 2110$.

Definition 5.3. We denote by $I_3(S)$ the number of separatrix connections, distinguishing the finite-to finite ones from the finite-to-infinite ones. That is, $I_3 = (SC_f^f, SC_f^\infty)$, where SC_f^f (respectively, SC_f^∞) is the number of separatrix connections connecting two finite singularities (respectively a finite and an infinite one). Even in this family there are also infinite-to-infinite (SC_∞^∞) separatrices, we do not need them to distinguish phase portraits.

Next topological invariant is defined for distinguishing the phase portraits in the subfamily of degenerate Riccati quadratic systems.

Definition 5.4. We denote by $I_4(S)$ a topological invariant which takes the following values:

$$I_4(S) = \begin{cases} 1 & \text{if there exists a trajectory connecting two infinite singularities of } (S); \\ 0 & \text{if there does not exist such a trajectory.} \end{cases}$$

Theorem 5.1. Consider the family \mathbf{QS}_{Ric} of Riccati systems and denote by \mathcal{P} the set of all the phase portraits that we have obtained for this family. The values of the affine invariant $I = (I_1, I_2, I_3, I_4)$ given in the Diagram 9 yields a partition of the set \mathcal{P} .

Furthermore, for each value of I in this diagram there corresponds a single phase portrait; i.e. S and S' are such that $I(S) = I(S')$, if and only if S and S' are topologically equivalent.

6 Appendix: Comparison between the phase portraits given in this paper and those presented in [13]

In this Appendix we confront the results obtained previously in [13, Fig.1] with our results obtained in this paper. Both articles had as a goal to produce phase portraits of the Riccati family of systems, i.e. to classify topologically the systems in this family. While the principal goals were the same, the methods used in the two papers are very different. While in [13] the authors used the usual classical methods (calculation of singularities finite and infinite, finding the separatrices and then the connections (the Riccati systems have no limit cycles), all calculations done with respect to a fixed normal form, the methods used in this paper are modern using the theory of algebraic invariants allowing to change normal forms, the recently obtained powerful tool of the topological configurations of singularities, the geometrical configurations of singularities as well as several other new methods involving the classifications of quadratic

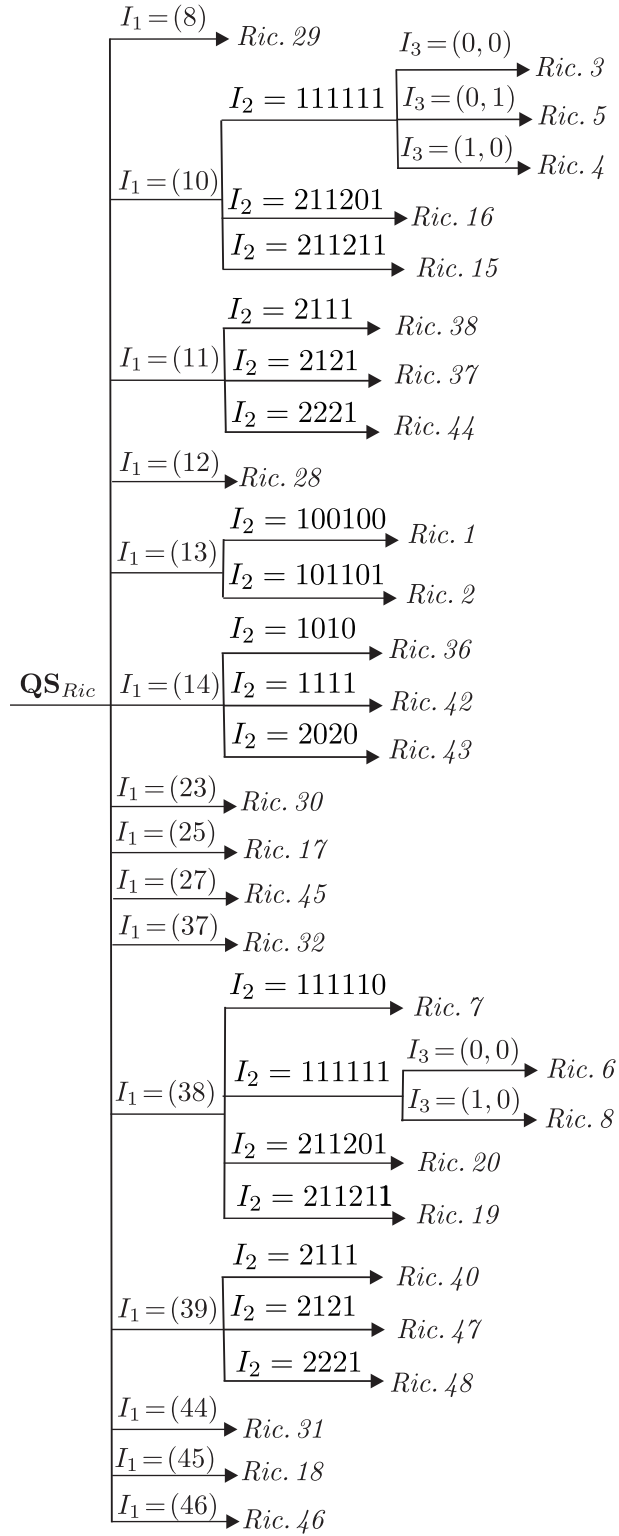


Diagram 9: The topologically non-equivalence of the phase portraits for the class \mathbf{QS}_{Ric}

systems modulo limit cycles. The affine equivalence relation is finer than the topological one. However, the affine equivalence relation plays a major role in topologically classifying families of

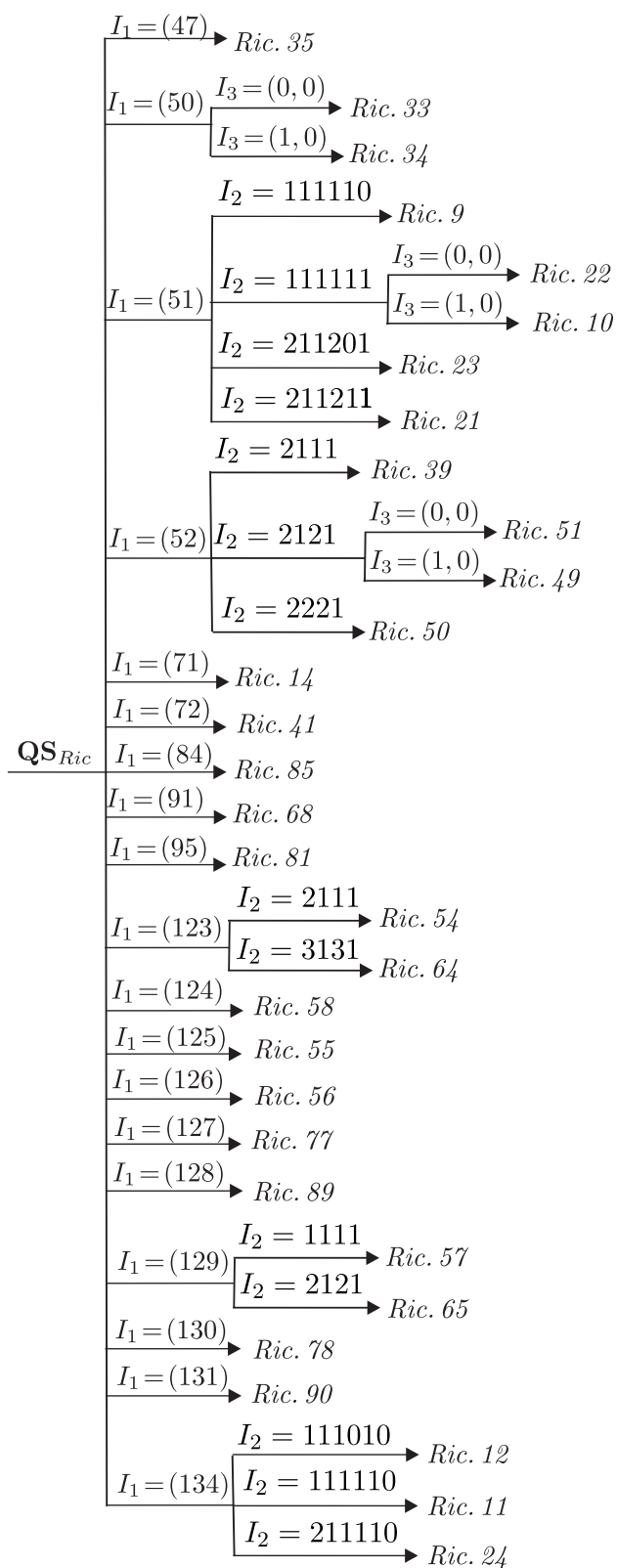


Diagram 9 (continuation): The topologically non-equivalence of the phase portraits for the class QS_{Ric}

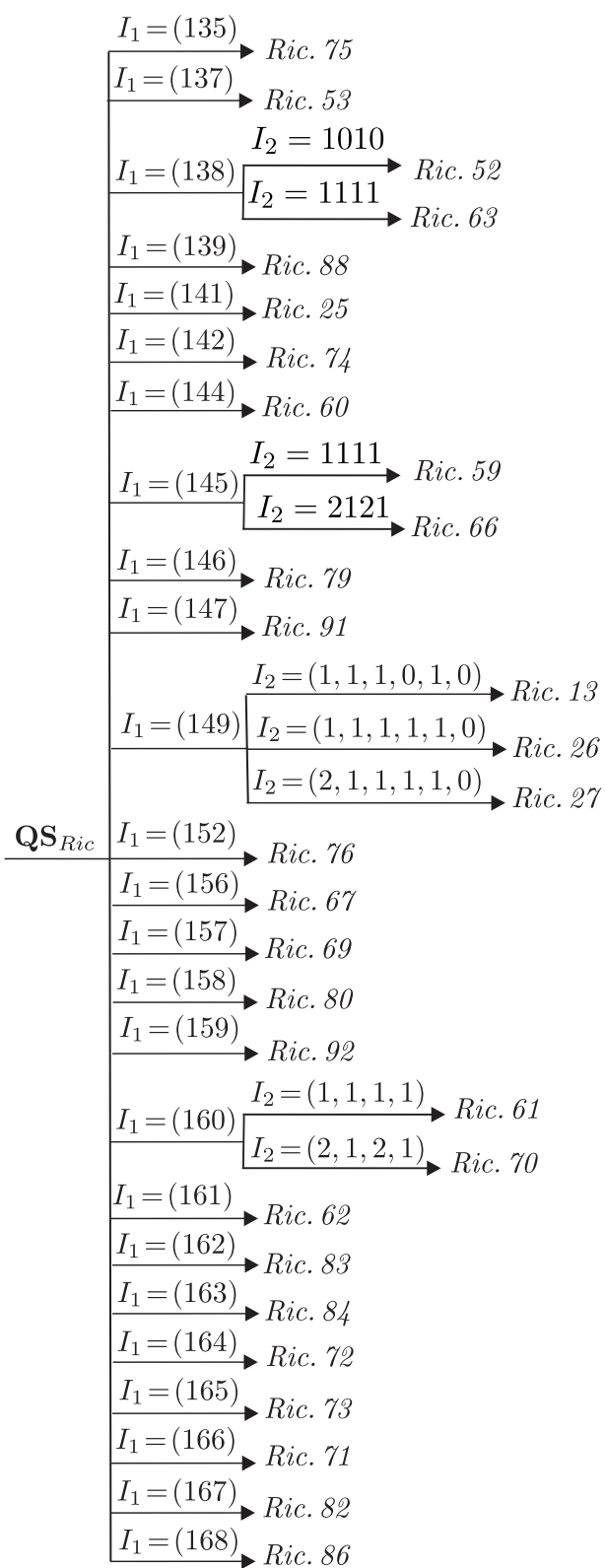


Diagram 9 (continuation): The topologically non-equivalence of the phase portraits for the class QS_{Ric}

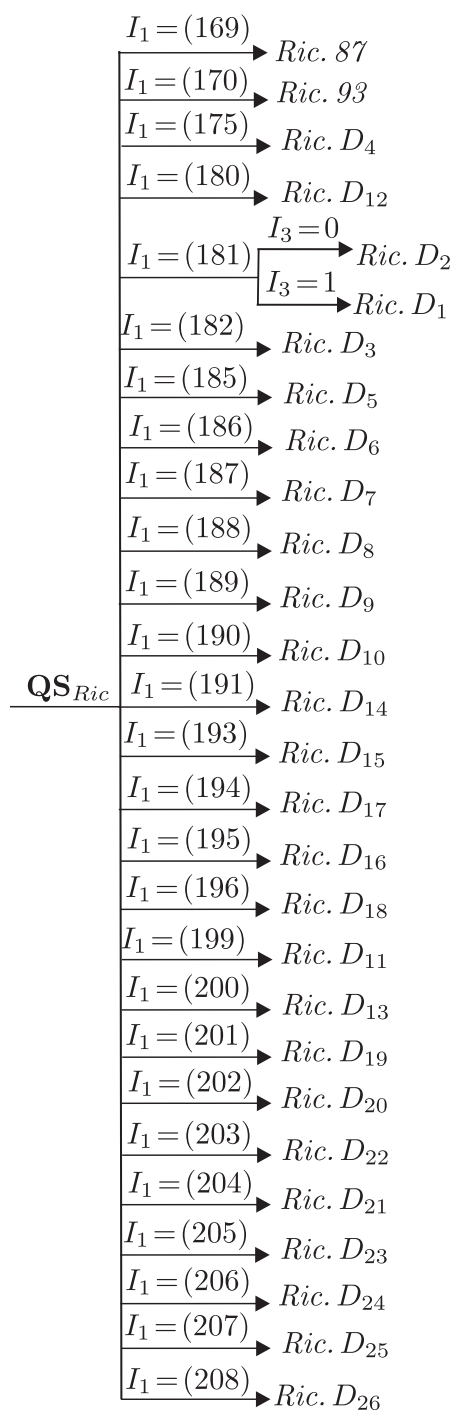


Diagram 9 (*continuation*): The topologically non-equivalence of the phase portraits for the class QS_{Ric}

polynomial vector fields firstly because it is via this equivalence relation that we get to normal forms eliminating superfluous parameters. Secondly, at least in the initial stages of calculating the main features of phase portraits of families of systems, features of an algebraic nature, we use affine invariant polynomials and these also appear in the initial stages of the construction of bifurcation diagrams done in the 12-dimensional space of the families of systems. Sometimes, in families with strong algebraic geometric features, like it is the case for Riccati systems these

turn out to even be complete bifurcation diagrams in terms of invariant polynomials. This is a family of systems with numerous phase portraits and the use of their geometric properties acts like a guiding flashlight in this labyrinth.

In this paper we obtain 119 topologically distinct phase portraits of the family (3), without any additional conditions, and we give them in Figures 5 and 6. From these 119 portraits, 93 correspond to non-degenerate systems and we denote them by *Ric.i* and 26 correspond to degenerate ones. The authors of [13] only considered quadratic Riccati systems (3) under the condition $n(b^2 + e^2 + l^2) \neq 0$ giving as reason that for $n = 0$ the systems are Liénard and for $b = e = l = 0$ the systems are Bernoulli. They denote their portraits by P_i with $1 \leq i \leq 74$.

Because of the wider scope of our paper, we cannot obtain a full comparison of the two works. We only confront their results with ours and start by pointing out some minor observations on portraits that have some typos or are wrong. The portraits P49 and P50 in [13] have small typos which are easy to observe and after correction they are both topologically equivalent to P30 and this portrait is equivalent with our portrait *Ric. 50*. In P69 there is an extra singularity on the vertical line. After removing it this phase portrait is equivalent to *Ric. 75*. There are also other three phase portraits P22, P25 and P58 which are wrong but here it is more difficult to decide what would the correct portraits be in this case.

We sum up the topological equivalence among the pictures P1–P74 and also their agreement with our phase portraits from Figure 5 in the following remark where in the left side there appear the numbers in this enumeration going from (1) to (45).

Remark 6.1. *We have checked the following topological equivalences of our phase portraits with those in [13]:*

1. *Ric. 1* \simeq *P70* ;
2. *Ric. 2* \simeq *P20* \simeq *P48* \simeq *P71*;
3. *Ric. 3* \simeq *P3*;
4. *Ric. 4* \simeq *P4*;
5. *Ric. 6* \simeq *P7* \simeq *P12*;
6. *Ric. 8* \simeq *P8* \simeq *P13*;
7. *Ric. 10* \simeq *P15* \simeq *P44*;
8. *Ric. 11* \simeq *P59*;
9. *Ric. 12* \simeq *P61*;
10. *Ric. 13* \simeq *P64*;
11. *Ric. 14* \simeq *P47*;
12. *Ric. 15* \simeq *P5*;
13. *Ric. 16* \simeq *P1* \simeq *P2*;
14. *Ric. 18* \simeq *P17* \simeq *P19* \simeq *P45* \simeq *P46*;
15. *Ric. 19* \simeq *P9* \simeq *P14*;
16. *Ric. 20* \simeq *P6* \simeq *P11*;
17. *Ric. 21* \simeq *P16*;
18. *Ric. 23* \simeq *P42* \simeq *P43*;
19. *Ric. 24* \simeq *P10* \simeq *P18* \simeq *P60*;
20. *Ric. 25* \simeq *P65*;
21. *Ric. 26* \simeq *P62*;
22. *Ric. 27* \simeq *P63*;
23. *Ric. 28* \simeq *P41*;
24. *Ric. 29* \simeq *P33*;
25. *Ric. 30* \simeq *P35* \simeq *P39*;

26. Ric. 31 \simeq P38 \simeq P40 \simeq P57;
27. Ric. 32 \simeq P34 \simeq P36;
28. Ric. 33 \simeq P37;
29. Ric. 34 \simeq P56;
30. Ric. 36 \simeq P72;
31. Ric. 37 \simeq P23;
32. Ric. 41 \simeq P53;
33. Ric. 42 \simeq P32 \simeq P55 \simeq P73;
34. Ric. 43 \simeq P74;
35. Ric. 44 \simeq P21;
36. Ric. 45 \simeq P26;
37. Ric. 46 \simeq P29 \simeq P31 \simeq P52 \simeq P54;
38. Ric. 48 \simeq P24 \simeq P27;
39. Ric. 49 \simeq P28;
40. Ric. 50 \simeq P30 \simeq P49 \simeq P50;
41. Ric. 51 \simeq P51;
42. Ric. 58 \simeq P66;
43. Ric. 60 \simeq P68;
44. Ric. 75 \simeq P67;
45. Ric. 76 \simeq P69.

We observe that sets of two or more phase portraits considered as distinct in [13] are in fact topologically equivalent. This is because sometimes phase portraits may be too complex and to distinguish them it is advisable to use invariants, affine or topological. As it can be seen there are only 45 topologically distinct phase portraits in [13] (plus 3 which are wrong and we could not compare them with ours).

From our 93 phase portraits in Figure 5 for non-degenerate Riccati systems, removing the ones which have the invariant infinite line filled up with singularities we get 87 topologically distinct phase portraits. The difference $87-45=42$ could correspond to the systems which are Riccati and also Liénard which are not investigated in [13]. Recall that we mentioned in the introduction that the Liénard systems are those Riccati systems (3) for which we have $n = 0$. However we will show that some of the missing phase portraits are in fact not Liénard but are omitted in [13]. We denote by \mathbf{QS}_{Lien} the family of systems of Liénard form, i.e. the systems (3) with $n = 0$.

It is interesting to note that all phase portraits can be split in three sets: (i) those which are realizable only for systems in the class \mathbf{QS}_{Lien} ; (ii) those which are realizable only for non-Liénard normal form (i.e. the systems (3) with $n \neq 0$) and (iii) phase portraits which are realizable for both normal forms, i.e. (3) with $n = 0$ and (3) with $n \neq 0$.

We point out that the last set can be divided in two subsets: (iii_a) those for which there exists an affine transformation which brings the corresponding Liénard normal form into non-Liénard normal form and (iii_b) those for which such kind of affine transformation does not exist.

This partition of the family of systems (3) is proved in Lemmas 6.1 and 6.2 below.

Lemma 6.1. *Assume that a Riccati system (3) belongs to the family \mathbf{QS}_{Lien} . Then there exists an affine transformation which brings this system to a non-Liénard form inside the family of Riccati systems if and only if the conditions $\eta = 0$, $\tilde{M} \neq 0$ and $\tilde{N} = \tilde{K} = B_2 = N_1 = 0$ are satisfied.*

Proof: Sufficiency. Assume that the conditions provided by the lemma are satisfied for a Riccati system except $N_1 = 0$. In this case according to [10] this system via an affine transformation can be brought to the canonical form (25) from [10], i.e. to the systems

$$\dot{x} = a + x^2, \quad \dot{y} = b + ex + fy.$$

For these systems we have $N_1 = 8ex^4$ and hence the condition $N_1 = 0$ gives us $e = 0$. So we arrive at the family of systems

$$\dot{x} = a + x^2, \quad \dot{y} = b + fy \tag{51}$$

which evidently are Liénard systems. After the linear transformation $x_1 = y$, $y_1 = x$ we obtain the systems

$$\dot{x}_1 = b + fx_1, \quad \dot{y}_1 = a - y_1^2.$$

Clearly these systems are Riccati but they are non-Liénard systems (i.e. have the form (3) with $n \neq 0$) and this completes the proof of the sufficiency.

Necessity. Assume that a Riccati system (3) is of Liénard normal form and there exists an affine transformation which brings this system to a non-Liénard form inside the family of Riccati systems. As it was mentioned earlier for a Liénard system in the family (3) the condition $n = 0$ is necessary. This condition implies $\eta = n^2[(g - 2m)^2 - 4ln] = 0$ and we get the subfamily of Riccati systems:

$$\frac{dx}{dt} = a + cx + gx^2, \quad \frac{dy}{dt} = b + ex + fy + lx^2 + 2mxy. \tag{52}$$

For these systems we have $C_2 = -x^2[lx + (2m - g)y]$ and $\widetilde{M} = -8(g - 2m)^2x^2$. Since there exists an affine transformation which brings this system to a non-Liénard form inside the family of Riccati systems (and this transformation is not the identity, otherwise we remain in the class of Liénard systems), we deduce that at infinity there must exist a second singular point besides $N_1[0 : 1 : 0]$. Considering the value of C_2 it is clear that the second singularity must be $N_2[g - 2m : l : 0]$ and this implies the condition $\widetilde{M} \neq 0$.

Therefore applying the linear transformation $x_1 = 2lx + (2m - g)y$, $y_1 = x$ we arrive at the family of systems

$$\begin{aligned} \dot{x}_1 &= al + b(2m - g) + fx_1 + (cl - eg - fl + 2em)y_1 + 2mx_1y_1, \\ \dot{y}_1 &= a + cy_1 + gy_1^2 \end{aligned} \tag{53}$$

for which $C_2 = (2m - g)x_1y_1^2$, i.e. the infinite singular points are $\widetilde{N}_1[0 : 1 : 0]$ and $\widetilde{N}_2[1 : 0 : 0]$.

Therefore the above systems belong to the family of Riccati systems if and only if the right hand part of the first equation depends only on x_1 . This implies $m = 0$ and $cl - eg - fl + 2em = 0$. On the other hand for systems (53) we calculate

$$\begin{aligned} \eta &= 0, \quad \widetilde{M} = -8(2m - g)^2y_1^2, \quad B_2 = 0, \quad \widetilde{N} = 4(g - m)my_1^2, \\ \widetilde{K} &= 4gmy_1^2, \quad N_1 = -8(g - 2m)^2(cl - eg - fl + 2em)y_1^4 \end{aligned}$$

and we observe that the conditions $m = 0$ and $cl - eg - fl = 0$ imply $\widetilde{N} = \widetilde{K} = N_1 = 0$. Conversely assume that the condition $\widetilde{N} = \widetilde{K} = N_1 = 0$ are fulfilled. It is clear that the conditions $\widetilde{N} = \widetilde{K} = 0$ yield $m = 0$. In this case $g \neq 0$ otherwise we get $\widetilde{M} = 0$ and therefore the condition $N_1 = 0$ implies $cl - eg - fl = 0$.

Since $g \neq 0$ we deduce that systems (53) with the conditions mentioned above are non-Liénard systems and this completes the proof of Lemma 6.1. ■

Lemma 6.2. *A Riccati system (3) is of Liénard normal form (i.e. $n = 0$) if and only if the conditions given in Diagram 10 are satisfied, correspondingly, taking into consideration the conditions provided by Lemma 6.1.*

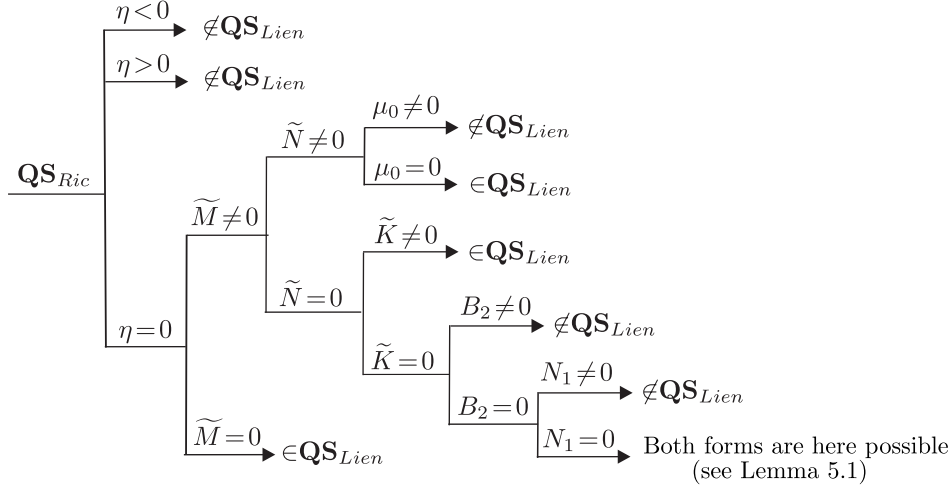


Diagram 10: The partition of the family \mathbf{QS}_{Ric} of Riccati systems

Proof: We consider the conditions provided by Diagram 10 taking into account that for the family (3) we have

$$\eta = n^2[(g - 2m)^2 - 4ln], \quad \mu_0 = g^2n^2, \quad \tilde{N} = 4(gn - m^2 + ln)x^2. \quad (54)$$

1: $\eta \neq 0$ (i.e. $\eta > 0$ or $\eta < 0$). Then a Riccati system (3) could not be a Liénard system because according to (54) the condition $\eta \neq 0$ implies $n \neq 0$.

2: $\eta = 0$, $\tilde{M} \neq 0$, $\tilde{N} \neq 0$, $\mu_0 \neq 0$. From (54) we get that $\mu_0 \neq 0$ implies $n \neq 0$ and we get non-Liénard systems.

3: $\eta = 0$, $\tilde{M} \neq 0$, $\tilde{N} \neq 0$, $\mu_0 = 0$. We claim that these conditions imply $n = 0$. Indeed suppose the contrary, that $n \neq 0$. Then considering (54) the condition $\mu_0 = 0$ yields $g = 0$ and then $\eta = 0$ implies $l = m^2/n$. However in this case we get $\tilde{N} = 0$ and this contradiction proves our claim.

4: $\eta = 0$, $\tilde{M} \neq 0$, $\tilde{N} = 0$, $\tilde{K} \neq 0$. We claim that these conditions imply $n = 0$. Indeed assuming $n \neq 0$ the condition $\eta = 0$ gives us $l = (g^2 - 4gm + 4m^2)/(4n)$ and then we get $\tilde{N} = g^2x^2$ and $\tilde{K} = 4gx(mx + ny)$. So $\tilde{N} = 0$ implies $\tilde{K} = 0$ which contradicts the conditions provided for this branch of Diagram 10.

5: $\eta = 0$, $\tilde{M} \neq 0$, $\tilde{N} = 0$, $\tilde{K} = 0$, $B_2 \neq 0$. These conditions imply $n \neq 0$ and for this it is sufficient to evaluate the invariant polynomial B_2 for Riccati systems (3). Indeed for these systems we calculate $B_2 = n\Phi(a, b, c, e, f, g, l, m, n, x, y)$, where Φ is a polynomial in the indicated parameters and variables. So the condition $B_2 \neq 0$ implies $n \neq 0$ and we are in the family of non-Liénard systems.

6: $\eta = 0$, $\tilde{M} \neq 0$, $\tilde{N} = 0$, $\tilde{K} = 0$, $B_2 = 0$, $N_1 \neq 0$. We claim that these conditions again imply $n = 0$. Indeed assuming $n \neq 0$ similarly as above we get that the condition $\eta = 0$ gives us $l = (g^2 - 4gm + 4m^2)/(4n)$ and then we obtain $\tilde{N} = g^2x^2 = 0$ which implies $g = 0$. Then we calculate

$$B_2 = -648(cm - fm + en)^4x^4, \quad N_1 = 16(cm - fm + en)x^2(mx + ny)^2/n$$

and evidently the conditions $B_2 = 0$ and $N_1 \neq 0$ are incompatible.

7: $\eta = 0$, $\widetilde{M} \neq 0$, $\widetilde{N} = 0$, $\widetilde{K} = 0$, $B_2 = 0$, $N_1 = 0$. According to Lemma 6.1 the systems in this subfamily due to an affine transformation can be presented in both (Liénard and non-Liénard) canonical forms.

8: $\eta = 0$, $\widetilde{M} = 0$. We claim that these conditions imply $n = 0$. Indeed assuming $n \neq 0$ the condition $\eta = 0$ gives us $l = (g^2 - 4gm + 4m^2)/(4n)$ and then we get $\widetilde{M} = -2[(g - 2m)x - 2ny]^2$. So evidently the condition $\widetilde{M} = 0$ implies $n = 0$ and we are inside the family of Liénard systems.

As all the cases provided by Diagram 10 are examined we deduce that Lemma 6.2 is proved. ■

Next we continue the comparison.

Considering the information from Diagram 10 together with that from Diagrams 5 to 8 we get the next corollary.

Corollary 6.1. *Taking into account Lemma 6.2 and Theorem 4.1 we deduce that the phase portraits Ric. 1 - Ric. 51, Ric. 53, Ric. 58, Ric. 60, Ric. 74 - Ric. 76 can be obtained for systems in Riccati form (3) which are non-Liénard.*

Similarly the phase portraits Ric. 28, Ric. 36, Ric. 43, Ric. 52 - Ric. 73, Ric. 77 - Ric. 93 can be obtained for systems in Riccati form (3) which belong to the family \mathbf{QS}_{Lien} .

As a consequence we conclude that the phase portraits Ric. 28, Ric. 36, Ric. 43, Ric. 53, Ric. 58 and Ric. 60 can be realized for systems in both Liénard and non-Liénard forms.

Since in the article [13] it is claimed that they determined all the phase portraits for Riccati systems (3) which are non-Liénard the authors should have found all the phase portraits from the first group. This group contains 57 phase portraits however in [13] are presented only 45 topologically distinct phase portraits (plus 3 wrongs ones) as it is mentioned in Remark 6.1.

Considering the list in Remark 6.1 and the Diagram 1 it can be easily seen that in [13] the following phase portraits are missed: Ric. 5, Ric. 7, Ric. 9, Ric. 17, Ric. 22, Ric. 35, Ric. 38, Ric. 39,

For each one of the above phase portraits we present an example of its realization in the families (i) - (iii) from [13].

$$\text{Ric. 5: } \dot{x} = x(x + 1), \quad \dot{y} = 4x - y - xy + y^2;$$

$$\text{Ric. 7: } \dot{x} = x(x + 1), \quad \dot{y} = -9/4 + x + 77x^2/4 - 8xy + y^2;$$

$$\text{Ric. 9: } \dot{x} = x^2, \quad \dot{y} = -1/9 + x - xy + y^2;$$

$$\text{Ric. 17: } \dot{x} = x(x + 1), \quad \dot{y} = 1 + 14x + 15y + 20x^2 + 10xy + y^2;$$

$$\text{Ric. 22: } \dot{x} = x(x + 1), \quad \dot{y} = 1 - 3x/8 + 2y + 7x^2/8 - xy + y^2;$$

$$\text{Ric. 35: } \dot{x} = x^2, \quad \dot{y} = 1 + x + 2x^2 - 2y - xy + y^2;$$

$$\text{Ric. 38: } \dot{x} = x(x + 1), \quad \dot{y} = -1 + x^2 - xy + y^2;$$

$$\text{Ric. 39: } \dot{x} = x^2, \quad \dot{y} = -2 - y + x^2 + 3xy + y^2;$$

$$\text{Ric. 40: } \dot{x} = x(x + 1), \quad \dot{y} = y + x^2/4 + y^2;$$

$$\text{Ric. 47: } \dot{x} = x(x + 1), \quad \dot{y} = 3x/8 + x^2/4 + y^2;$$

$$\text{Ric. 53: } \dot{x} = x, \quad \dot{y} = 1 + y^2;$$

$$\text{Ric. 74: } \dot{x} = x, \quad \dot{y} = 1 + x^2/4 + xy + y^2;$$

Acknowledgments. The work of the first and second authors are partially supported by the Agencia Estatal de Investigación grant PID2019-104658GB-I00, the H2020 European Research Council grant MSCA-RISE-2017-777911 and the AGAUR (Generalitat de Catalunya) grant 2022-SGR 00113. The second author also is partially supported, and by the Acadèmia de Ciències i Arts de Barcelona. The work of the third and the fourth authors was partially supported by the grants: NSERC Grants No. RN000355 and No. RN001102; the fourth author was partially supported by the grant No. 21.70105.31 SD.

References

- [1] J.C. Artés, B. Grunbaum and J. Llibre, On the number of invariant straight lines for polynomial differential systems, *Pacific J. of Math.* 184 (1998), 207–230.
- [2] J. C. Artés, R. Kooij and J. Llibre, *Structurally stable quadratic vector fields*, Memoires of the American Mathematical Society, vol 134, no. 639, American Mathematical Society, 1998, 108 pp.
- [3] J. C. Artés, J. Llibre and A. C. Rezende, *Structurally unstable quadratic vector fields of codimension one*, Birkhäuser/Springer, Cham, 2018, vi+267 pp.
- [4] J.C. Artés, J. Llibre and A.C. Rezende, *Structurally unstable quadratic vector fields of codimension one*, Birkhäuser/Springer, Cham, 2018, vi+267 pp.
- [5] J.C. Artés, J. Llibre, D. Schlomiuk and N. Vulpe, *Geometric configurations of singularities of planar polynomial differential systems [A global classification in the quadratic case]*. Birkhäuser/Springer, Cham, [2021], ©2021. xii+699 pp. ISBN: 978-3-030-50569-1; 978-3-030-50570-7
- [6] J. C. Artés, J. Llibre, D. Schlomiuk and N. I. Vulpe, Global topological configurations of singularities for the whole family of quadratic differential systems, *Qual. Theory Dyn. Syst.* 19 (2020), no. 1, Paper No. 51, 32 pp.
- [7] J.C. Artés, J. Llibre, D. Schlomiuk and N. Vulpe, From topological to geometric equivalence in the classification of singularities at infinity for quadratic vector fields, *Rocky Mountain J. of Math.* **45** (2015), 29–113.
- [8] J. C. Artés, R. Oliveira and A. C. Rezende, Structurally unstable quadratic fields of codimension two: families possessing either a cusp point or two finite saddle nodes, *J. Dynam. Differential Equations*, DOI: <https://doi.org/10.1007/s10884-020-09871-2> (2020), 43 pp.
- [9] V.A. Baltag and N.I. Vulpe, Total multiplicity of all finite critical points of the polynomial differential system, *Differ. Equ. Dyn. Syst.* **5** (1997), 455–471.
- [10] C. Bujac, D. Schlomiuk and N. Vulpe, On families $\mathbf{QSL}_{\geq 2}$ of quadratic systems with invariant lines of total multiplicity at least 2, *Qual. Theory Dyn. Syst.* 21 (2022), no. 4, Paper No. 133, 68 pp.
- [11] J.H. Grace and A. Young, *The algebra of invariants*, New York, Stechert, 1941.
- [12] M. Jungers, Historical perspectives of the Riccati equations, *ScienceDirect*, www.sciencedirect.com, IFAC PapersOnLine 50-1 (2017), 9535–9546.
- [13] J. Llibre, B.D. Lopes, P.R. da Silva, Bifurcations of the Riccati Quadratic Polynomial Differential Systems, *International Journal of Bifurcation and Chaos*, Vol. 31, No. 6 (2021) 2150094 (13 pages).
- [14] J. Llibre, D. Schlomiuk, The geometry of quadratic differential systems with a weak focus of third order, *Canad. J. Math.* 56 (2004), no. 2, 310–343.
- [15] P.J. Olver, *Classical Invariant Theory*, London Mathematical Society student texts: **44**, Cambridge University Press, 1999.
- [16] D. Schlomiuk and N. Vulpe, Planar Quadratic Vector Fields with invariant lines of total Multiplicity at least Five, *Qual. Theory Dyn. Syst.*, **5** (2004), no. 1, 135–194.

- [17] D. Schlomiuk and N. I. Vulpe, Geometry of quadratic differential systems in the neighborhood of infinity, *J. Differential Equations*, **215** (2005), no. 2, 357–400.
- [18] D. Schlomiuk and N. Vulpe, Planar quadratic differential systems with invariant straight lines of total multiplicity four, *Nonlinear Anal.*, **68**, no. 4 (2008), 681–715.
- [19] D. Schlomiuk and N. Vulpe, Integrals and phase portraits of planar quadratic differential systems with invariant lines of at least five total multiplicity, *Rocky Mountain J. Math.*, **38**, no. 6 (2008), 2015–2075.
- [20] D. Schlomiuk and N. Vulpe, The full study of planar quadratic differential systems possessing a line of singularities at infinity, *J. Dynam. Differential Equations*, **20**, no. 4 (2008), 737–775.
- [21] D. Schlomiuk and N. Vulpe, Integrals and phase portraits of planar quadratic differential systems with invariant lines of total multiplicity four, *Bul. Acad. Ştiinţe Repub. Mold. Mat.*, **1** (56) (2008), 27–83.
- [22] D. Schlomiuk, N. Vulpe, Global topological classification of Lotka-Volterra quadratic differential systems,
- [23] D. Schlomiuk, X. Zhang, Quadratic differential systems with complex conjugate invariant lines meeting at a finite point, *J. Differential Equations* 265 (2018), no. 8, 3650–3684.
- [24] K.S. Sibirskii, *Introduction to the algebraic theory of invariants of differential equations*, Translated from Russian, Nonlinear Science: Theory and Applications, Manchester, University Press, Manchester, 1988.
- [25] J. Sotomayor and R. Paterlini, Quadratic vector fields with finitely many periodic orbits, in *Geometric dynamics*, Lecture Notes in Mathematics, vol. 1007, Springer, Berlin, 1983, pp. 753–766.
- [26] Y. Q. Ye et al., *Theory of limit cycles*, translated by Y. L. Chi, Translations of Mathematical Monographs, vol. 66, American Mathematical Society, Providence, RI, 1986, xi+435 pp.